Biogenesis of the parasitophorous vacuole membrane (PVM) and regulation of its major component, the early transcribed membrane proteins (ETRAMPs) of *Plasmodium falciparum* (Welch, 1897) blood stages

Dissertation with the aim of achieving a doctor degree

at the Faculty of Mathematics, Informatics and Natural Sciences

Department of Biology

of Universität Hamburg

submitted by Leonie-Sophie Hecht

2015 in Hamburg

LANGUAGE CERTIFICATE

I am a native speaker, have read the present PhD thesis and hereby confirm that it complies with the rules of the English language.

Toronto, Canada, August 24, 2015
Place, Date

Tatianna Wong

Dissertationsgutachter:

1. Gutachter: Prof. Dr. Tim-Wolf Gilberger

2. Gutachter: Dr. Tobias Spielmann

Tag der Disputation: 29.01.2016

Zusammenfassung

Malaria stellt nach wie vor eine massive Bedrohung für die Menschheit da. Trotz zahlreicher Versuche gibt es immer noch keinen kommerziell erhältlichen Impfstoff und Resistenzen gegen alle bekannten Malaria-Medikamente breiten sich immer weiter aus. Die Malariaerreger, Parasiten der Gattung *Plasmodium*, werden von weiblichen Anopheles-Mücke, während einer Blutmahlzeit, übertragen. Malaria Tropica, die schwerste Form der Malaria im Menschen, wird von Blutstadien der Spezies *P. falciparum* ausgelöst. In dieser Phase und auch in der symptomlosen Leberphase sind, bedingt durch die obligat, intrazelluläre Lebensweise des Parasiten, nur dessen invasiven Stadien außerhalb der Wirtszellen zu finden.

Innerhalb ihrer Wirtszellen, Hepatozyten bzw. Erythrozyten, entwickeln sich die Plasmodien stets in einem spezialisierten Kompartimentes, der Parasitophoren Vakuole (PV), die von einer Membran (PVM) umgeben ist. Diese entsteht während des Invasionsprozesses aus der Wirtszellmembran, die jedoch sofort durch parasiteneigene Proteine und Lipide modifiziert wird. Bei der überlebensnotwendigen Modifikationen der Wirtzelle durch den Parasiten und bei der Aufnahme von Nährstoffen, müssen sowohl die Parasiten Plasma Membran, als auch die PVM passiert werden. Dieses Kompartiment wurde vielseitig untersucht, aber nie wurde die Biogenese der PV analysiert. Mit Hilfe der seit kurzem verfügbaren vier-dimensionalen-Mikroskopie für Blutstadien-Entwicklung von *P. falciparum* konnte in dieser Arbeit die Biogenese dieses Kompartiments genau untersucht werden. Durch die Sekretion von artifiziellen Reportern (Fusionen von einem Signal Peptid (SP) mit Fluoreszenzproteinen unter Kontrolle von stadienspezifischen Promotoren) in das PV-Lumen, konnte die Entwicklung der PV über die kompletten 48 Stunden der Blutphase beobachtet werden. Außerdem wurden die proteinspezifischen Lokalisationen endogener PV Proteine durch die Fusion mit Fluoreszenzproteinen analysiert. Durch die Expression eines artifiziellen Reporters unter der Kontrolle der 5´untranslationierten Region (5´UTR) des Genes für das *early transcribed membrane protein2* (*etramp2*) konnte erstmals auch die PV früher Ringstadien, direkt nach der Invasion, visualisiert werden. Dabei konnten für die amöboiden Formen der Ringstadien distinkte Proteinlokalisationen, in den Enden der amöboiden Verlängerungen, und kaum im

Rest der PV beobachtet werden. Diese zuvor als spezifisch für Komponenten des *Plasmodium* Translokons für exportierte Proteine (PTEX) beschriebene Lokalisation, scheint demnach eine generelle Lokalisation vieler PV Proteine in diesem Stadium darzustellen. Die Reporterzellline, unter der Kontrolle der *etramp2* 5´ UTR wurde außerdem zur Untersuchung einer postulierten translationellen Repression der *etramp2* mRNA im Schizontenstadium genutzt. Es konnte jedoch keine vollständige Repression beobachtet werde, sondern eine Expression des Reporters bereits im späten Schizontenstadium, kurz vor dessen Ruptur. Während der frühen Trophozoitenentwicklung erschien die PV ebenmäßig bis auf einige Extensionen, die vom Parasiten ausgingen. Diese Extensionen repräsentierten überwiegend die kürzlich beschriebene Cavity, eine mit dem Parasitencytosol verbundene Struktur unbekannter Funktion.

Es konnte gezeigt werden, dass die PV Biogenese während des späten Trophozoitenstadiums zwei neu entdeckte Phasen aufweist: die Strawberry-Phase und die Gap-Phase. Die mehrere Stunden andauernde Strawberry-Phase beginnt zeitgleich mit der Zentralisierung der Fressvakuole (FV), welche charakteristisch für den Übergang zum Schizontenstadium ist. Diese Phase ist dadurch gekennzeichnet, dass die PV rau erscheint und Reporterproteine in distinkten Bereichen lokalisieren, kontinuierlich unterbrochen von Bereichen ohne GFP-Signal.

Die Gap-Phase beginnt im Anschluss an die Strawberry-Phase und ist dadurch gekennzeichnet, dass eine oder mehrere Lücken in der Reporterproteinverteilung auftauchen. Das GFP schien von bestimmten Arealen der PV ausgeschlossen zu sein. Das Ende der Gap-Phase ist durch die sichtbare Segmentierung der neu gebildeten Merozoiten gekennzeichnet. Diese distinkten und reproduzierbaren Phasen der PV Morphologie, beobachtet für alle Reporterzelllinen, lassen Rückschlüsse auf generelle, strukturelle Veränderungen zu. Die Strawberry-Phase könnte die Einleitung der Schizogony repräsentieren und die Gap-Phase deren Ende und den Übergang zur Segmentierung der Tochterparasiten. Die beobachten Phasen können somit als Sub-Phasen der Schizontenentwicklung bezeichnet werden, die es auf molekularer Ebene weiter zu erforschen gilt.

Summary

Malaria still represents a serious threat to humankind. An effective vaccine is still not available and resistances to all common anti-malarial drugs are widespread. The causative agent of malaria - parasites of the genus *Plasmodium* - are transmitted during a blood meal of an infected, female *Anopheles* mosquito. The severest form of malaria in humans, falciparum malaria, is caused by the blood stages of *P. falciparum*. Due to its obligate intracellular lifestyle, only the invasive parasite stage can be found outside of the host cell. Inside their host cells, hepatocyte during the symptomless liver stage and erythrocyte during the blood stage, the parasites reside in a highly specialized compartment, the parasitophorous vacuole (PV) which is surrounded by a membrane (PVM). The PV forms during the invasion process out of host cell membrane, which is immediately altered and supplemented with parasite derived proteins and lipids. In order to modify its host cell, proteins are exported into the host cell cytoplasm. Those parasites proteins have to pass the parasites plasma membrane as well as the PVM. The same applies also for nutrients taken up by the parasites.

Many aspects of this parasite specific compartment have been analyzed before, however its biogenesis had not been examined yet. In this thesis the PV biogenesis was analyzed through the entire development of *P. falciparum* blood stages by using the recently established 4d-microscopy technique. Utilizing artificial reporters, which were secreted to the lumen of the PV and expressed under the control of stage-specific promoters, this compartment could be observed over the entire 48 hours blood stage development. Furthermore, protein-specific localizations of PV-resident proteins, fused to fluorescent proteins, were examined.

An artificial reporter under the control of the 5´ untranslated region (5´UTR) of the *early transcribed membrane protein2* (*etramp2*) gene was used to visualize the PV of early ring stage parasites immediately after the invasion for the first time. These experiments revealed that PV proteins localize to the far end of arm-like extensions during the amebic phase of ring stage parasites while the marker was barely detectable in the remaining PV. This localization was previously described to be specific for compounds of the *P. falciparum* translocon for exported proteins

(PTEX). However, the observation shown in this work suggest that this is a general localization of several PV proteins during that stage. The reporter cell line, under the control of the *etramp2* promoter region, was further used to examine the putative translational repression of *etramp2* mRNAs during the schizont stage. This reporter, as well as IFAs against ETRAMP2, showed no complete translational repression and an onset of translation in the very late schizont stage, shortly before its rupture.

During the early trophozoite development the PV appeared smoothly, except for some protrusions, extending from the parasite. These protrusions observed, were mainly identified as the recently identified cavity, an extension of unknown function, bound to the parasites cytosol.

During the PV biogenesis of later stages of trophozoite development two newly identified phases were observed: the strawberry-phase and the gap-phase.

The strawberry-phase always occurred concomitantly with the centralization of the parasites food vacuole (FV), an event characteristic for the transition of the trophozoite to the schizont stage. This new phase is characterized, by a rough appearance of the PV and a discontinuous distribution of the reporter-protein within the PV.

The strawberry-phase was immediately followed by the gap-phase and was characterized by gaps in the reporter-protein distribution. The GFP seemed to be excluded from those distinct areas of the PV. The end of the gap-phase was characterized by the segmentation of newly formed daughter merozoites.

These distinct and reproducible phases of the PV morphology were observed for all reporter cell lines, suggesting general, structural changes. The strawberry-phase may represent the onset of schizogony and the gap-phase its end and the transition to the stage of daughter parasites segmentation. Therefore, they probably represent sub-stages of schizont development, which have to be characterized in more detail on the molecular level in the future.

TABLE OF CONTENT

Table of Figures

List of Tables

Abbreviations

3d	Three-dimensional
4d	Four-dimensional
ACT	Artemisinin combination therapy
AMA	Apical Membrane Antigen
Apo	Apolipoproteins
C-	Carboxy
CRT	Chloroquine Resistance Transporter
DAPI	4'6-Diamino-2-phenylindol
DDT	Dichlordiphenyltrichlorethan
DNA	Desoxyribonucleicacid
et al.	et alii
ETRAMP	Early transcribed membrane protein
EXP-1	Exported protein-1
EXP-2	Exported protein-2
FKBP	FK 506 binding
DIC	Differential interference contrast
GFP	Green fluorescent protein
L-FABP	human liver fatty-acid binding
HBsAg	Hepatitis B surface antigen
IMC	Inner membrane complex
iRBC	Infected Red blood cell

hpi	Hours post invasion
HSP	Heat shock protein
LSA	LIverstage Antigen
DHFR	Dehydrofolate reductase
mRNA	Messenger ribonuclei acid
MAHRP	Membrane associated histidine rich protein
MSP	Merozoite surface protein
N-	Amino-
PCR	Polymerase chain reaction
PEXEL	*Plasmodium* export element
PfEMP1	*Plasmodium* falciparum erythrocyte membrane protein-1
PNEP	PEXEL negative exported proteins
PPM	Parasites plasma membrane
PTEX	*Plasmodium* translocon for exported proteins
PV	Parasitophorous vacuole
PVM	Parasitophorous vacuole membrane
RBC	Red blood cell
RC	Red blood cell cytosol
REX	Ring Exported Protein
RPMI	Rosswell Park Memorial Institute
SP	Signal peptide
TEM	Transmission electron microscopy
TM	Transmembrane domain

UIS	Upregulated in infective sporozites
UTR	Untranslated region
WHO	Wold Health Organization
WPC	Whole parasite-based vaccine
Wt	Wild type
µ	Micro
µl	Microliter
µm	Micrometer

Chapter 1: Introduction

1.1 Malaria

Malaria is a vector-born parasitic disease, caused by eukaryotic, obligate intracellular protozoans of the genus *Plasmodium*. The parasites are transmitted to their vertebrate hosts during the blood meal of an infected, female mosquito of the genus *Anopheles*. There are over 200 different *Plasmodium* species, but only five of them are known to be human pathogenic, namely *P. falciparum, P. vivax, P. ovale, P. malariae and P. knowlesi. P. knowlesi*, originally known to infect monkeys, is the most recent species discovered to be infective for human beings. The most virulent species is *P. falciparum,* which is responsible for most of the malaria associated deaths. There are over 3 billion people living at the risk of an infection and over half a million people died in 2013 (WHO, 2014). Death occurs mainly in children under the age of 5 and predominately in sub-Saharan Africa (Fig. 1.1).

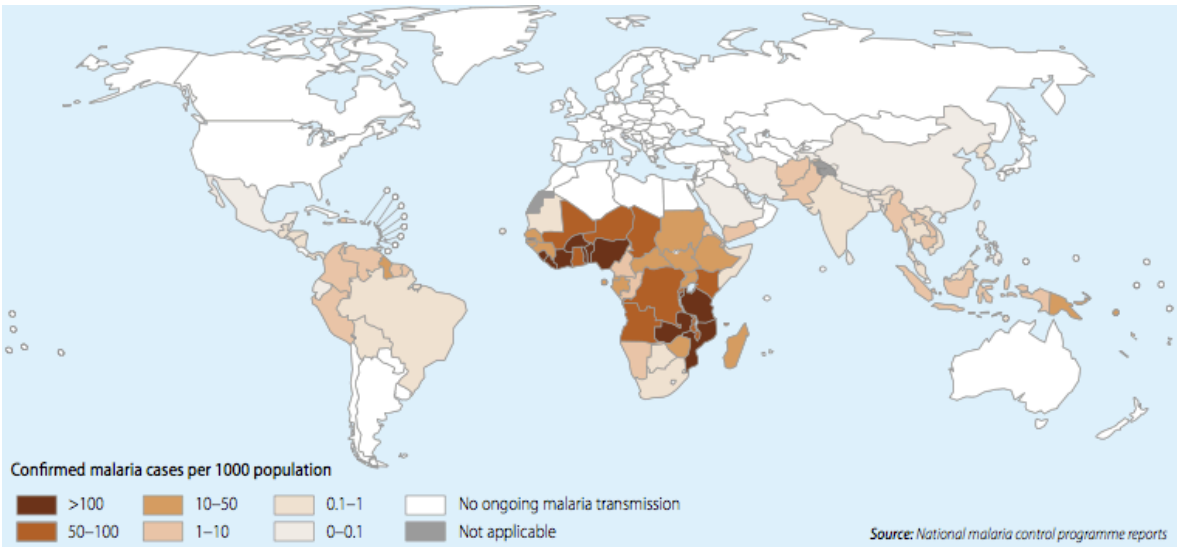

Fig.1.1 Countries with ongoing Malaria transmission (WHO Malaria Report, 2014)

1.2 Pathophysiology

All clinical symptoms of malaria are caused by the asexual blood stage development of *Plasmodium* parasites in the human blood. The time to occurrence of symptoms after an infective bite of an *Anopheles* mosquito depends on the duration of the liver phase, which precedes the blood stage and varies in length with *Plasmodium* species. In the case of falciparum-Malaria, this latency period takes about 12 days, for *P. vivax* and *P. ovale* (*Malaria tertiana*) it takes 12-18 days and for *P. malaria* 15 to 50 days (Bartoloni and Zammarchi, 2012).

The primary symptoms of malaria are similar for all species and resemble the symptoms of the common flu, including nausea, ague, emesis, headache, body aches, sweating, diarrhea, malaise and fever (reviewed in Miller *et al.*, 2002). The rupture of iRBCs causes the characteristic periodic fever attacks of malaria. This rupture occurs at the end of each reproduction cycle, when newly formed daughter parasites are release into the blood stream together with pyrogenic agents that accumulated in the iRBCs (Schofield *et al.*, 2002; White *et al.*, 2014). The five human pathogenic *Plasmodium* species are known to cause different courses of the disease. Eponymic and characteristic for these malaria types are the periodicity of the fever attacks, occurring in a three and four days time period, respectively. *P. malaria* causes the malaria quartana, Quartana malaria (Pm). *P. vivax* and *P. ovale* are the causative agents of the so called malaria tertiana. The most severe form of malaria is the malaria tropica or falciparum malaria, caused by *P. falciparum.* Malaria tertiana and quartana characterized by comparably mild course of the disease. The Quartana malaria is characterized through very low blood parasitaemia and a mild course of the disease. However, the blood stage parasites are able to persist for extremely long periods. It is believed, if untreated, it could lead to a lifelong infection of the human host (Collins and Jeffery, 2007). This course of the disease is mostly complication-free. But malaria tertiana is known to relapse, resulting from the activation of quiescent hepatic hypnozoites, characteristic for *P. vivax* and *P. ovale* (Shute *et al.*, 1946; Cogswell *et al.*, 1992; Shanks and White, 2013; Dembélé *et al.*, 2014) and for *P. vivax* severe courses of the disease have been reported (reviewed in Price *et al*., 2009).

The most severe form of malaria is the malaria tropica or falciparum malaria, caused by *P. falciparum*. The uniqueness of *P. falciparum* infected red blood cells (iRBC) is the ability to avoid splenic clearance by adhering to the vascular endothelium. This cytoadherence ability can cause obstruction of blood vessels and is a major contributor of the severity of *P. falciparum* infection (Good and Milon, 1992). This can lead to impaired consciousness, coma and death if the brain is affected (Medana and Turner, 2006; Kyes *et al.*, 2007). This symptom complex is called cerebral malaria and is the main cause of fatal malaria cases. And some cases of malaria, the infections can also lead to severe complications like anemia, splenomegaly and very rarely to spleen rupture, acute renal failure or respiratory failure (White *et al.*, 2014). Pregnant woman face an especially high risk of developing severe malaria. The massive sequestration of iRBC in the placenta contributes to complications during pregnancy, such as maternal morbidity, low birth weight and preterm delivery (Desai *et al.*, 2007). *P. knowlesi* was beeing described as human pathogenic since 2007 and it is prevalent mainly in the southeast of Asia, but only a limited number of cases has been described until now. From the cases known to be caused by *P. knowlesi* it can be concluded that this Malaria type has a comparable latency period and course of the disease to falciparum Malaria (RKI; Case report, 2014; Ahmed and Cox-Singh, 2015).

1.2.1 Strategies against malaria

There are several, efficient and inexpensive drugs available against malaria, such as quinine and artemisinin. However, drug resistant *P. falciparum* isolates have been reported to all known commercially available drugs. The antifolates, like pyrimethamine, sulphadoxine and proguanil, are usually not recommended anymore, due to the fact that resistances to this class of drugs develop quickly under drug pressure and are widespread (Gregson and Plow, 2005; Sridaran *et al.*, 2010). These drugs inhibit the *de novo* tetrahydrofolate synthesis, which is needed by the parasites as a co-factor in protein synthesis (Müller and Hyde, 2010).

Quinine is derived from the Cinchona tree (*Cichona officinalis*) and the commonly used derivatives in treatment are the safe and inexpensive, synthetic 4-aminochinolin-derivatives Chloroquine and Amodiaquine (Dondorp *et al.*, 2009). These compounds affect blood stage parasites. They accumulate in the parasite's food vacuole, where they inhibit the hemoglobin degradation by forming complexes with toxic heme moieties and interfere with other detoxification mechanisms (Sidhu *et al*., 2002; Johnson *et al*., 2004). The heavy use through the decades eventually led to chloroquine resistance as well, in *P. falciparum* and *P. vivax* strains. The first resistant *P. falciparum* strains were detected in Colombia and at the Cambodia-Thailand border during the late 1950s. It took nearly 20 years for the resistance to reach Africa, via South America and India (Wellems and Plowe, 2001).

Artemisinin is extracted from the wormwood *Artemisia annua*, and was used in Chinese medicine for over 2000 years against febrile illnesses (Jiang *et al.*, 1982). Artemisinin and its derivatives, like artesunate, artemether and dihydroartemisinin, have a short elimination half-life and a rapid onset of action. Because of the shorter exposure of the parasite to sub lethal doses in the hosts` blood, the chances for the development of resistant parasites are reduced. To further reduce the chance for the development of resistance, the artemisinins are combined with longer-acting partner drugs including artemether- lumefantrine, artesunate-amodiaquine, artesunate-mefloquine, and dihydroartemisinin- piperaquine (Laufer *et al.*, 2009; WHO Report, 2014), in a so-called Artemisinin combination therapy (ACT). The idea is that the drug with the longer half-life would eliminate any parasites escaping the action of artemisinins, thereby eliminating the parasites potentially exposed to sub-lethal doses of the drug. However, *Plasmodium* strains resistant against Artemisinin have been reported and confirmed (Gordi *et al.*, 2001; Noedl *et al.*, 2009; Dondorp *et al.*, 2009; Dondorp *et al.*, 2010; Phyo *et al.*, 2012). Recently described mutations of the gene encoding a Kelch propeller domain protein (PF3D7_13436700) have been connected with resistance against artemisinin (Ariey *et al.*, 2014).

In the mid 1960s, malaria eradication seemed to be on its way, with the widespread usage of anti- malarial drugs like pyrimethamine and chloroquine and the use of the insecticide dichlorodiphenyltrichloroethane (DDT). In addition, the mosquito vectors evolved resistance against DDT. For these reasons, new drug development is still highly needed (Talisuna *et al.*, 2004).

1.2.1.1 Malaria vaccines

Despite of large efforts in the past decades, research into malaria vaccines has so far failed to deliver a commercially available vaccine that induces sterile and long lasting immunity (Crompton *et al.*, 2010). The reasons for this are not fully clear but may include the mainly intracellular life cycle, antigenic variation and polymorphisms of parasites surface proteins and the lack of knowledge regarding the human immune system.

There are different strategies to obtain a protective vaccine against any pathogen: immunizations can be done with the killed pathogen, the attenuated pathogen or the pathogen's proteins or subunits of proteins (Hill *et al.*, 2011). For malaria, all of the three different life cycle stages of the parasite are the target for vaccine development: the pre-erythrocytic, erythrocytic and the vector stages of parasites development.

There are many vaccine candidates serving as targets proteins of liver and erythrocytic stages, like AMA1 (Sagara *et al.*, 2009), EBA-175 (El Sahly *et al.*, 2010), MSP1 (Ogutu *et al.,* 2009) und SERA5 (Horii *et al.,* 2010). Some of the candidates, namely LSA-1, AMA-1 and MSP1 have already been tested, but non of the vaccines passed the phase II clinical trials (Ogutu et al., 2009; Sagara *et al*., 2009, Cummings *et al*., 2010).

The most promising and advanced subunit candidate is the RTS,S/AS01 vaccine that targets the parasites pre-erythrocytic stages. It consists of regions of the circumsporozoite protein (CSP) that are recognized by the human immune system combined with fused (25%) and free hepatitis B surface antigen (75%) and

formulated with the AS01 adjuvant (Casares *et al.*, 2010). Previous studies established that RTS,S/AS01 has the ability to provide some protective immunity. The most recent and final results of the phase 3, individually randomized, controlled trial were published in April 2015. It was reported that the RTS,S/AS01 prevented a substantial number of cases of clinical malaria over a 3 - 4 year period in young infants and children. Overall vaccine efficacy against clinical malaria and severe courses of the disease, was in the 30% range. Therefore the vaccine has the potential to make a substantial contribution to malaria control when used in combination with other effective control measures, like insecticide-treated bednets, especially in areas of high transmission (RTS,S Clinical Trials Partnership, 2015).

Another vaccination strategy is the whole parasite-based vaccine (WPV). The idea to produce a vaccine based on attenuated parasites already came up in 1967 by Nussenzweig and colleagues. Their work showed that vaccination with radiation-attenuated Sporozoites (the parasite stage passed from the mosquito to the human) (RAS) protected mice as well as humans from malaria infection (Nussenzweig *et al.*, 1967; Nussenzweig and Nussenzweig, 1989). One problem in producing the inactivated Sporozoites is to find the optimal level of radiation, to ensure DNA damage without reducing infectivity and immunogenicity of the sporozoites (Ménard *et al.*, 2013). Recently the idea of WPV by using RAS has been resumed by Sanaria CEO Stephen Hoffman and colleagues. They were able to produce high numbers of infective, attenuated, aseptic, purified, cryopreserved sporozoites that are administered intravenously. The report of some preliminary clinical trials showed their success with the PfSPZ vaccine (Seder *et al*., 2013).

1.3 *Plasmodium* life cycle

There are two major developmental phases in the human host, the liver or exo-erythrocytic stage and the blood or erythrocytic stage. First the liver stage, were a single but massive multiplication step takes place (see section 1.2.1) occurs. Secondly, the blood or erythrocytic stage, were the parasites develop in the host cells erythrocyte and continuously multiply (see section 1.2.2).

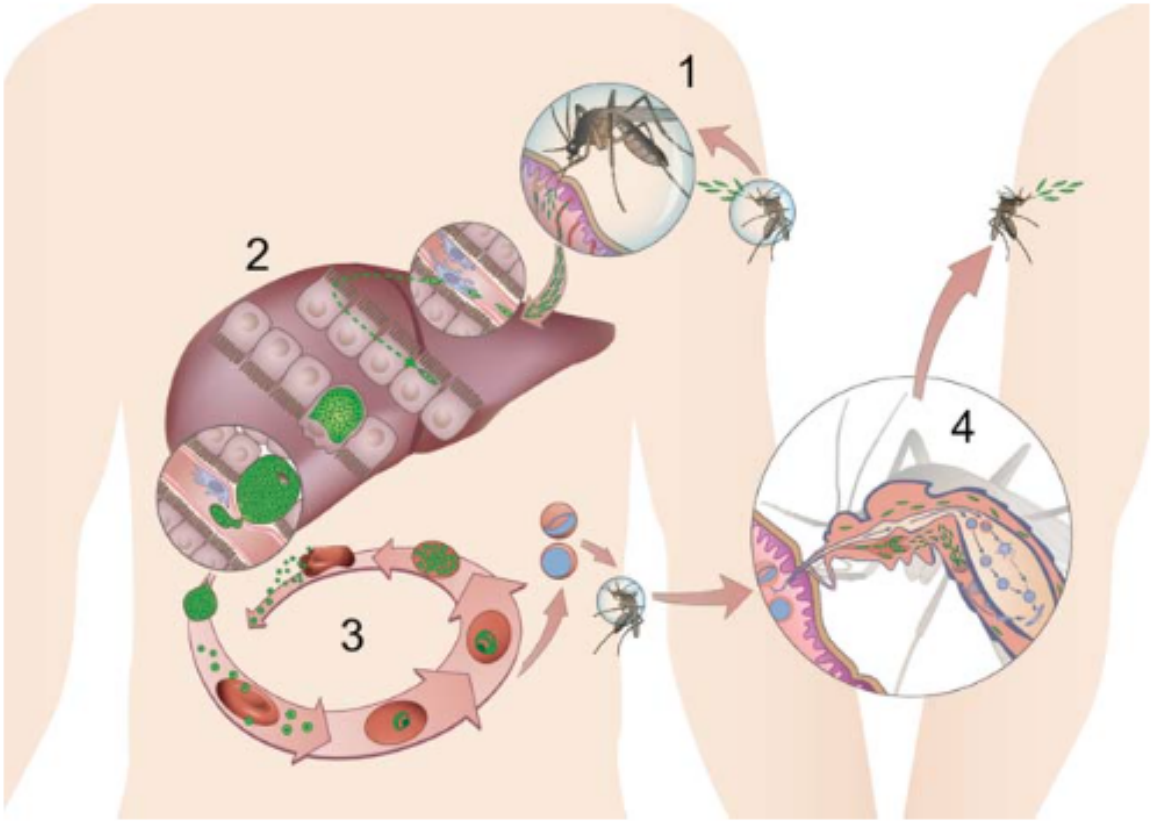

Fig. 1.2.: ***Plasmodium falciparum*** **life cycle:** 1. Parasites are transmitted during the blood meal of an *Anopheles* mosquito. 2. Liver stage development, which ends with the release of thousands of Merozoites into the blood stream 3. Asexual blood stage development: Some parasites form sexual stages, which are taken up by a mosquito during another blood meal. 4. Sexual development of the parasite in the anopheline vector that leads to the production of new sporozoites that enter the salivary glands (picture taken from Sturm and Heussler, 2007)

1.3.1 *Plasmodium* liver stage development

The infectious sporozoites reside in the salivary glands of the anopheline vector. During a blood meal the sporozoites are inoculated into the skin of the human host. The sporozoites invade small blood vessels in the skin and travel through the human blood stream to the liver (Mota *et al.*, 2002). Sporozoites cross the sinusoidal endothelial cell layer by traversing Kupffer cells or fenestrated endothelium cells, and finally reach the hepatocytes (Tavares *et al.*, 2013). After transmigration of several hepatocytes the sporozoite reaches a hepatocyte in

which it will develop (Prudencio *et al.*, 2007). During invasion of this hepatocyte, a parasitophorous vacuole (PV) is formed wherein the parasite develops. The PV is surrounded by host cell membrane, which invaginated during the invasion process and is termed parasitophorous vacuole membrane (PVM) (Meis *et al.*, 1983b; Bano *et al.* 2007). In this specialized compartment (see section 1.3.5) the exo-erythrocytic schizogony, the parasite's first asexual replication, takes place (Menard *et al.*, 2013). During liver stage development the parasite modifies the protein content of the PVM (see section 1.3.5.1) with parasite proteins like UIS4 or EXP1, which are detectable shortly post infection (Aly, 2008; van de Sand, 2005). During liver stage development a massive karyokinesis without any cytokinesis takes place, resulting in multi-nucleic syncytium. In order to form the new daughter cells, the parasites´ plasma membrane (PPM) invaginates, until every nucleus is surrounded and the new merozoites are formed, this process is termed schizogony. During this process the PVM gets more and more permeable (Sturm *et al.*, 2009), until it completely breaks down to release the merozoites into the host cell cytoplasm. Thereafter the merozoites are packed into membrane sacs formed out of host cell membrane, so called merosomes, that are released into the liver sinusoids (Sturm *et al.*, 2006; Graewe *et al.*, 2011) and in this way reach the blood circulation (Fig. 1.3).

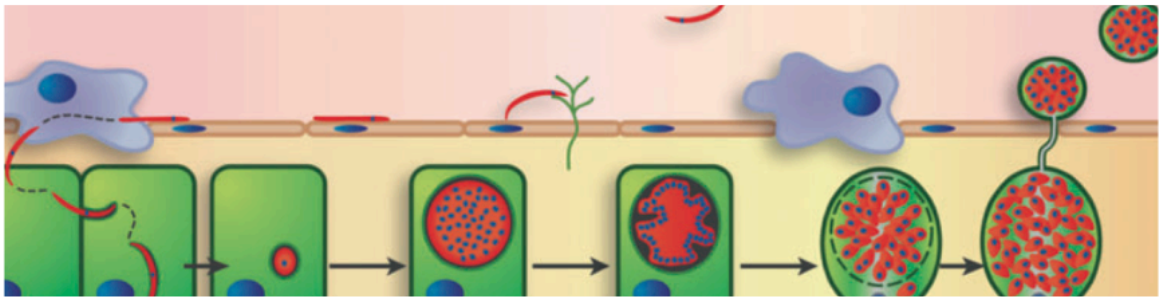

Fig. 1.3: Schematic of *Plasmodium* spp. Liver stage development: red: parasite; blue: nucleus; green: hepatocycte; purple: kupffer cells. (Picture taken and modified from Rankin *et al.,* 2010)

1.3.2 *Plasmodium* blood stage development

For *P. falciparum,* each blood stage multiplication cycle takes 48 hours, and starts with the invasion (see section 1.3.3) of - initially liver stage – and in subsequent cycles, blood stage-derived merozoites into the red blood cell. After invasion the merozoite develops into a so-called ring stage parasite, that is named based on the ring-like appearance in Giemsa-stained blood smears. It has been shown that living ring stages are not always ring-shaped: they are highly mobile within the RBC and change their shape from circular to amebic and vice versa (Grüring *et al.*, 2011) (Fig. 1.2.2). During this early developmental stage, the parasites remodel their host cell, in order to create ideal conditions for their development. Approximately 19 hours post invasion a transition phase to the next developmental stage (the trophozoite stage) starts. This transition phase takes 2 to 4 hours and is, *inter alia,* marked by the arrest of the parasite in the RBC periphery and by its smaller, condensed circular shape (See schematic overview Fig. 1.5). At this stage the parasite starts to incorporate the hemoglobin of the host cell and degrades it in its food vacuole. This process is required for the parasite to gain energy and amino acids, and to make space in the host cell for its growth. Due to the digestion of hemoglobin, toxic heme is released and converted to a nontoxic polymer (hemozoin) by a parasite-specific heme polymerizing activity. These hemozoin crystals accumulate inside the parasites food vacuole and in Giemsa-stained parasites are visible as what is known as “brown malaria pigment” (Slater, 1992).

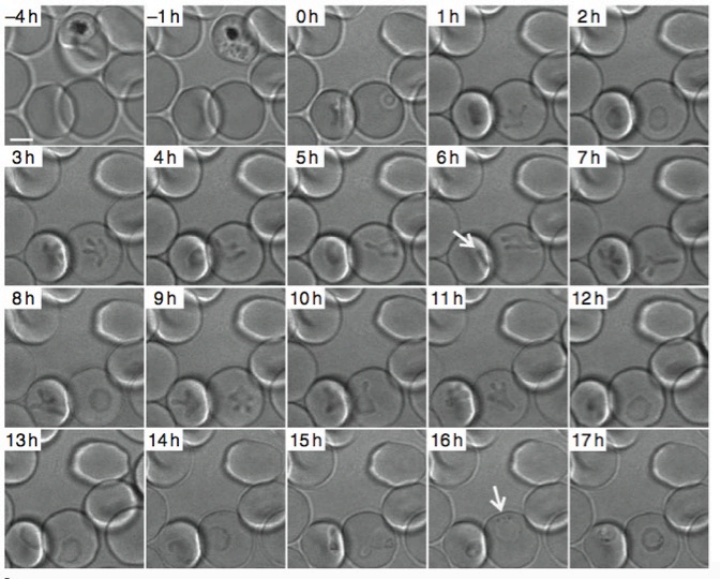

Fig. 1.4 Time-lapse microscopy of early blood stage parasites. Differential interference contrast (DIC) images of confocal time- lapse microscopy of the different shapes of ring stage parasites are shown. Taken in 1 hour intervals; time points given in the left upper corner of each image. Arrow time point 6 h, laterally seen ring stage; arrow time point 16 h, haemozoin foci. (Picture taken from Grüring *et al.,* 2011)

The trophozoite stages covers approximately 22 to 36 hours post invasion. During this time the parasites grows until it occupies most of the host cell. DNA replication starts around 32 hours post invasion and approximately 36 hours after invasion the trophozoites turn in to schizont-stage parasites. During this stage the nuclear division and parasites growth goes on until the mature schizont harbors 8 to 32 daughter nuclei. Then schizogony takes place and a corresponding number of mononuclear daughter merozoites are formed.

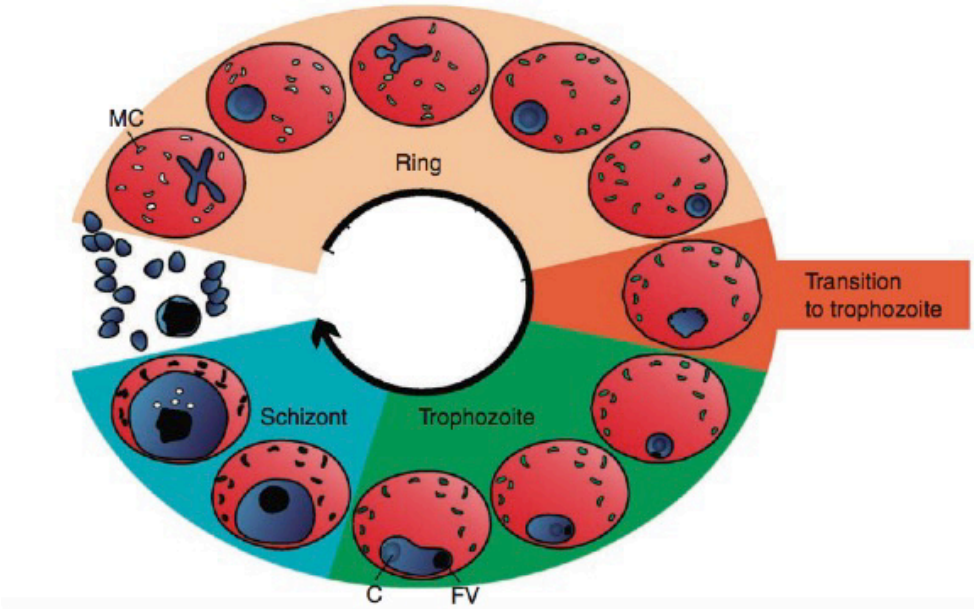

Fig. 1.5 Schematic overview of the asexual blood stage development of *P. falciparum* parasites. In red the erythrocyte; in blue the developing parasite; MC= Maurer´s clefts; C= cavity; FV= Food vacuole (Picture taken from Grüring et al., 2011)

1.4 Asexual Blood stage biology

1.4.1 Cell biology

A defining feature of eukaryotic cells is the presence of membrane-bound organelles- eponymic the nucleus [Eukarya, comes from the Greek ευ (eu, "well") and κάρυον (karyon, "nut" or "kernel")], like mitochondria, the Golgi apparatus and, in plant cells, the chloroplasts. *Plasmodium* parasites belong to the domain Eukarya and therefore contain the canonical set of organelles like the nucleus, the Golgi, the ER, and mitochondria. In addition they contain parasite-specific organelles, including secretory organelles such as rhoptries and micronemes (see section 1.3.2), a lysosome-like compartment referred to as the food vacuole, the inner membrane complex consisting of membrane sacs underneath the parasite plasma membrane and a complex four membrane bound plastid, the apicoplast (Deponte, 2012). The apicoplast is a secondary plastid, acquired by secondary endosymbiosis. This plastid has lost its ability to provide energy by photosynthesis (Agrawal and Striepen, 2010) but is still essential for parasites survival (vanDooren and Striepen, 2013) and a good example for the complexity and specialization of

the organelles of *P. falciparum* parasites.

1.4.2 Apical organelles and invasion

To invade the host cell, *Plasmodium* parasites have to recognize and bind receptors on the host cell surface. In the case of *Plasmodium* blood stage parasites, the merozoite makes the contact to the RBC via proteins residing on its surface. The initial contact is mediated by GPI anchored proteins, like the merozoite surface protein-1 (MSP-1) (O'Donnell *et al.*, 2000). The invasion process then starts with a re-orientation of the parasites, until the merozoites´ apical end faces the RBC membrane (Fig. 1.6, B). The parasites possess special apical organelles, named the rhoptries, micronemes and dense granules, which then discharge their contents. Some of the released proteins are used to establish a tight junction between parasite plasma membrane (PPM) and RBC membrane. The rhoptry neck (RON) proteins play a role in this process. These proteins are inserted into the host cell membrane and interact with AMA-1 (apical membrane protein-1) located on the parasite to form the tight junction (Hehl *et al.*, 2000; Triglia *et al.*, 2000, Besteiro *et al.*, 2009; Riglar *et al.*, 2011; Tyler *et al.*, 2011). The tight junction moves from the apical to the posterior end of the merozoite (fig. 1.6; C-D). This movement is driven by the parasites actin- myosin motor (Keeley and Soldati, 2004; Baum *et al.*, 2005). During the invasion process the parasitophorous vacuole (PV) is formed in which the parasite resides in the host-cell cytoplasm (Cowman and Crabb, 2006). After the parasites entered the host cell, its membrane is sealed by parasites proteases (fig. 1.6; E). As a result of this, the parasite grows inside the parasitophorous vacuole and is never in direct contact with the host cell cytosol (See section 1.3.5) (Cowmanand Crabb, 2006).

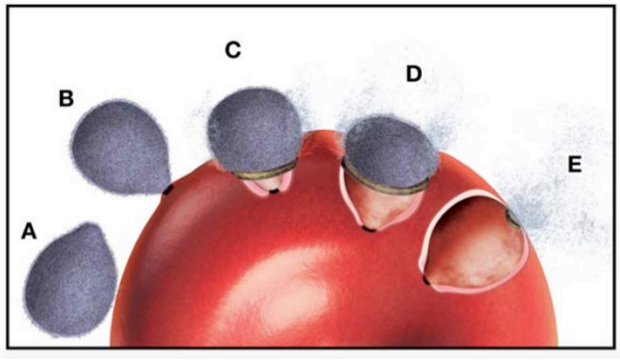

Fig. 1.6: Steps of the invasion process of a merozoite into a RBC. (A) The merozoite re-orientates at the RBC surface until (B) its apical end faces the RBC membrane and a tight junction is formed. C-D the merozoite pushes itself into the RBC in a process depending on its actin-myosin-motor. (E) The completion of the invasion process and sealing of the membrane (Picture taken from Crabb and Cowman, 2006).

1.4.3 Protein export and host cell remodeling

After the successful invasion of a RBC, the parasite immediately starts to remodel its host cell. To achieve this, parasites proteins are transported into the host cell. These exported proteins have to overcome the parasites plasma membrane (PPM) as well as the parasitophorous vacuole membrane. A recently identified translocon was originally identified as a complex of five different proteins, including HSP101, EXP2 and TRX2, as well as PTEX88 and PTEX150, residing at the PVM (deKoning-Ward *et al.*, 2009) is described in detail in section 1.3.5.1.

There are two different groups of exported proteins in *Plasmodium* parasites. The first group contains a conserved export motif termed the *Plasmodium* export element (PEXEL). The PEXEL motif consists of 5 amino acids (RxLxE/Q/D) and is cleaved in the ER by the parasite protease Plasmepsin V (Marti *et al*., 2004; Klemba *et al.*, 2005; Chang *et al.*, 2008; Russo *et al.*, 2010; Boddey *et al.*, 2013). The second group of exported proteins does not cotain a well defined export motif, but most of them have a transmembrane domain (TM) and an N-terminus that functionally resemble the N-terminus of the plasmepsin V processed PEXEL proteins (Spielmann and Gilberger, 2010; Grüring *et al*., 2012). This second group of exported proteins is referred to as PEXEL negative exported proteins (PNEPs).

1.4.3.1 Host cell modifications

The *P. falciparum* parasites are known to modify the RBCs surface, in order to avoid splenic clearance, iRBCs are sequestered from the blood circulation adhesion to the endothelium of small blood vessels. The major ligand for this cytoadherence is the *Plasmodium falciparum* erythrocyte membrane protein 1 (PfEMP-1), which is anchored in the RBC membrane in structures called knobs (Baruch *et al.*, 1995; Smith *et al.*, 1995; Su *et al.*, 1995). The knobs contain a number of different exported parasite proteins of which KAHRP (knob-associated histidine-rich protein), is a major component and is required for knob formation and efficient PfEMP-1 mediated binding to endothelial cells (Crabb *et al.*, 1997; Waller *et al.*, 1999).

Another unique modification of the iRBC are the membranous structures in close proximity to the RBC membrane, called Maurer´s Clefts (Maurer, 1902; Aikawa *et al.*, 1971). Trager *et al.* described Maurer's clefts as narrow clefts scattered throughout the cytoplasm of the infected cell bounded by a double membrane (Trager *et al.*, 1966). The current opinion of the function of the Maurer´s clefts is that they are important for protein trafficking and sorting within the RBC (Wickham *et al.*, 2001). Both, KAHRP and PfEMP1 transiently associate with Maurer´s clefts before relocating to the host cell membrane (Wickham *et al.*, 2001; Kriek *et al.*, 2003) and a number of MC resident proteins are known to be essential for PfEMP1 trafficking (Cooke et al., 2006; Maier et al., 2007; Spycher et al., 2008; Maier et al., 2008). However, the details of the transport and sorting processes remain unclear (Mundwiler-Pachlatko and Beck, 2013).

1.4.4 PV/PVM

The parasitophorous vacuole (PV) is a highly specialized compartment, in which the *Plasmodium* parasites reside and develop (Liehl *et al.*, 2015). The PV separates the parasite from direct contact with the host cell cytosol (Fig. 1.7). The PV membrane (PVM) is the interface between host cell and parasite and it is both, a gate and a barrier. It protects the parasite of potential harms and still allows the parasite to take up nutrients (Lingelbach and Joiner, 1998).

The PVM originates from the erythrocyte plasma membrane, but it is extensively modified by lipid material secreted from the parasites rhoptries (Dluzewski, 1992; Ward, 1993; Lingelbach and Joiner, 1998). The PVM remains tightly attached to the parasite plasma membrane (PPM), leading to a restricted vacuolar space between the(se) two membranes (Cesbron-Delauw *et al.*, 2008). Despite the difficulties to isolate the two membranes for direct proteomic and functional analysis, a number of PVM-associated proteins (see section 1.3.5.1) have been identified by immunofluorescence assays (IFAs), immunoelectron microscopy (IEM) or selective permeabilization techniques (Simmons, 1987; Stenzel, 1989; Spielmann, 2003; Spielmann; 2012). The analyses of Nyalwidhe and Lingelbach, identified for the PV proteome mainly following classes chaperones, proteases, and metabolic enzymes, consistent with the thought function of this compartment (Nyalwidhe and Lingelbach, 2006).

1.4.4.1 PVM protein set-up

In order to allow parasites growth, the parasite modifies and expands the PVM during its development (Cesbron-Delauw *et al.*, 2008).

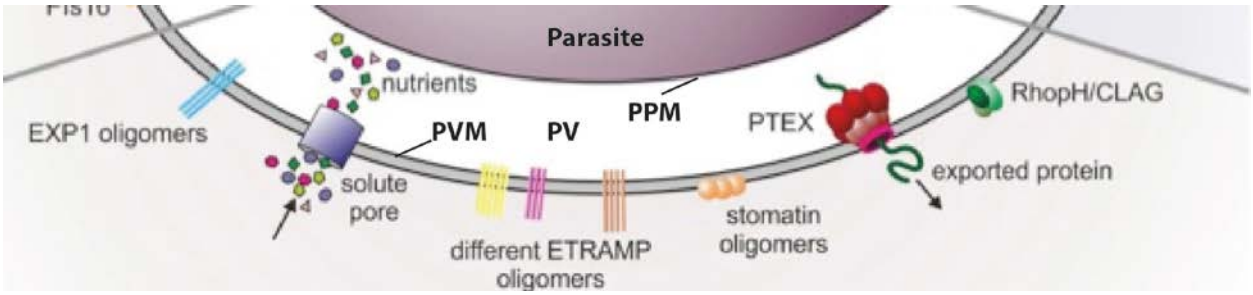

Fig. 1.7 Model for blood stage specific protein set-up of the PVM. This part of the schematic drawing**,** taken and modified from Spielmann et al., 2012, shows the protein content of the parasites PVM, during its asexual blood stages. EXP1: Exported protein 1; ETRAMP: Early transcribed membrane proteins; PPM: Parasite plasma membrane; PTEX: *Plasmodium* translocon of exported proteins; PV, Parasitophorous vacuole; PVM: Parasitophorous vacuolar membrane; RhopH/CLAG: rhoptry protein (RhopH) and cytoadherence-linked asexual gene (CLAG) complex.

The PVM of *Plasmodium* parasites contains solute pores, which were identified by patch clamp experiments, and are permeable for molecules up to a size of 1400

Da. Precursors, like monosaccharides, amino acids, and purine nucleotides, can cross the PVM by diffusion through this channel (Desai *et al.*, 1993; Desai and Rosenberg, 1997).
Most recently *P. falciparum* aquaporin (PfAQP), multifunctional channel protein, residing at the PPM, was shown to transport water and several solutes across the cell membrane (Chen, 2015).
Nutrients enter the lumen of the PV, where they get into contact with transporters at the PPM to get taken up into the parasite (Schwab *et al.*; 1994; Desai and Rosenberg, 1997). Prominent PVM extensions, also called tubovesicular network (TVN), are increasing the surface of the membrane and possible the PVM-mediated exchange, protein trafficking and nutrients uptake, in contact with the host cell cytosol. The TVN was also reported to be essential for parasites nutrient uptake (Lauer *et al.*, 1997; Eksi *et al.*, 2011).

Parasites proteins, destined for the host cell need to pass the PV membrane (see section 1.3.3). Hence, it needs to have the capacity to sort resident and exported proteins and the activity to transport exported proteins in to the host cell cytoplasm. The *Plasmodium* translocon of exported proteins (PTEX) was recently described as PVM resident (deKoning-Ward *et al.*, 2009) and it consists of five proteins: HSP101, EXP2 and TRX2, as well as PTEX88 and PTEX150 (deKoning-Ward *et al.*, 2009; Bullen *et al.*, 2012). In the PTEX machinery the EXP2 represents the membrane-associated pore, which interacts with PTEX150. PTEX150 binds HSP101, which unfolds the proteins at the PV in order to translocate them (fig. 1.8) (deKoning-Ward *et al.*, 2009; Bullen et al., 2012; Gehde et al., 2009; Beck *et al.*, 2014). These PTEX components were shown to be essential for parasites protein export (Elsworth *et al.*, 2014; Beck *et al.*, 2014).
Most recently PTEX components were shown to reside at the end of tubovesicular extensiions, which might differ from the TVN, in *P. berghei* liver stages (Matz *et al*., 2015).

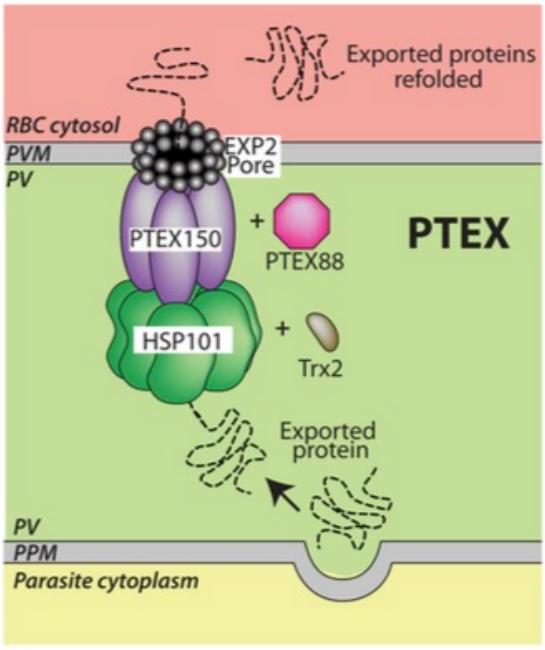

Fig. 1.8 Model of *Plasmodium* transolocon PTEX (Modiefied from Bullen *et al.,* 2012)

The Exported Protein 1 (EXP-1) is the earliest known PVM protein (Simmons *et al.*, 1987; Stenzel and Kara, 1989). Attempts to disrupt the gene encoding EXP-1 failed and it therefore may be essential for parasite survival (Maier *et al.*, 2008). EXP-1 is a single pass transmembrane protein, with a N-terminal signal peptide. And it is inserted into the PVM facing the host cell with its C-terminus (Günther *et al.*, 1991; Ansorge *et al.*, 1997). Most recently EXP-1 was described as a glutathione s- transferase, with a supposedly crucial degradation function in the hematin metabolism (Lisewski *et al.*, 2014). The *exp1* gene is among the most highly transcribed genes during the ring and early trophozoite stages of *Plasmodium* blood stages (Bozdech *et al.*, 2003; LeRoche *et al.*, 2004). Exp-1 is known to form oligomers at the PVM but the physiological relevance of this is unknown (Spielmann *et al.*, 2006a). A second group of integral PVM proteins are the early transcribed membrane proteins (ETRAMPs) and family of proteins described in more detailed in section 1.3.5.2.

1.4.4.2 Early Transcribed Membrane Proteins

The *etramps* belong to a multigene family, which is specific for the genus *Plasmodium*. ETRAMPs show a conserved domain structure (Fig. 1.9), including a signal peptide (SP), a short cationic N-terminal-domain, a transmembrane domain (TM) and highly charged more variable C-terminal domain (Spielmann and Beck, 2000; Spielmann *et al.*, 2003).

Fig. 1.9 General structure ETRAMPs. Signal peptide (SP), a short cationic N-terminal-domain (K-rich N-term), a transmembrane domain (TM) and highly charged C-terminal domain (Picture taken from Spielmann *et al.,* 2003)

Most ETRAMPs are expressed during the asexual stage of *P. falciparum*, but some are also exclusively transcribed in gametocytes or in pre-erythrocytic stages (LeRoch, 2005; Bodzech, 2003; Spielmann, 2003; McKellar, 2010). Some *etramps* are known to be among the most highly transcribed genes in *P. falciparum* (LeRoch, 2003; Daily, 2004) and accordingly show high protein levels in the PVM (Spielmann, 2006).

Table 1: ***P. falciparum*** **ETRAMPs and its localization throughout the life cycle stage**

Etramp	Gene	Stage	Reference
2	PF3D7_0202500	BS	Spielmann *et al*. (2003)
4	PF3D7_0423700	BS,Gam	Spielmann *et al*. (2003)
5	PF3D7_0532100	BS;LS	Birago, *et al*. (2003) Spielmann *et al*. (2003)
8	PF3D7_0829600	SPZ	Silvie *et al*. (2014)
10.1	PF3D7_1001500	BS	Spielmann *et al*.(2003); MacKellar *et al*. (2010)
10.2	PF3D7_1033200	BS	Spielmann *et al*. (2003)
10.3	PF3D7_1016900	BS,Gam	MacKellar *et al*. (2010)
11.1	PF3D7_1102700	BS	Spielmann *et al*. (2006c)
11.2	PF3D7_1102800	BS	Spielmann *et al*. (2003)
12	PF3D7_1240100	BS	Spielmann *et al*. (2003)
13	PF3D7_1302200	LS	Spielmann *et al*. (2003); Mueller *et al.*, 2005a
14.1	PF3D7_1401400	BS	Spielmann *et al*. (2003)
14.2	PF3D7_1476100	Gam	Spielmann *et al*. (2003)

BS: Blood stage; LS: Liver Stage, Gam: Gametocytes; SPZ: Sporozoites

For *P. falciparum* there are 14 ETRAMPs known (Table 1), expressed at different but specific stages of the parasite's life cycle (Spielmann *et al.*, 2003; MacKellar *et al.*, 2011; Müller et al. 2005a; Spielmann *et al.*, 2012). In 2010 there have been attempts to delete the gene encoding ETRAMP10.3, but this was not successful. The authors concluded from this that this ETRAMP has essential functions in *P. falciparum* blood stage development (MacKellar *et al.*, 2010). Two members of the ETRAMP family were previously identified as the liver stage-specific genes *uis3* and *uis4* (uis; upregulated in infective sporozoites) in the rodent malaria parasites *P. yoelii* and *P. berghei* and each was shown to be essential for liver stage

development (Matuschewski *et al.*, 2002; Kaiser *et al.,* 2004; Mueller *et al.*, 2005a,b; Mikolajczak *et al.*, 2007). Recent attempts to delete rodent *P. yoelii* (Py) genes, encoding *etramps,* were mainly successful. Only two *pyetramp* genes (PY02667 and PY07506) appeared to be essential for the survival of blood stages, since several attempts to delete these genes failed (MacKellar *et al.*, 2011). However, it should be noted that several of these ETRAMPs are much more closely related among each other than *P. falciparum* ETRAMPs are related.

For some ETRAMPs it has been shown, that they interact with host proteins. The rodent *P. yoelii* ETRAMP UIS3, had been shown to interact with human liver fatty-acid binding protein (L-FABP) (Mikolajczak *et al.*, 2007). Additionally ETRAMP5 was found to interact with human apolipoproteins ApoA1, ApoB, and ApoE (Vignali *et al.*, 2008). These studies suggest that PVM proteins can be important in direct interactions between parasite and its host cell proteins (MacKellar *et al.*, 2010).

Spielmann and colleagues showed that the PVM contains ETRAMPs and EXP-1 organized into oligomeric arrays (Fig. 1.7). They provided evidence that different ETRAMPs are present in separate arrays, leading to a mosaic distribution of clustered integral PVM proteins. ETRAMPs can form oligomers independently of other *Plasmodium* proteins or lipid rafts, indicating that ETRAMPs alone are sufficient to create different microdomains in a biological membrane and are therefore capable to form and/or maintain defined subdomains of the PVM (Spielmann *et al.*, 2006a). Together the EXP-1 and the ETRAMPs, together are the major protein component of the PVM. The high transcript abundance at specific *P. falciparum* developmental stages, their immediate expression after invasion (see section 1.4.1) of RBCs, the failed attempt to disrupt one of the multigene family members and their high abundance at the parasite host cells interface all together suggest a distinct and crucial role of ETRAMPs for parasites development and PVM formation/maintenance.

1.4.5 Regulation of gene expression

Eukaryotic cells need to regulate their gene expression. There are different possibilities of regulative mechanisms:

1. Epigenetic regulation: inheritable DNA or histone modification, capable of influencing gene expression to activate or inactivate transcription.
2. Transcriptional regulation: regulation of the copy number of mRNA through regulation of transcription rate (based on promotor/enhancer regions).
3. Translational regulation of mRNAs: controlling translation of specific proteins.
4. Post-translational regulation: proteolytic cleavage, phosphorylation or acetylation, regulate the activity or stability of proteins.

1.4.6 Gene regulation in *Plasmodium*

Like in many eukaryotic organisms, transcriptional regulation may be a dominant mode of expression regulation in *Plasmodium* parasites (Bozdech *et al.* 2003), although there is also evidence of posttanscriptional regulation (LeRoch *et al.*, 2004; Mair *et al.*, 2006; Foth *et al.*, 2008). In contrast to transcriptional regulation, posttranslational regulation has the advantage of speed and allows the parasite to rapidly adapt to drastic changes in environmental conditions as well as to rapid transition steps between developmental stages (Caro *et al.*, 2014). In *P. berghei* (Pb), the liver stage specific ETRAMP UIS4 is regulated at both, the RNA and the protein level (Silvie *et al.*, 2014). The detailed analysis in this work showed that only traces of the UIS4 protein were detectable at the sporozoite stage, while mRNA was clearly abundant. In contrast, immediately after host cell infection, large amounts of UIS4 were found (Silvie *et al.*, 2014). The discrepancy in the mRNA and protein levels suggested translational repression of UIS4 in the sporozoite stage. Interestingly, this study could exclude a role of the 5´ or 3´ untranslated regions (UTR) as cis-regulatory elements involved in UIS4 repression in sporozoites. Instead the presence of a secondary mRNA structures that might be recognized by an unknown repression complex was suggested. miRNA mediated regulation, known from other eukaryotes, although in principle an option, is not operational in *Plasmodium* parasites (Silvie *et al.*, 2014; Baum *et al.*, 2009).

In female gametocytes, translational repression was shown to play a crucial role. A stock of mRNA encoding for ookinete proteins are stored and not translated in so called messenger ribonucleoprotein particles (mRNPs) (Mair *et al.*, 2006; Mair *et al.*, 2010). These mRNPs contain the DDX6 RNA helicase DOZI, which binds to a U-rich motif in most repressed 3´UTRs (Braks *et al.*, 2008; Mair *et al.*, 2006). However, DOZI is known to be down-regulated in Pb sporozoites (Mueller *et al.*, 2011). Instead two genes, encoding proteins with PUF (Pumilio and fem-3 mRNA binding factor) region, PUF 1 and PUF 2, are up- regulated in Pb sporozoites (LeRoch *et al.*, 2005). In *Plasmodium* parasites PUF2 is known to mediate latency in mosquito sporozoites (Gomes-Santos *et al.*, 2011, Lindner *et al.*, 2013a, Mueller *et al.*, 2011). However, PUF proteins are known to interact with the mRNAs 3´UTR and in the case of uis4 the flanking regions were ruled out for mediating translational repression (Silvie *et al.*, 2014). The mode of repression for *uis*4 therefore remains unclear. In salivary gland sporozoites several transcripts are known that accumulate but are translated only later in the life cycle. For example, liver stage-associated proteins 1 and 2 (LSAP-1/PFL0065w and LSAP-2/PFB0105c) are among the most abundant transcripts in the salivary gland transcriptome (LeRoch *et al.*, 2004) but no proteins are detectable in sporozoites (Florens *et al.*, 2002; Lasonder *et al.*, 2008). There are more *etramp*s expressed in *P. falciparum* sporozoites, namely *etramp*8, *etramp*13 and *etramp*14.2 (LeRoch *et al.*, 2005). For all, high mRNA levels were observed in sporozoites but the corresponding proteins were not detected (Florens *et al.*, 2002, Lasonder *et al.*, 2008, Lindner *et al.*, 2013b), suggesting that also these *etramp*s are transcribed but not translated (Silvie *et al.*, 2014). For *P. falciparum* blood stages a similar translational repression has been suggested for another member of the *etramp* multigene family, namely *etramp2* (Spielmann *et al.*, 2003; Spielmann *et al.*, 2006a). In late blood stage schizonts the mRNA of *etramp*2 was observed by Northern blot (Fig. 1.10,A), but in the Western blot analysis the corresponding protein was not detected (Fig. 1.10,B). It is therefore possible that this is a general theme for ETRAMPs and hat their mRNAs are already produced in large amounts in the stage preceding their expression.

Fig.1.10 Discrepancy in mRNA and protein levels of ETRAMP2 A: Northern blot analysis: while the control 18s rRNA shows a constant level of?all over the *P. falciparum* life cycle, the mRNA of *etramp2* is missing in trophozoite stages (time points 4 and 5). A clear signal for *etramp2* mRNA is found in late blood stage schizonts (time point 7). B: Western blot analysis showed contradictory results to the findings of the Northern blot analysis: the endogenous ETRAMP2 protein was not/barely detectable in trophozoite to schizont stage parasites (22-32 and 32-42 hours post invasion; hpi). A, lanes 1-7: highly synchronized asexual blood stage cultures harvested at 0–6, 6–12, 12–18, 18–24, 24–30, 33–39, and 40–4 hpi; B, parasites developmental ranges 2-12; 12-22; 22-32 and 32-42 hpi; pictures taken and modified from Spielmann *et al.,* 2003.

1.5 Time-lapse microscopy

Visualizations of morphological details of *P. falciparum* blood stages, were usually obtained by the analyses of fixed samples. This is an important and informative technique, but for the examination of biogenesis of biological structures this technique could be prejudicial. Highly dynamic processes, like the biogenesis of biological structures could not be analyzed, using fixed, dead cells. Live cell imaging over extended periods of time was not possible for the asexual stages of these parasites.

Until, Spielmann and Grüring established 4d microscopy for *P. falciparum* blood stages (Spielmann and Grüring, 2012) and therefore they paved the for way structural and morphological studies of the biogenesis of biological structures. This imaging technique enables the generation of 3d reconstructions of infected RBCs, in regular time intervals, to generate a 4D dataset (3D time lapse imaging) (Grüring and Spielmann, 2012).

Using this technique Grüring and colleagues made their pioneering discovery that the ring stage development of the parasites appeared to be a highly motile stage, shown in detail in section 1.2.2 (Grüring *et al*., 2011). Furthermore they identified an extension, depriving from the parasite, which was shown to be filled with host cell cytosol, occurring at parasites from the ring stage to the schizont stages, in different but distinct patterns. These striking discoveries emphasize the advantages of the imaging of non-fixed, living parasites under health-keeping conditions.

To image intracellular, erythrocytic stages of *P. falciparum* over longer time periods, it is crucial to ensure parasites survival and to avoid phototoxicity. The differential interference contrast (DIC) microscopy is thereby used to visualize and enhance the contrasts of unstained sample material. In the case of *P. falciparum* blood cultures, structures visualized are infected and not infected erythrocytes, including the different developmental parasites stage. But in order to analyze structural processes of the parasites, different morphologies and structures within the parasites would not be visualizable or distinguishable from other structures. Hence, transgenic parasites were used, expressing marker proteins, like the green fluorescent protein (GFP). With the help of these marker proteins the desired parasites structure/ dynamic process can be visualized at particular time points during parasite development. In order to examine the biogenesis of the PV of very early ring stages, the knowledge about early expression of some ETRAMPs can be used (see sections 1.3.5.2 and 1.4.1), and the regarding *etramp* promoter region could be used to achieve very early expression of marker proteins.

1.6 Aims of this thesis

The *Plasmodium* parasites reside in its parasitophorous vacuole (PV) over the entire intracellular development, from invasion to egress. But only very little information have been raised about the biogenesis of the PV and the PVM through *P. falciparum*s life cycle. In this thesis, the biogenesis of this highly specialized compartment will be examined by using confocal microscopy for 4d (time- lapse) and 3d imaging (Grüring and Spielmann, 2012). Taking advantage in using fluorescent marker proteins, which are expressed at different time points of blood

stage development in the parasites PV, different developmental stages will be elucidated. For the first time the PV of very early rings stages parasites will be observed, by expressing the marker protein under the control *etramp2* promoter region, whereby a very early onset of translation will be ensured. The etramp2 is thought to be translational repressed in blood stage schizonts, but immediately translated after reinvasion of a new RBC (see section 1.4.1) (Spielmann *et al.*, 2003). Given that reporter construct, this putative translational repression of *etramp2* will be analyzed.

Chapter 2: Material and Methods

2.1 Materials

2.1.1 Technical and mechanical devices

Type	Specification	Distributor
SDS-PAGE chamber	Protean	Bio-Rad, München
Agarose-gel chamber	Sub Cell GT basic	Bio-Rad, München
Analytical balance	SBA32	Scaltec, Göttingen
Autoclave	V120	Systec, Wettenberg
Centrifuges	J2-HS Ultracenrifuge	Beckmann, München
	Eppendorf 5415 D	Eppendorf, Hamburg
Confocal microscope	Olympus FV1000	Olympus, Hamburg
Gel documentation	Gel-Soc XR	Bio-Rad, München
Electro blotter	Phase	Bio-Rad, München
Elecotropocator	X-Cell	Bio-Rad, München
Developer	Curix 60	AGFA-Gevaert, Mortsel/Belgie
Developer cassette	Cronex Quanra III Cassette	Dupnont, Neu Isenburg
Fluorescence microscope	Axioscope M1	Zeiss, Jena
Hamamatsu Digital camera	Orca C4742-95	Hamamatsu Photonics K.K., Japan
Incubator *P. falciparum* culture	B6200	Heraeus, Hannover
Ice machine	AF-10	Scotsman, Vernon Hills/USA
Laboratory scale	MC1 Laboratory LC 2200P	Sartorius, Göttingen
Laboratory scale	ATICON	Acculab, Gelsenkirchen
Magnetic stirrer	19R3001	Heidolph, Schwabach
Microwave	Micromaxx MM41568	Medion, Mülheim

Type	Specification	Distributor
Ultrapure Water Purification System	Milli-Q	Millipore, Bedfort/USA
PCR Mastercycler	Epgradient	Eppendorf, Hamburg
pH-Meter	211 Microprocessor	Hanna Intruments, Kehl
Photometer	Uvikon 933	Kontron, Offenbach
Pipettes	20µl, 100µl, 200µl, 1000µl	Gilson, Middleton/USA
Pipettor	Pipetus®-akku	Hirschmann, Eberstadt
Power-supply	Power PAC 300	Bio-Rad, München
Roller mixer	SRT6	Bibby Scientific, Staffordshire/UK
Shaking incubator	GFL 1083	Eppendorf, Hamburg
Sterile bench	Sterigard®III Advance	Baker, Standford/USA
Thermoblock	Thermomixer 5436	Eppendorf, Hamburg
UV-Transilluminator	PherOlum289	Biotec Fischer, Reiskirchen
Vortexer	Genie 2	Scientific Industries, USA
Waterbath	1004	GFL, Burgwedel

2.1.2 Labware and disposables

Labware and disposables	Manufacturer/Distributor
Bacteria culture tubes (13 ml)	Sarstedt, Nümbrecht
CEA RP NEW Medical X-Ray screen film blue sensitive	AGFA Healthcare NV, Mortsel/Belgium
Chromatography paper	GE Healthcare, Buckinghamshire/UK
Cover slip 24x65 mm, thickness 0.13-0.16 mm	R. Langenbrincl, Laboratory and Medicine technique; Emmendingen
Cryotubes	Nunc, Langenselbold
1.5 ml Eppendorf reaction tubes	Eppendorf, Hamburg

Labware and disposables	Manufacturer/Distributor
Falcon tubes (15 ml and 50 ml)	Sarstedt, Nümbrecht
Glass slides	Engelbrecht, Edermünde
IFA Glass slides	Thermo Scientific, Braunschweig
Latex Powder-free gloves	Kimberly Clark, Koblenz
Microscopy dishes, uncoated, hydrophobic	Ibidi, Martinsried
Multiply-µStrip Pro 8-Strip PCR reaction tubes	Sarstedt, Nümbrecht
Nitrocellulose Transfer Membrane Protane®	Whatman GmbH, Dassel
One way canulas	Braun, Meisungen
One way syringe	Braun, Meisungen
Parafilm	Pechiney, Mühltal
Pasteurpipettes	Brand, Wertheim
Plastic pipettes (5 ml, 10 ml and 25 ml)	Greiner, Solingen-Wald
5 cm and 10 cm Petri dishes	Sarstedt, Nümbrecht
Pipette tips	Sarstedt, Nümbrecht
Filter tips	Eppendorf, Hamburg
Sterile filter, 0.22 µm	Sarstedt, Nümbrecht
0.2 cm Transfection cuvette	Bio-Rad, München

2.1.3 Chemicals and biological reagents

Reagents	Manufacturer/Distributor
Acetic acid	Merck, Darmstadt
Acrylamid	Roth, Karlsruhe
Agar	Becton Dickinson, Heidelberg

Reagents	Manufacturer/Distributor
Agarose	Invitrogen, Karlsruhe
AlbumaxTM II	Invitrogen, Karlsruhe
Albumin bovine fraction V, BSA	Biomol, Hamburg
Ammoniumpersulfat, APS	Merck, Darmstadt
Ampicillin	Roche, Mannheim
BactoTM Yeast Extract	Becton Dickinson, Heidelberg
Blasticidin	Invitrogen, Karlsruhe
Bromphenolblue	Merck, Darmstadt
Calcium Chloride	Sigma, Steinheim
N-cyclohexyl-3-aminopropanesulfonic acid (CAPS)	Sigma, Steinheim
Concanavalin A G-250	Sigma, Steinheim
Coomassie Brilliant Blue	Merck, Darmstadt
Desoxyribonucleosidtriphosphates (dNTPs)	Roche, Mannheim
DAPI (4´, 6-Diamidino-2´-phenylindol)	Roche, Mannheim
di-Sodiumhydrogenphophate	Roth, Karsruhe
DPBS (Dilbecco´s Phosphate Buffered Saline)	PAN Biotech, Aidenbach
1,4-Dithiothreitol	Biomol, Hamburg
Developing solution G150	AGFA, Leverkusen
Ethanol	Merck, Darmstadt
E-64 Protease Inhibitor	Sigma-Aldrich, Hamburg
Ethidium Bromide	Sigma, Steinheim
EDTA (Ethylenediaminetetraacetic acid)	Biomol, Hamburg
Fixing solution G334	AGFA, Leverkusen

Reagents	Manufacturer/Distributor
Gentamycin	Rathiopharm, Ulm
Giemsas Azur-Eosin-Methylenblue solution	Merck, Darmstadt
Glucose	Merck, Darmstadt
Glycerin	Biomol, Hamburg
HEPES (4-(2-hydroxyethyl)-1-piperazineethanesulfonic acid)	Roche, Mannheim
Hypoxanthiine	Biomol, Hamburg
Isopropanol	Merck, Darmstadt
Percoll	GE Healthcare Lifescience, Freiburg
Potassium chloride	Merck, Darmstadt
Potassium dihydrogen phosphate	Roth, Karlsruhe
Mangan chloride	Merck, Darmstadt
Magnesium chloride	Merck, Darmstadt
Methanol	Sigma, Steinheim
Milkpowder	Roth, Karlsruhe
MOPS (3-(N-morpholino)propanesulfonic acid	Sigma, Steinheim
TEMED (N,N,N,N-Tetramethylendiamin)	Merck, Darmstadt
Sodium hydroxide	Merck, Darmstadt
Sodium choride	Gerbu, Gaiberg
Sodium-Didodecylsulfat (SDS)	Serva, Heidelberg
Sodium dihydrogen phosphate	Roth, Karsruhe

Reagents	Manufacturer/Distributor
Sodium hydroxide	Merck, Darmstadt
Peptone	Merck, Darmstadt
Rubidium chloride	Sigma, Steinheim
RPMI Medium	Applichem, Karlsruhe
RPMI Phenol red free	Applichem, Karlsruhe
Saponin	Serva, Heidelberg
Sorbitol	Sigma, Steinheim
Sucrose	Sigma, Steinheim
TE (Tris EDTA)	Invitrogen, Karlsruhe
Tris-Base	Merck, Darmstadt
Triton X-100	Biomol, Hamburg
Tryptophan	Merck, Darmstadt
WR 99210	Jacobus Pharmaceuticals, Washington/USA
Xylencyanol	Sigma, Steinheim

2.1.4 Kits and Standards

Kits and Standards	Manufacturer/Distributor
MACS®	Miltenyi Biotec GmbH, Bergisch Gladbach
NucleoSpin®Plasmid-Kit	Macherey-Nagel, Düren
NucleoSpin®ExtractII-Kit	Macherey-Nagel, Düren
Plasmid Midi Kit	QIAGEN
Western Blot Detection Kit	Pierce, Rockford/USA
1kb DNA GeneRuler™	MBI, Fermentas
Protein PageRuler™	MBI, Fermentas

2.1.5 Stock solutions, buffers and media for *P. falciparum* culture

RPMI-complete Medium	15.87g RPMI 1640, 1g Na_2Co_3, 2g Glucose, 5g Albumax^{TM} II, 0.0272g Hypoxanthine, 0.5ml Gentamycin (40mg/ml), pH 7.2, fill up to 1L with dH_2O, sterile filter
Synchronization solution	5% D-Sorbitol (w/v) in dH_2O
Cryo-Freezing solution	37,8g D-Sorbitol, 8,1g NaCl, 350 ml
Thawing-solution	Glycerol, add 1L dH_2O, sterile filter
Transfection Buffer	120mM KCl, 0.15mM CaCl2, 2mM EGTA, 5mM $MgCl_2$, 10mM K_2HP0_4, 10 mM KH_2PO_2, 25mM HEPES pH7.6, sterile filter
Saponin lysis buffer	0.03% Saponin in PBS
Blood	sterile, humane erythrocyte-concentrate blood group 0^+ (Blood bank, UKE; Hamburg)
Selection drug WR99210	Stock solution: 20mM WR in DMSO (dilute 1:1000 in fresh medium)
10x HT-PBS	5.7g Na_2HPO_4, 1.25g NaH_2PO_4, 15.2g $NaCl_2$ fill up to 1L with dH_2O, pH 7.4
10% Giemsa stain	10 ml Giemsa Azur-Eosin-Methylenblue solution, 90 ml dH_2O
90% percoll solution (stock)	45ml percoll, 5 ml 10xPBS
80% percoll solution	0.8g sorbitol, 8.9 ml stock (90%)+ 1,1ml RPMI complete medium
60% percoll solution	0.8g sorbitol, 6.7 ml stock (90%)+ 3,3ml RPMI complete medium
40% percoll solution	0.8g sorbitol, 4.4 ml stock (90%)+ 5.6ml RPMI complete medium
Parasite lysis buffer	4% SDS, 0.5% Triton X-114, 0,5xPBS

2.1.6 Stock solutions, buffers and media for *E. coli* culture

Antibiotic	100mg/ml Ampicillin in 70% Ethanol
LB-Medium	1% Yeast extract, 0.5% Peptone, 1% $NaCl_2$ in dH_2O; autoclave
LB-Agar	LB-Medium, 1.5% Agar
LB-AMP selection media/ Agar	LB-Medium or LB-Agar, autoclave, cool down to 50°C add Ampicillin to a final concentration of 100 mg/ml
Glycerol stabilate	50% (v/v) Glycerol in LB-medium

2.1.7 Buffers for competent *E. coli* cells

Solution I: TFBI	30mM sodium acetate, 50mM $MnCl_2$, 100mM $NaCl_2$, 10 mM $CaCl_2$, 15% Glycerol
Solution II: TFBII	10mM MOPS, 75 mM $CaCl_2$, 10mM $NaCl_2$, 15% Glycerol

2.1.8 Buffers and solutions for molecula biology work

Sodium acetate	3M, pH 5.2
Ethanol	100%
TE-Buffer	10mM Tris-HCl, pH 8.0, 1mM EDTA
DNA separation	
50x TAE Buffer	242g Tris-Base, 57.1ml glacial acetic acid, 100ml 0.5M EDTA, fill up to 1L with dH_2O
6x DNA-loading dye	30% glycerine 10 mM Tris-HCl pH 7.4, 10mM EDTA pH8, one spatula tip of Bromphenolblue, fill up to 10 ml with dH_2O

2.1.9 Buffers and solutions for biochemical work

Protein separation using SDS-PAGR	
Electrophoresis buffer	0.1% SDS, 192 mM Glycine, 25mM Tris
Ammoniumpersulfate (APS)	10% (w/v) in dH_2O
Stacking gel buffer	1M Tris-HCL, pH 6.8
Running gel buffer	1.5M Tris-HCL, pH 8.8
Stacking gel (for two gels, 5%)	0.75ml stacking gel buffer, 4.35ml dH_2O, 750µl Acryl amide (40%), 6µl TEMED, 60µl SDS (10%), 60µl APS (10%)
Running gel (for two gels, 12%)	2.5ml running gel buffer, 4.2ml dH_2O, 3ml Acryl amide (40%, 4µl TEMED, 100µl SDS (10%), 100µl APS (10%)
6xSDS loading buffer	375mM Tris-HCl pH 6.8, 12% (w/v) SDS, 60% (v/v) Glycerin, 0.6M DTT, 0.06% (w/v) Bromphenolblue

2.1.10 Bacterial and *Plasmodium* strains

Bacterial strain	
E.coli XL-10 gold	Tetr Δ(mcrCBhsdSMRmrr) 173 endA1 supE44 thi-1 recA1 gyeA96 relA1 lac Hte [F´proAB laclqZ ΔM15 Tn10 (Tetr) Amy Camr]
Plasmodium strain	
3D7	Cloned line derives from NF54 strain (isolated from an airport malaria case)

2.1.11 Enzymes for DNA amplification and ligation

T4 DNA Ligase [3U/µl]	NEB, Ipswich/USA
Phusion™ High Fidelity DNA Polymerase	NEB, Ipswich/USA

FirePol® DNA-Polymerase [5U/µl]	Solis Biodyne, Taipei/Taiwan
Taq Polymerase	NEB, Ipswich/USA

2.1.12 Restriction enzymes

KpnI (GGTACC)	NEB, Ipswich/USA
AvrII (CCTAGG)	NEB, Ipswich/USA
XhoI (CTCGAG)	NEB, Ipswich/USA

Futher restriction enzymes

2.1.13 Primary antibodies

Antigen	Organism	Ditution	Usage
Ama1			IFA
Etramp 2	Rabbit	1:250	IFA
Etramp 4	Rabbit	1:300	IFA
Etramp 5	Rabbit	1:300	IFA
Etramp 10.1	Rabbit	1:300	IFA
GFP	Monoclonal Mouse /Rabbit	1:500	IFA

2.1.14 Secondary antibodies

Antigen	Conjugate	Ditution	Usage	Source
Mouse	ALEXA-488	1:2500	IFA	Invitrogen, Karlsruhe
Rabbit	ALEXA-488	1:2500	IFA	Invitrogen, Karlsruhe
Rabbit	ALEXA-594	1:2500	IFA	Invitrogen, Karlsruhe
Mouse	ALEXA-594	1:2500	IFA	Invitrogen, Karlsruhe

2.2 Cell biological and molecular procedures for *P.falciparum*

2.2.1 *P.falciparum* culture

P.falciparum (strain 3D7) parasites were cultivated according the standard procedures (Trager and Jensen, 1979). Parasites were kept in 5 10 ml Petri dishes (Sarstedt) in 0+ donor blood at 5 % hematocrit and were incubated at 37°C in a 5% CO_2, 1% O_2 and 94% N_2 gas mixture. Cultured parasites were fed daily and adjusted to the desired parasitaemia.

2.2.2 Giemsa smears

A drop of parasites culture was given on a glass slide and smeared to obtain a cell monolayer. Infected RBC were air-dried and fixed in methanol for 20 seconds. The blood smear was subsequently stained in a 10% Giemsa solution for 10 to 20 minutes. Slides were viewed using a Zeiss standard 20 light microscope.

2.2.3 Parasites synchronization

A culture, containing mostly ring stage parasites, was spun down for 3 minutes at 1800g and resuspended in five pellet volumes of 5% D-Sorbitol (Sigma). This suspension was incubated at 37°C for 5 to 10 minutes. The so synchronized parasites were centrifuged for 3 minutes at 1800g. After removing the supernatant, the pellet was washed one time with malaria culture medium, centrifuged for 3 minutes at 1800g and subsequently suspended in malaria culture medium. If obvious cell lyses was visible, blood was added to obtain 5% hematocrit.

2.2.4 Parasite freezing

To obtain a stabilate suitable for long term storage in liquid nitrogen, a ring stage rich parasite culture was centrifuged, the supernatand removed and and the pellet was resuspended in 1 ml of freezing solution. The solution was transferred to a cryotube and stored at -80°C until transfer into liquid nitrogen.

2.2.5 Thawing of parasites

The cryotube containing frozen parasites culture was thawed, in a water bath, at 37°C until completely thawed. After centrifugation of the thawed culture, the supernatant was removed and the pellet was resuspended in 1 ml pre-warmed thawing solution. After centrifugation the supernatant was removed and the pellet was resuspended in pre-warmed malaria culture medium and the suspension was put in a 5 or 10 ml Petri dish and blood was added to obtain a 5% hematocrit.

2.2.6 Transfection of *P. falciparum*

100µg plasmid DNA was precipitated in 1/10 volume 3M sodium acetate pH 5.2 and 3 volumes of 100 % ethanol. Precipitated DNA was centrifuged for 30 minutes at 16.000 g. The supernatant was removed and the pellet was washed in 1 ml 80% ethanol (in H_20). After centrifugation, the supernatant was again removed and the pellet was air-dried und sterile conditions. The dry DNA pellet was dissolved in 15µl sterile TE buffer. The dissolved DNA was then mixed with 385µl cytomix (see section 2.1.5). The solution was mixed with the pellet of 10 ml *P. falciparum* culture, containing 5-10% ring stage parasites. Electroporation was conducted in a 2 mm cuvette (Biorad) at 310V and 950µF. After transfection, the iRBC were immediately resuspended in malaria culture medium. After five hours 3nM the medium was changed and 3nM of the antifolate drug WR99210 was added to the culture. Medium change was conducted daily until day 10 post-transfection. After this time period the medium was changed every other day. Transfected parasites were visible in Giemsa staining 17-30 days after transfection.

2.2.7 Saponin lysis

Saponin was used to selectively lyse the erythrocyte membrane and the parasitophorous vacuolar membrane (PVM) and contemporary keep the parasites plasma membrane intact. For the saponin lysis, 10 ml culture of iRBC was centrifuged and the supernatant was removed. The pellet was mixed with 5-10 pellet volumes of 0.03% saponin (sigma) dissolved in 1xPBS and incubated for 10 minutes on ice. The lysed iRBC were washed three times using 1ml 1xPBS or until

the supernatant was clear. The pellet was resuspended in 100µl lysis buffer (see section 2.1.5).

2.2.8 Magnetic Activated Cell Sorting (MACS)

In order to separate later parasite stages from early stages at least two 10 ml culture plates with at least 5 % parasitaemia of highly synchronized culture were harvested and than magnetically separated using the MACS kit according to the manufactuters´ manual.

2.2.9 Percoll gradient

To separate iRBC from uninfected and to separate the different parasites stages from one another a Percoll gradient centrifugation was made. Therefore a 10ml culture was centrifuged, the supernatant was removed and the pellet was washed with 1xPBS one time. In a 2ml Eppendorf tube the percoll gradient was prepared. After washing, the pellet was resuspended in 100µl 1xPBS and carefully layered over the gradient. After 5 minutes of centrifugation at 16,000g the desired parasites phases were transferred to a fresh tube and extensively washed with 1ml 1xPBS.

2.2.10 E-64 Protease inhibitor treatment

In Order to prevent Schizonts from rupture, and therefore obtain an enriched schizont culture, a well-characterized protease inhibitor, E64 (Sigma Aldrich), was used. The E-64 was prepared according to the manufactures´ protocol to obtain a 1 mM stock solution. The supernatant of a 10 ml cell culture plate was discarded and 10 ml of fresh and preheated RPMI medium were added, containing the protease inhibitor in a finale concentration of 10 µM.

2.3 Microscopy

2.3.1 Live cell imaging

Live cell imaging was carried out using a Zeiss Axioscope M1 microscope (Zeiss) equipped with a 100x/1.4 oil immersion lens. Pictures were taken with a

Hamamatsu Orca camera (Hamamatsu) and Zeiss Axioscope software (Zeiss). Images were processed in photoshop CS5.5 (Adobe). iRBC were taken from the culture and incubated with DAPI (1mg/ml) for 20 minutes at 37°C. A drop was put on a glass slide and covered with a cover slip and immediately imaged.

2.3.2 IFA with acetone fixed parasites

500 µl of infected red blood cells were centrifuged for 30 sec at 1800 g and the supernatant was discarded. The pellet was resuspended in 500 µl 1x PBS and one drop was put per well on a 10 well glass slide. The slide was air dried for 2 hours. The cells were than fixed in acetone; 30 minutes at RT. The residual acetone should than evaporate for 20 minutes at RT. Afterwards the cells on the wells were re-hydrated by adding a drop of 1x PBS. The wells were washed twice with 1x PBS before adding the regarding antibodies diluted in 3%BSA/PBS solution. Primary antibodies were incubated at RT for one hour in a humid chamber.

After removal of the antibodies the wells were washed five times with 1xPBS. The secondary antibodies and DAPI (1 µg/ml) staining were diluted in 3% BSA/PBS solution and incubated for one hour in humid chamber at RT.

2.3.3 Bodipy-TR-C5-ceramide staining

Bodipy-TR-C5-ceramide staining was prepared according to the manufactures´ protocol to obtain a 5 µM stock solution in 1xPBS. The stock solution was prepared under sterile condtions and filter sterilized PBS was used for the dilution.

For live cell imaging: 500 µl iRBC were removed from culture and washed once with 1xPBS. A tiny residue of the PBS was left over to resuspend the pellet in it. Then 100 µl of 5 µM Bodipy-TR-C5-ceramide were added and incubated for 15 min at 37° C, followed by a washing step with 1x PBS. The cells were than prepared as described for live cell imaging.

For 3d reconstruction: The parasites culture was prepared as described for confocal microscopy but with an additional 10 minutes incubation step for the Bodipy-TR-C5-ceramide staining.

2.3.4 Confocal microscopy and 4d imaging

For time lapse microscopy the parasites cultures were arrested on the bottom of a sterile, uncoated, hydrophobic, 35mm µ-dish (Ibidi), using culture grade 0.5 mg/ml concanavalin A (Sigma). Concanavalin A added to the surface of the glass bottom dish (described in Spielmann *et al*. 2003) for 10 minutes at 37°C. Washed three times with sterile dPBS (Sigma-Aldrich) and the culture, washed and resuspended in dPBS was added and allowed to settle for 5 minutes at RT. Unbound cells were washed off using dPBS for at least three times. Pre-warmed and pre-aborbed (1:10 dilution of donor blood in RPMI medium; incubated overnight at 4°C, centrifuged until blood is removed) medium was added to the dish and than the dish was closed and sealed with parafilm. Cells were viewed at 37°C using an Olympus FluoView FV1000 confocal microscope equipped with an Olympus Cellcubator. Using the multi area time lapse function of the FV Software and a motorized stage, multiple cells (10-15) were observed in each experiment. Focus was maintained using the Olympus ZDC autofocus system. A 60/x1.4 immersions oil lens and the Fluoview software FV10-ASW version 4.0.1 were used. Cells were viewed using either the 488nm (GFP and DIC) and/or the 594 nm (mCherry, Bodipy-TR-C5-ceramide and DIC) laser lines. For long term imaging usually following settings were used: 4 µs dwell time, 512x512 dpi (resolution), 15-30 z-stacks (0.2-04 µm step size), zoom level 3.5-5 and laser levels 0.1-5% for the 488nm and 1-15% for the 594nm. For 3d reconstruction following dissenting settings were used: 8-10 µs dwell time and zoom levels between 10 and 12. All experiments were analyzed with the Imaris software version 7.0.1 to 8.0.2. For further processing the ImageJ software was used (http://rsb.info.nih.gov/ij). Single images were processed with Photoshop CS5.5 (Adobe).

2.4 Bacterial cultures

2.4.1 Transformation of *E. coli*

100 µl of competent *E. coli* cells were thawed slowly on ice. The plasmid DNA was added and incubated on ice for 30 minutes. Transformation of the *E. coli* cells was achieved by heat shock, at 42°C for 45 sec, and than back on ice immediately and

incubation for 2 minutes. To let the *E. coli* cells grow initially, 900 µl LB-Medium was added and the suspension was incubated for one hour, shaking at 37°C and subsequently plated on a agar plate containing Ampicillin. The plate was incubated over night at 37°C and bacterial colonies screened for positive clones as described in section 2.5.5.

2.4.2 Freezing of *E. coli*

Bacteria from a single colony were transferred to a 100 x 16 mm bacterial incubation tube (Sarstedt) containing 5 ml of LB-Ampicillin medium, using a pipette tip. The bacterial culture was shaken overnight at 200 rpm and 37°C. The next day 1 ml of the bacterial culture was centrifuges for 30 seconds at 6000 rpm, the supernatant was discarded and the pellet was resuspended in 500 µl LB-Medium (without any antibiotics) and 500µl glycerol (merck) was added and the suspension was mixed and immediately frozen at -80°C.

2.5 Molecular biological methods

2.5.1 Amplification of DNA sequences

In order to amplify specific DNA sequences, a Polymerase-chain reaction (PCR) was conducted, genomic *P. falciparum* 3d7 or plasmid DNA served as templates. A list of used primers can be found in the section 2.6. The required sequence information were taken from the *Plasmodium* genomic resource (www.plasmodb.org) and/or the National Center for Biotechnology Information (http://www.ncbi.nlm.nih.gov). A proofreading Taq Polymerase was used in order to avoid the occurrence of mutations during the PCR. The PCR set up has been as follows: 94°C for 2 minutes as Taq Polymerase activation; 20 seconds 94°C denaturation, to split the double stranded DNA in single strands; 45 seconds at 50 °C annealing (primer binding to the DNA sequences); 20 seconds at 72°C elongation, the Polymerase produces the newly formed DNA strand. The elongation time was adjusted to the length of the amplified sequence, regarding manufactures´ manual. These steps were repeated for at least 35 times.

PCR steps	**Temperature**	**Time**
Taq activation	94°C	2 minutes
Step1 Denaturation	94°C	20 seconds
Step 2 Annealing	50°C	45 seconds
Step3 Elongation	72°C	20 seconds
Repeat step 1 to step 3; 35 times		
Final elongation	72°C	2 minutes
Store at	4°C	∞

2.5.2 Isolation of bacterial plasmids (mini- and midi-preps)

For plasmid mini-preparations a single bacteria colony was transferred to a bacteria culture tube (Sarstedt), containg 5 ml of LB-Ampicillin medium. The bacteria/medium suspension was shaken over night at 37°C and 200 rpm. Next day 2 ml bacteria culture were centrifuged 30 seconds at 11000 rpm and the supernatant was discarded. The preparation of plasmid DNA was carried out according to manufactures´ protocol. For the preparation of higher amounts of bacterial DNA, to 100 ml LB-Ampicillin medium a single bacteria colony was added and incubated overnight at 37°C at 200 rpm. DNA isolation was carried out according to the manufactures´ protocol

2.6 Primers and plasmids

Vektor:	Source:
pARL1-GFP	Struck *et al*. 2005
pARL2mCHerry	Grüring *et al*, 2012
pARL2-mito-2A- FKBPmCherry	P. Mesen-Ramirez, unpublished

Primers for sequencing

GFP(272)_rev ccttcgggcatggcactc
mCherry_rev gcgcatgaactccttgatgatggc

2.7 Protein analysis

2.7.1 SDS PAGE

Proteins were separated using sodium dodecyl sulphate-polyacrylamide gel (SDS PAGE). SDS gels were prepared with 12% acrylamide and the protein samples

were loaded in 1xSDS buffer. For protein separation a BioRad Mini Protean® tetra cell system was used, running for one hour at 200 Volts.

2.7.2 Western blot analysis

Separated proteins were transferred to a nitrocellulose membrane. Before proteins could be transferred, the membrane was soaked in 5 mM CAPS buffer and laid on three layers o blotting papers. The SDS gel was carefully layered upon the membrane and another three pre-soaked blotting papers were put on top. In a BioRad Wet blotting system transfer of the proteins to the membrane three took place. Blotting was carried of at 15 V overnight at 4°C. Afterwards the membrane was transferred to 50 ml Falcon reaction tube and blocking solution was added. The blocking was carried out at RT for one hour on a Stuart SRT6 Lab roller. After blocking the primary antibody was added, diluted in blocking solution. Incubation lasted for at least one hour at RT. The membrane was than washed 5 times with 1xPBS before the secondary antibody was added. After at least one hour the membrane was washed again and the Enhanced Chemiluminscence (ECL) solution was added. The ECL solution was freshly prepared (1:1 of both reagent solution were mixed) and incubated with the membrane for 5 minutes at RT on the lab roller mixer. The membrane was than laid between two transparent overhead transparencies and a medical X-ray film blue sensitive was exposed to the membrane as long as needed to obtain appropriate signal intensity.

Chapter 3: Results

3.1 Analysis of the putative translational repression of ETRAMP2 in *P. falciparum* blood stage schizonts

The translational repression of ETRAMP2 might play a crucial role in the early blood stage development of *P. falciparum* erythrocytic stages (see chapter 1, section 1.4.1). In previous studies, the mRNA of *etramp2* was found in schizont stages, but no protein was detectable. Shortly after reinvasion of the released merozoites, the ETRAMP2 was detectable in early ring stage parasites (Spielmann *et al*., 2003). This suggested that this mRNA was stored and only expressed for a crucial function during invasion and/or early developmental in the RBC. In order to examine this potential regulation a reporter construct under the *etramp*2 5´ untranslated region (UTR) was generated. The 3´UTR of the *etramp*2 gene had previously been ruled out as a mediator for the translational repression (Heiber & Spielmann, unpublished). Therefore a unrelated standard 3´UTR was chosen, the terminator region of the *P. berghei dyhydrogenase folate reductase thymidylate synthase* gene (*Pbdt*) (Fig. 3.1.1, A). The reporter consisted of green fluorescent protein (GFP) fused to the signal peptide (SP) of the Exported Protein-1 (EXP-1). The rational of using this SP-EXP1-GFP reporter was that a signal peptide per default transports GFP to the PV which will by lysed after each cycle of replication of the parasite and hence no accumulation of the reporter will obscure the expression timing of the protein. This reporter construct with the configuration 5´UTR-*etramp2-exp-1sp-gfp-PbDT*-3´-UTR is herein after named SP-EXP-1-GFP^{etramp2}.

3.1.1 Visualization of GFP expressed in the parasitophorous vacuole under the control of the etramp2 promoter of *P. falciparum* blood stages

The SP-EXP-1-GFP^{etramp2} expressing parasites were firstly analyzed by fluorescence microscopy. Representative parasites are shown in fig. 3.1.1. The

marker protein was found in the periphery of ring stage parasites, co- localized with the membrane marker Bodipy-TR-C5-Ceramide (fig. 3.1.1). In trophozoite stage parasites the SP-EXP-1-GFP^{etramp2} was not detectable (fig. 3.1.1). These findings were corresponded to the early onset of expression under the control of the *etramp2* promoter. The presence of the GFP marker protein in the parasite periphery, co-localized with the membrane staining, indicated a typical PV localization.

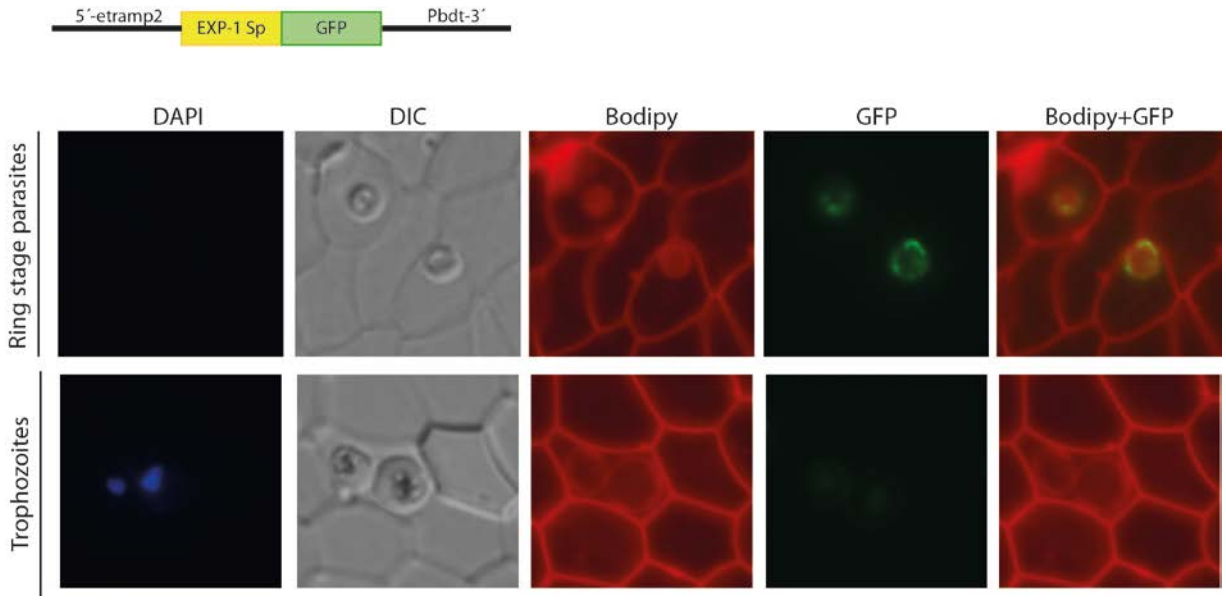

Fig. 3.1.1 live cell images of SP-EXP-1-GFP^{etramp2} expressing parasites. A schematic drawing of the SP-EXP-1-GFP^{etramp2} construct is shown above the image panels. Live cell fluorescence microscopy images of ring stages (upper row) and trophozoite stage parasites (bottom row) are shown. DAPI: nuclear staining; DIC: Differential interference contrast (DIC); GFP: GFP fluorescence; Bodipy: membrane staining with Bodipy-TR-ceramide; size bar: 5 µM.

Next, the SP-EXP-1-GFP^{etramp2} expressing parasites were analyzed in individual cells over time using 3D time- lapse to obtain information about the expression dynamics under the *etramp2* promoter. In fig. 3.1.2 an extracted time sequence of a representative time-lapse experiment is shown. The time sequence started with a schizont stage parasites, showing no expression of the SP-EXP-1-GFP^{etramp2} (fig. 3.1.2, -120 to -90 min). Unexpectedly, 60 minutes before rupture, the SP-

EXP-1-GFP^{etramp2} was observable inside the parasite (fig. 3.1.2; -60 min). Shortly before schizonts rupture, expression of the GFP reporter increased further (Fig. 3.1.2; -30 min). Thereafter, the infected RBC ruptured and the merozoites were released (fig. 3.1.2; 0). Two of the merozoites reinvaded into new RBCs (fig. 3.1.2; 30 min; red asterisks). These early ring stage parasites already expressed the SP-EXP-1-GFP^{etramp2} reporter (fig. 3.1.2; 30 min). These observations indicated that under the control of the *etramp2* promoter, the reporter is already expressed shortly before rupture, in late schizont stages.

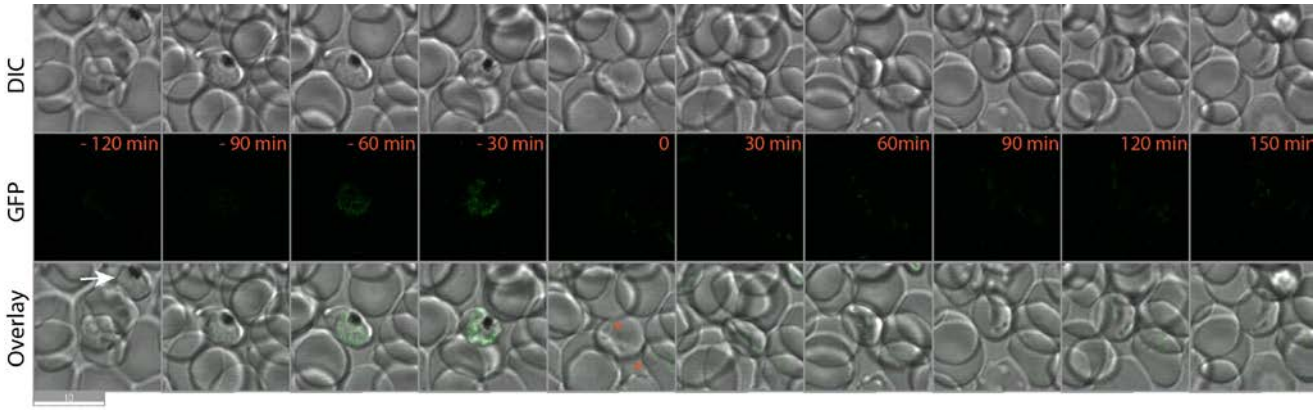

Fig. 3.1.2 Time- lapse microscopy of SP-EXP-1-GFP^{etramp2} parasites. Stacks were taken in 30 minutes intervals; single sliced images shown in the upper row: the DIC Channel; middle row: the GFP Channel; bottom row: the overlaid signals of the DIC and the GFP channels. The time points before schizont rupture and post reinvasion (red numbers); reinvasion of new RBCs (red asterisk); size bar: 10 µM.

3.1.2 Systematic analysis of SP-EXP1-GFP^{etramp2} expression pattern in late stage parasites

According to the findings of the previous section, an early onset of the expression of the SP-EXP-1-GFP^{etramp2}, shortly before schizont rupture, was strongly suggested (section 3.1.1). In order to test the consistency of these finding in different cells, more time- lapse experiments focused on the late developmental stages were conducted. To ensure that only results from properly developing cells were included, only schizonts that released vital merozoites (as judged by reinvasion into new RBCs), were scored. The reinvasion of RBCs was used as time point zero.

In four independent time- lapse experiments (including multiple imaging areas and cells) conducted to assess the timing of expression of the SP-EXP-1-GFP^{etramp2} reporter, a total number of 20 schizonts met the requirements and were scored. All of these 20 schizonts showed the early onset of SP-EXP-1-GFP^{etramp2} expression (fig. 3.1.3, complete data shown in Appendix fig. A1; A-B).

Of the 20 cells, 15 showed detectable expression 90 min before rupture and 5 showed detectable expression from 60 min before schizont rupture (summarized in fig. 3.1.3, Appendix figure A1). For all analyzed schizonts, the intensity of the GFP signal increased over time (summarized in fig. 3.1.3, Appendix figure A1). These data indicated that the proteins expressed from an episomal plasmid under the *etramp2* promoter are not translationally expressed in late schizonts.

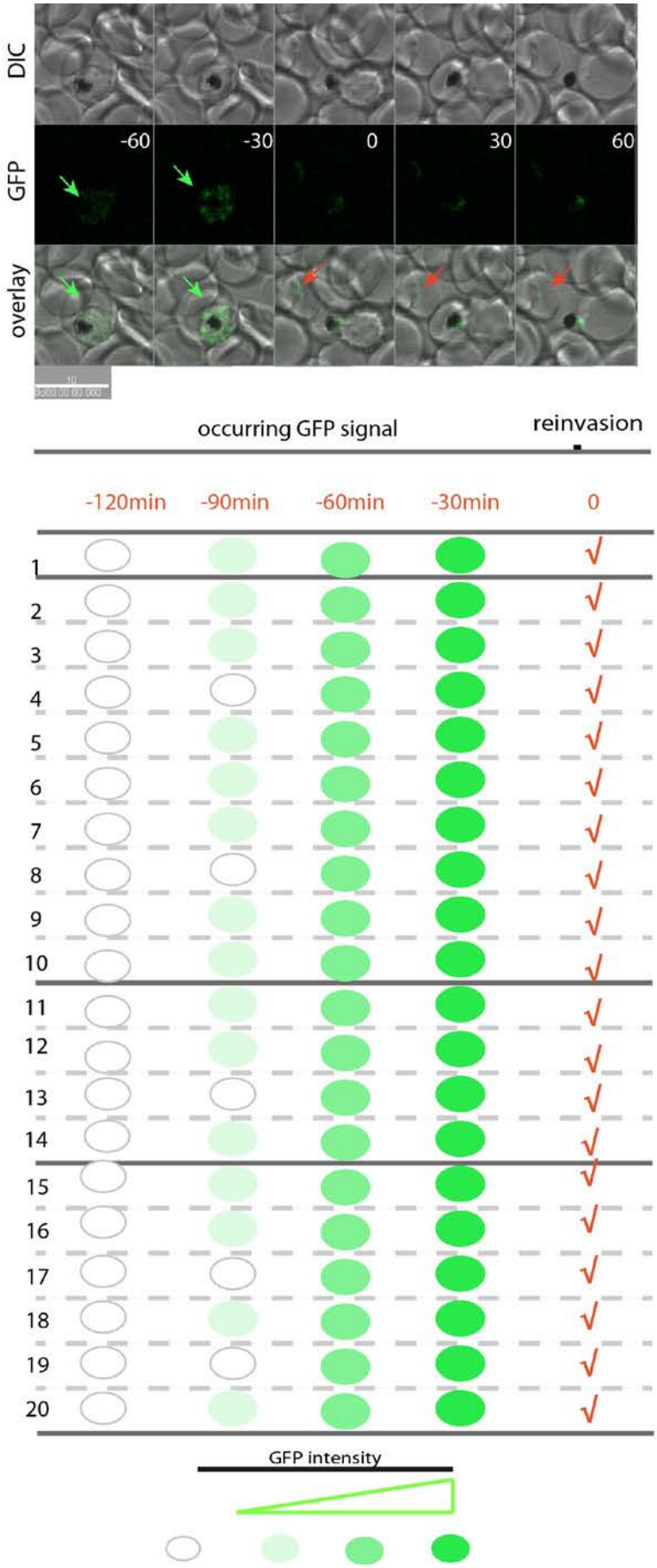
DIC
GFP
overlay
-60
-30
0
30
60
occurring GFP signal
reinvasion
-120min
-90min
-60min
-30min
0
1
2
3
4
5
6
7
8
9
10
11
12
13
14
15
16
17
18
19
20
√
GFP intensity

Fig. 3.1.3 Time-lapse microscopy experiments of SP-EXP-1-GFP*etramp2* schizont stages. Four time-lapse experiments (indicated by bolt lines, in summary table) focused on schizonts were carried out. A short sequence of single sliced images of an example cell is shown atop of the summarizing table: stacks were taken in 30 minute intervals (white numbers); DIC channel (upper row); GFP signal (middle row); overlay: merged DIC and GFP signals. GFP marker protein expression shortly before schizonts rupture is indicated by green arrows; reinvaded parasite indicated by red arrows; size bar: 10µM. The table below summarized all counted schizonts; the time points of onset and the intensity of the GFP marker signal before rupture (different green shaded elipses; white elipse: no GFP signal detectable); reinvasion was used as time point zero (red hooks).

3.1.3 Endogenous ETRAMP2 is detectable shortly before schizonts rupture

The expression of SP-EXP1-GFP*etramp2* already in late schizonts may be an artifact due to the episomal nature of the encoding plasmid or the fact that usually multiple copies of plasmid are present per cell. This could lead to an overrepresentation of the regarding mRNA, which could dilute out repressing factors, this might lead to expression or poor repression of the mRNA. In order to rule this option out, immunofluorescence analyses (IFA) were carried out, using an antibody against endogenous ETRAMP2 (α-Etr2). Firstly, the IFAs were carried out with late schizonts from a synchronized parasite culture expressing SP-EXP1-GFP*etramp2*. Antibodies against GFP (fig 3.1.4; α-GFP) were used in addition to the α-Etr2 antibodies (fig. 3.1.4; α-Etr2). Clear signals for both, ETRAMP2 and GFP, were observable in late schizonts (α-Etr2 and α-GFP in Fig. 3.1.4, A). Both signals were found in close proximity to each other, surrounding the newly formed daughter nuclei, but not or only partially co-localizing. These data confirmed the live cell imaging. Next, IFA was carried out, using the α-Etr2 antibody with wild type 3D7 *P. falciparum* parasites (Fig. 3.1.4, B). The signal for the endogenous ETRAMP2 (shown in green) was evident for both observed stages, the late schizonts and the early ring stages (Fig. 3.1.4, B). In schizonts the GFP signal was detectable al over the parasites, whith some foci in its periphery and in rings stage parasites the signal was detectable all over the parasites as well, this might be due to the high intensity of the detected GFP /(Fig. 3.1.4; B). The intensity of the ETRAMP2 signal

in schizont stages was lower than the ETRAMP2 signal intensity in the ring stage parasite (fig. 3.1.4; B).

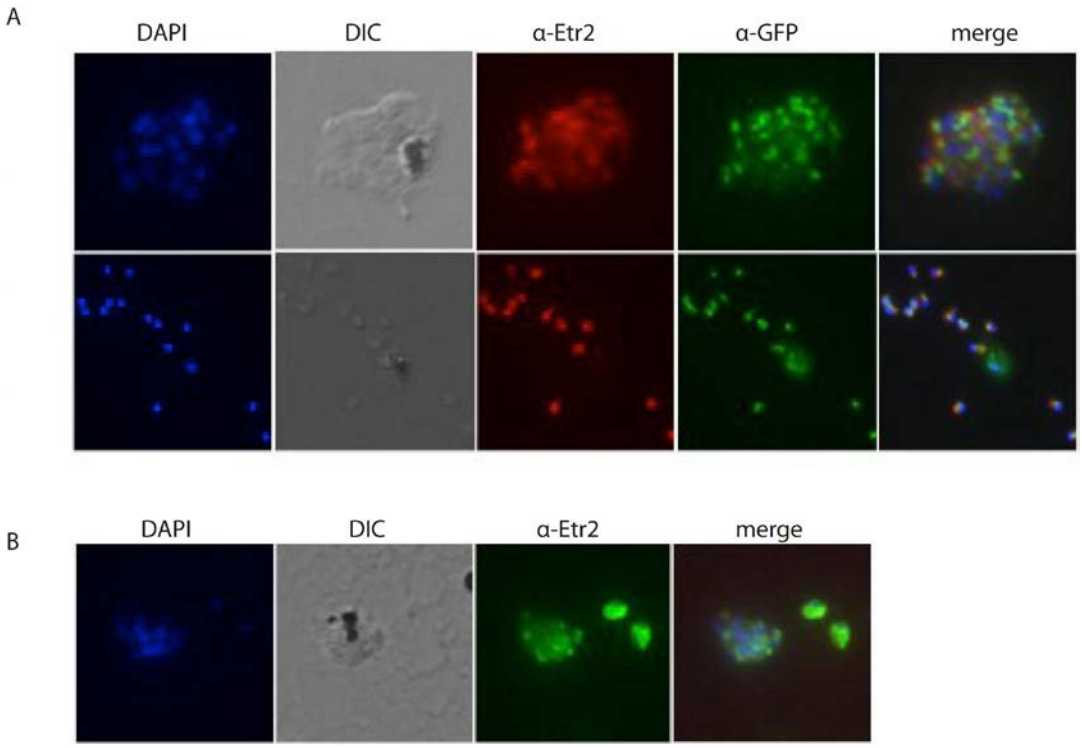

Fig 3.1.4 Immunofluorescence analyses (IFAs) for the detection of endogenous ETRAMP2 in SP-EXP-1-GFP^{etramp2} and wild type parasites. (A) Acetone fixed IFA of two SP-EXP-1-GFP^{etramp2} expressing schizonts; (B) acetone fixed IFAs of wild type 3d7 parasites; the image shows a schizont stage parasite next to two ring stage parasites. DAPI: nuclear staining; DIC: Differential interference contrast; α-Etr2: anti ETRAMP2 antibody; GFP: α-GFP: anti-GFP antibody; merge: overlaid signals of DAPI; α-Etr2 and α-GFP (A) of DAPI and α-Etr2 (B).

From these findings it can be concluded that ETRAMP2 is not translational repressed, at least not in very late schizonts. However, expression in very late blood stage schizonts will lead to the presence of the reporter during invasion of newly formed merozoites and in the early ring stage development, suggesting a potentially crucial function of ETRAMP2 in one or both if these processes.

3.2 Biogenesis of the parasitophorous vacuole

To study the biogenesis of the parasitophorous vacuole (PV) several cell lines expressing different marker proteins were generated. The different kind of reporter cell lines should express the marker proteins at different time points of the parasites development at the parasites PV to allow the visualization of this compartment and its biogenesis.

There are two general types of markers: the first consists of artificial reporters containing a targeting sequence to bring the marker to the correct location (section 3.2.1). The second are proteins resident in the compartment of study. The latter may also show protein specific sub- compartment localizations (section 3.2.2). To obtain appropriately timed expression, different promoters driving the expression of the reporters were used.

3.2.1 Visualization of the PV with artificial reporters

3.2.1.1 Visualization of the PV of ring stages

There was no translational repression of *etramp2* verifiable and the artificial reporter SP-EXP1-GFP^{etramp2} protein was expressed shortly before schizonts rupture and in the parasitophorous vacuole of ring stage parasites immediately after reinvasion (see section 3.1.1). However, this represented a promoter system to obtain reporter expression in freshly invaded ring stages, which so far was not available in malaria research. This system was used to visualize the PV biogenesis from early ring stage on using the SP-EXP1-GFP reporter trafficked to this compartment.

Time- lapse microscopy was used to image the SP-EXP1-GFP^{etramp2} cell line over the entire asexual life cycle in RBCs. A representative experiment is shown in fig. 3.2.1. In the trophozoite and schizont stages of the SP-EXP1-GFP^{etramp2} -expressing parasites, no GFP signal was visible (Fig. 3.2.1; -14.5 - 1.5 hours before rupture). In the DIC channel proper parasites growth was confirmed (fig. 3.2.1). In late schizonts, 1 hour and 30 minutes before rupture, a clear and strong

GFP signal was observable, confirming the observation of the onset of expression driven by the *etramp2* 5´UTR shortly before schizont rupture (section 3.1). Already 30 minutes post rupture two newly invaded ring stage parasites, expressing the SP-EXP1-GFP^{etramp2}, were detected. These young parasites developed for two more hours before this experiment was stopped. This phase of development was covered in 15 experiments with similar results.

A further representative time lapse experiment showed the PV biogenesis in SP-EXP1-GFP^{etramp2} expressing parasites over the ring stage (fig. 3.2.2) which is not covered in the experiment shown in fig. 3.2.1. In this experiment, two ring stage parasites in a single host cell are shown until they reach the trophozoite stage (Fig. 3.2.2). During ring stage development, the parasites are known to change between a circular and an amebic shape (Grüring et al., 2011). The first time point in the shown experiments, the rings are in their circular shape and the SP-EXP1-GFP^{etramp2} signal detected around the parasites with some areas of even distribution and some gaps without fluorescence. In the second time point the GFP seemed to accumulate in more discrete foci. The 30 minutes later, one of the parasites still in its circular shape, and the other changed to the amebic form, which led to a drastic change of SP-EXP1-GFP^{etramp2} distribution in its PV (Fig. 3.2.2, 1.5 to 2h). The SP-EXP1-GFP^{etramp2} accumulated in the rounded ends of the amebic extensions and was barely visible in other areas around the parasite. At time point 4, both rings were amebic and this distinct pattern of accumulation of the reporter at the far end of the amoeboid arms was very clearly observable for both parasites. Back in a ring shaped form, the GFP was again spread evenly around the parasites (Fig. 3.2.2, 1.5 to 2.5 h).

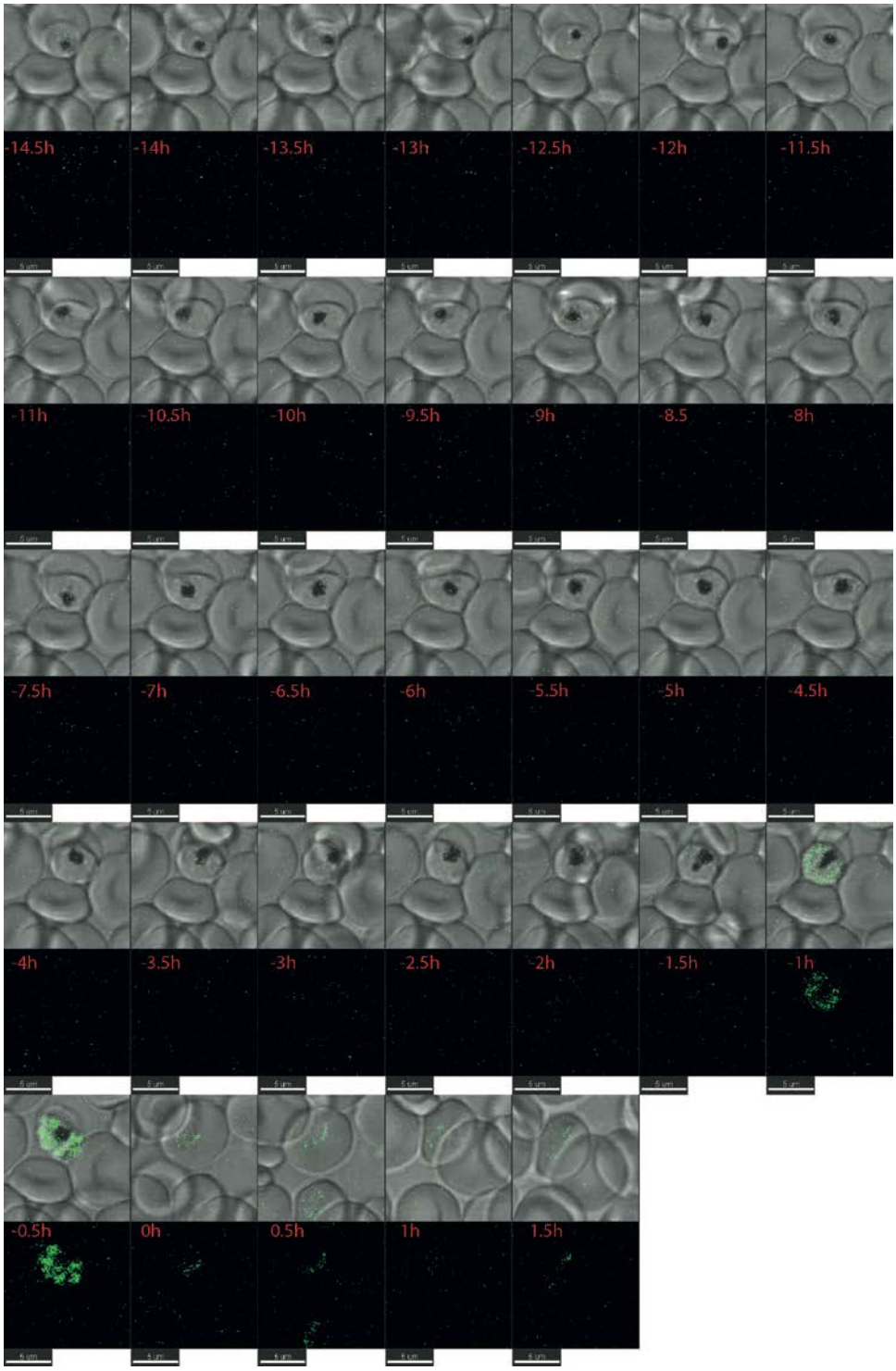

Fig. 3.2.1 Time- lapse microscopy of SP-EXP1-GFP*etramp2* parasites, covering trophozoite to re-invaded ring stages. Stacks were taken in 30 minutes intervals (red numbers). The upper row shows the overlay of the single sliced images of the DIC channel and the GFP signal; bottom row: single sliced images of the GFP signals. Scale bar: 5µM; One representative experiment of n= 15.

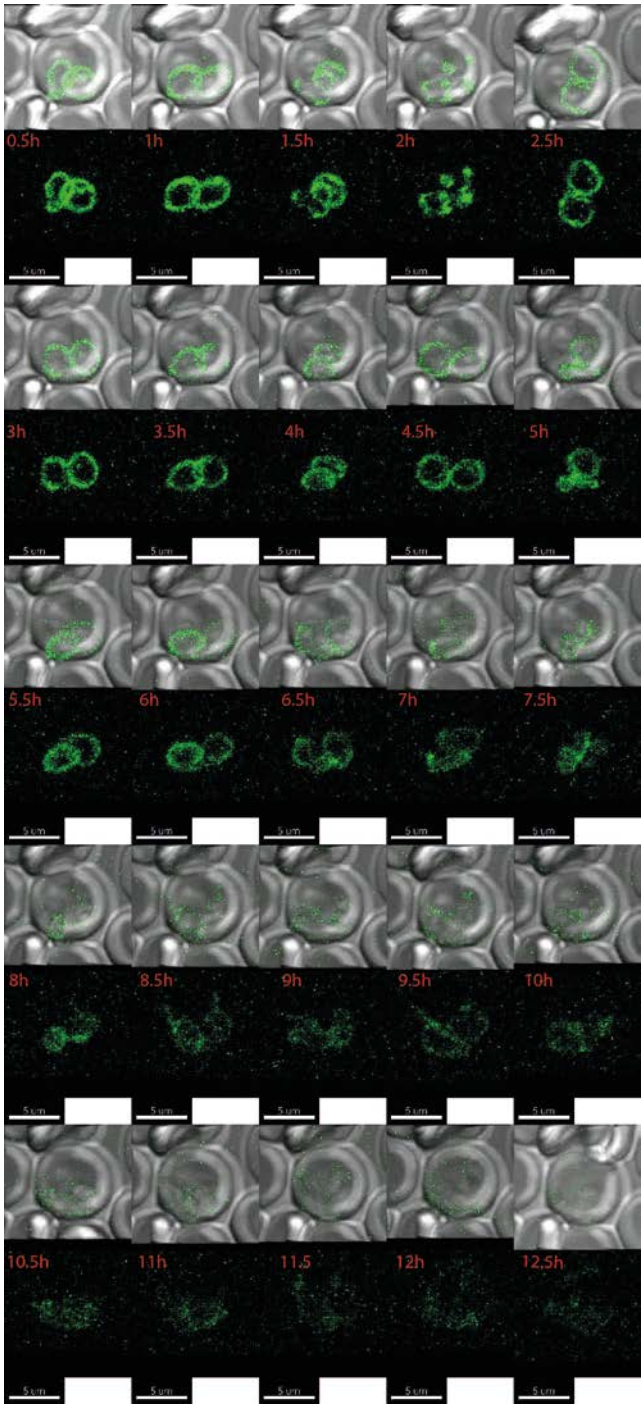

Fig. 3.2.2 Time-lapse microscopy of PV SP-EXP1-GFP*etramp2* parasites covering the ring stage. Images were taken in 30 minutes intervals, represented as red numbers (1 to 25). 3d reconstructions are shown. The upper row: overlay of the DIC channel and the GFP signal; Bottom row: signals of the GFP. Scale bar: 5 µM. One representative of n= 8 analyzed experiments.

The transition from ring stage to trophozoite stage had been described by Grüring *et al*. (Grüring *et al.,* 2011) and was characterized by an arrest of the parasites at a particular position in the RBC and a condensation of the parasite into a smaller circular form. Both features were confirmed by time-lapse microscopy of the SP-EXP1-GFP^{etramp2} –cell line. In the experiment shown in Fig 3.2.2 this is evident after 7.5 and 8 hours of observing the parasites (Fig. 3.2.2; 7.5h to 8h). Already from the next time point on, a noticeable growth of the parasites was observable. The early trophozoite development was accompanied by the gradual disappearance of the GFP signal and the appearance of small hemozoin foci in the parasite (fig. 3.2.2, 10.5h to 12.5h).

The remarkable accumulation of the SP-EXP1-GFP^{etramp2} at the far end of the extensions of amebic parasites was observed in all ring stage parasites observed during time-lapse experiments. A more detailed analysis using 4d microscopy experiment is shown in Fig. 3.2.3. The 3d reconstructed GFP signal over time revealed the previously described accumulation of the SP-EXP1-GFP^{etramp2} as “capping” structures at the end of the extensions of amoebic rings (fig. 3.2.3; B: time point 3, 9 and 10; white arrows). These cap-like structures were exclusively found in the extensions of amebic ring stage parasites, in all 35 analyzed time-lapse microscopy experiments. After the parasites changed their shape back to the circular form, the SP-EXP1-GFP^{etramp2} was evenly distributed in the PV again (fig. 3.2.3; time points 5, 10 and 13).

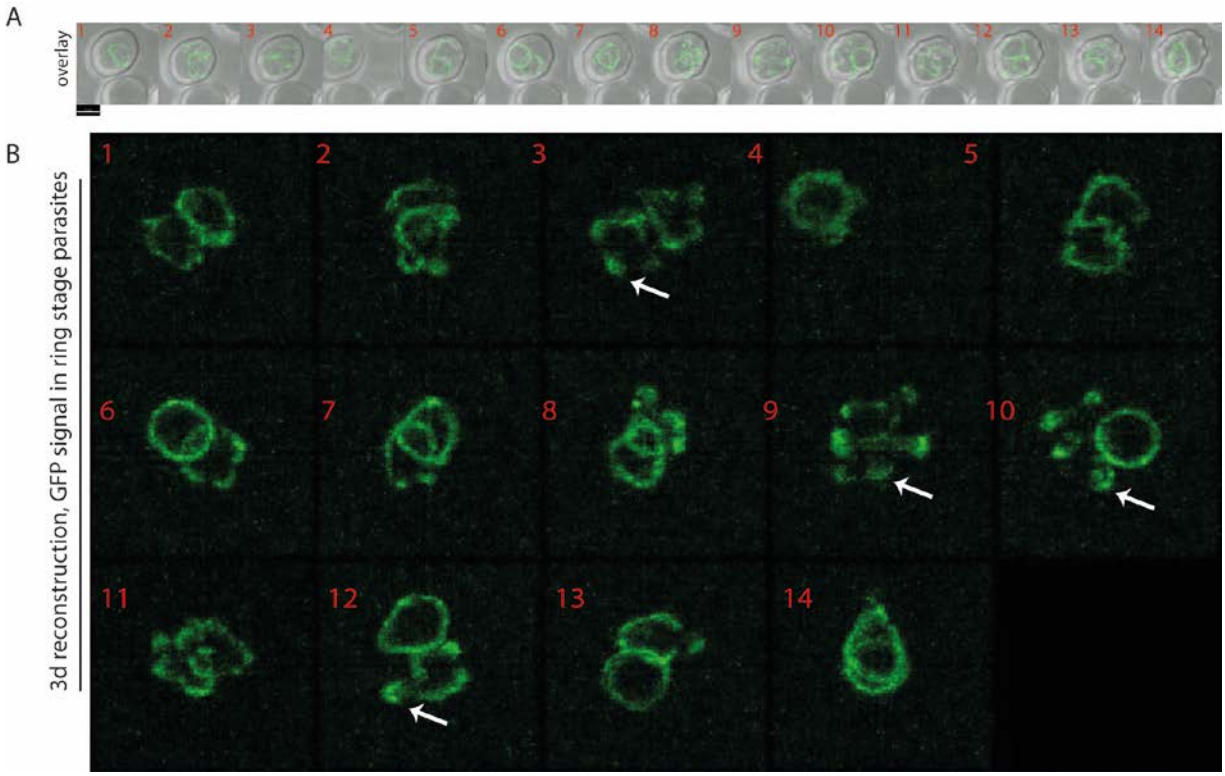

Fig. 3.2.3 4d microscopy revealed SP-EXP1-GFP^{etramp2} cap-like structures at the far end of amebic extensions. Time- lapse microscopy experiment of SP-EXP1-GFP^{etramp} ring stage parasites, stacked images had been taken in 30 minutes intervals. (A) The overlaid 3d reconstructions of the SP-EXP1-GFP^{etramp2} - and DIC signals. (B) The regarding GFP-channel 3d reconstructions. Time points 1 to 14 are shown (red numbers); white arrows show examples of caps; size bar: 3µM; n=35.

3.2.1.2 Visualization of the PV of trophozoite and schizont stages

For the examination of the PV biogenesis of trophozoites and schizonts a well-characterized artificial PV reporter, Rex2ΔTM-SP-GFP, was used (Haase *et al*., 2009; Grüring *et al.,* 2011). The expression of this reporter is driven by the *chloroquine resistance transporter* (crt) *gene* promoter, leading to expression from early trophozoite to the schizont stage (Grüring *et al*., 2011). The PV localization of Rex2ΔTM-Sp-GFP was confirmed by the use of fluorescent live cell microscopy (Fig. 3.2.3), showing a co-localization with Bodipy-TR-C5-ceramide as a membrane marker in infected RBCs.

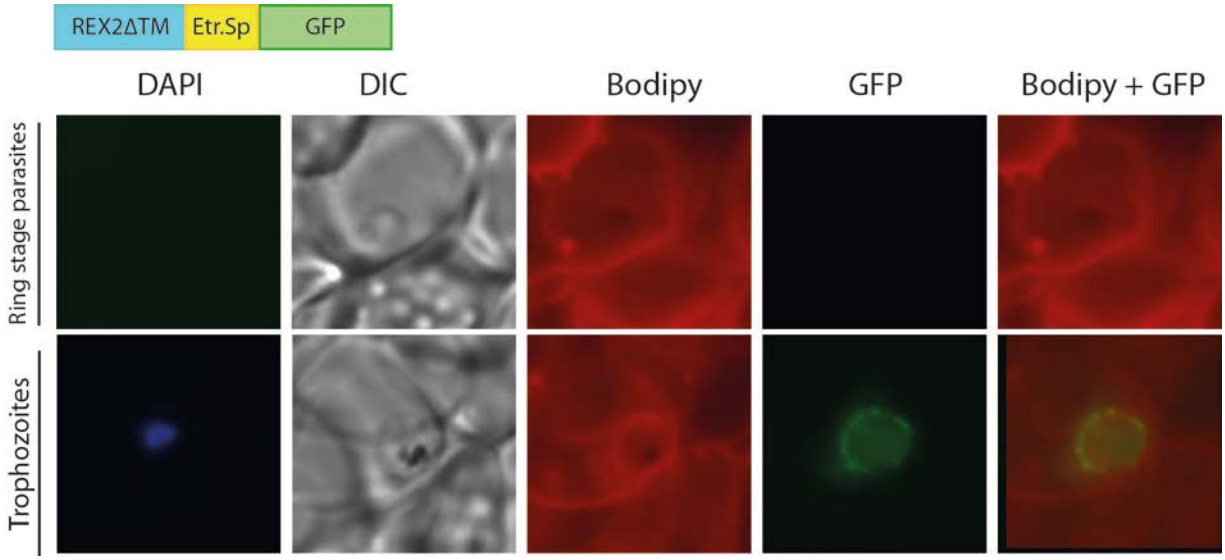

Fig. 3.2.4 Rex2ΔTM-SP-GFP localized at the PV of trophozoite and is absent in ring stages. Schematic depiction of the Rex2ΔTM-Sp-GFP (Haase *et al*., 2009; Grüring *et al*., 2011) construct is shown above the image panels. The images show live cell fluorescent microscopy of the Rex2ΔTM-Sp-GFP cell line stained with Bodipy-TR-C5-ceramide. DAPI: Nuclear staining; Bodipy-TR-C5-ceramide: membrane staining.

Next the cell line expressing Rex2ΔTM-SP-GFP was used in time- lapse microscopy experiments to visualize the PV in trophozoites and schizonts (Fig. 3.2.5). A representative experiment is shown in fig. 3.2.5. Imaging in this experiment started with a late trophozoite stage. The parasite's food vacuole, represented by the focus of hemozoin, resided in the parasites periphery and the GFP signal was evenly distributed around the parasite (Fig. 3.2.5; 14 hours before rupture). During the transition to the schizont stage, a rapid movement of the food vacuole to a more central position had previously been reported to occur 10-15 hours before rupture (Grüring *et al*., 2011). In the shown experiment this event took place between 12 and 13 hours before rupture (Fig. 3.2.5). Around this time, the previously smooth PV, now appeared rougher, with small foci in close proximity, forming a bead on a string pattern. This rough appearance was reminiscent of the surface of a strawberry and hence was termed the 'strawberry' phase. The strawberry phase was reproducible, regarding its appearance and its time of onset, in all 8 independent time-lapse microscopy experiments where sufficient resolution was present to detect this phase. The observed parasites entered the strawberry phase 15 to 11 hours before schizont ruptures and this

phase persisted for 4 to 6 hours. In fig. 3.2.5 the parasites reached the strawberry phase 12 hours before rupture and persisted for 4 hours (Fig. 3.2.5; 12 to 9 hours before rupture). Thereafter the Rex2ΔTM-SP-GFP signal took up a smooth appearance again (Fig. 3.2.5; 8 hours before rupture).

One hour later, the next remarkable change in the Rex2ΔTM- SP -GFP distribution in the parasites PV occurred: the circumferential GFP signal around the parasites looked interrupted. This phase of PV development was termed the 'gap-phase'. In the shown experiment, there are two visible gaps in the PV in close proximity of the parasites food vacuole (fig. 3.2.5; 8 hours before rupture, white arrows), which then combined to a larger gap (fig. 3.2.5; 7 hours before rupture). In the following time points a gap was visible at the opposite side to the previous location, indicating either a new gap or movement of the old gap (fig. 3.2.5; time point 7 to 10). These gaps occurred reproducibly in other experiments in a similar time frame, respective to host cell rupture in all eight cells observed over time of Rex2ΔTM-Sp-GFP cell line with sufficient quality to detect this phase. In these eight cells the gap phase started immediately after the strawberry phase and was observable 8 to 5 hours before rupture and lasted 3 to 5 hours. In the parasite shown in figure 3.2.5 the gap-phase, occurred 8 hours before rupture and persisted for 5 hours (Fig. 3.2.5; -8h to -4h).

The gap phase was followed by the phase where the new merozoites are formed, a phase that was previously described (Grüring *et al*., 2011). In the experiment shown in Fig. 3.2.5, this phase took place 3 to 1 hour before rupture. This was evident by the localization of Rex2ΔTM-Sp-GFP at invaginations reaching from the periphery into the schizont, until each of the newly formed nuclei was surrounded (fig. 3.2.5). Followed by the rupture of the host cell and the release of merozoites, of which two invaded new RBCs (fig. 3.2.5; 0 h).

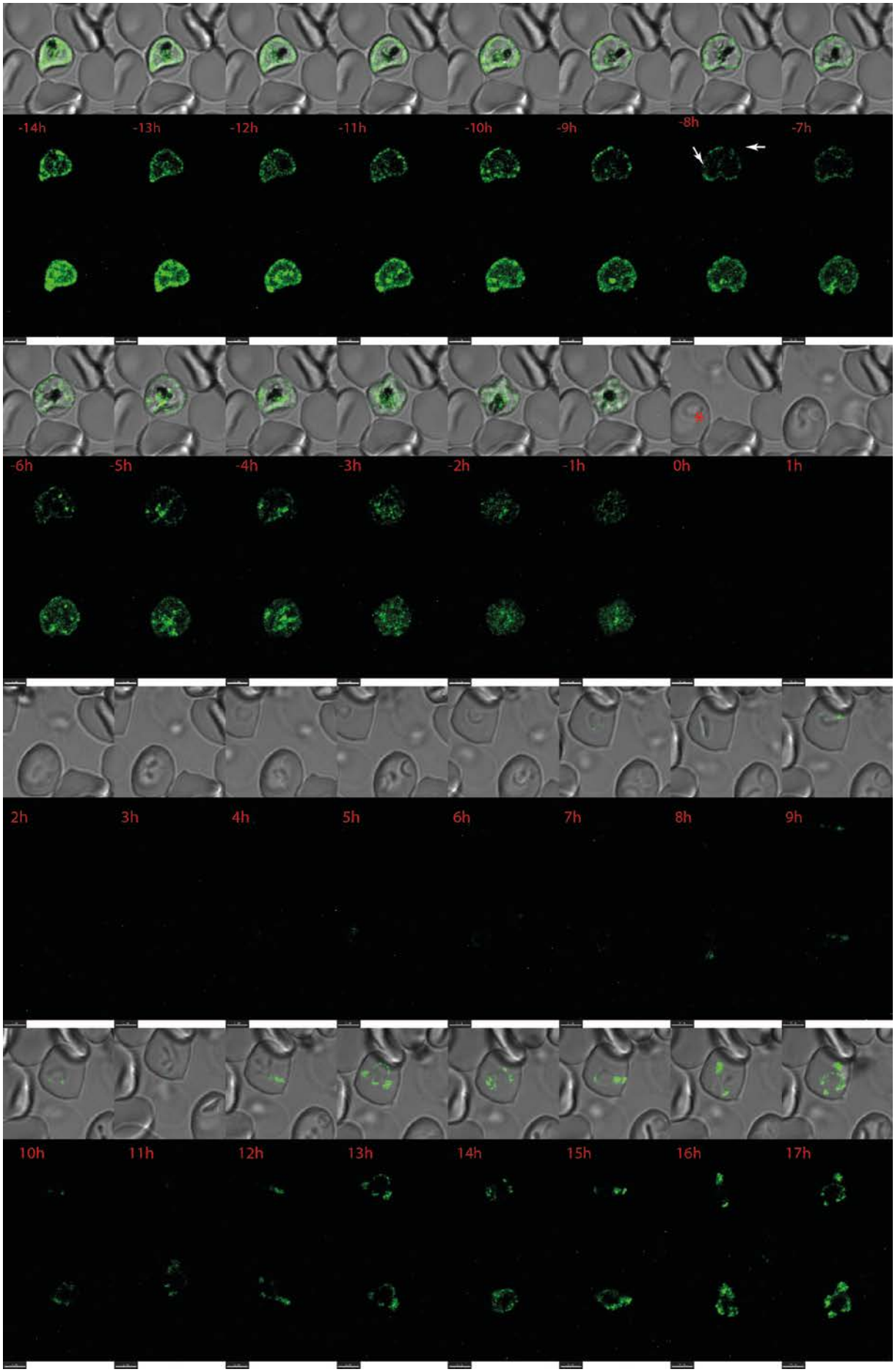
-14h
-13h
-12h
-11h
-10h
-9h
-8h
-7h
-6h
-5h
-4h
-3h
-2h
-1h
0h
1h
2h
3h
4h
5h
6h
7h
8h
9h
10h
11h
12h
13h
14h
15h
16h
17h

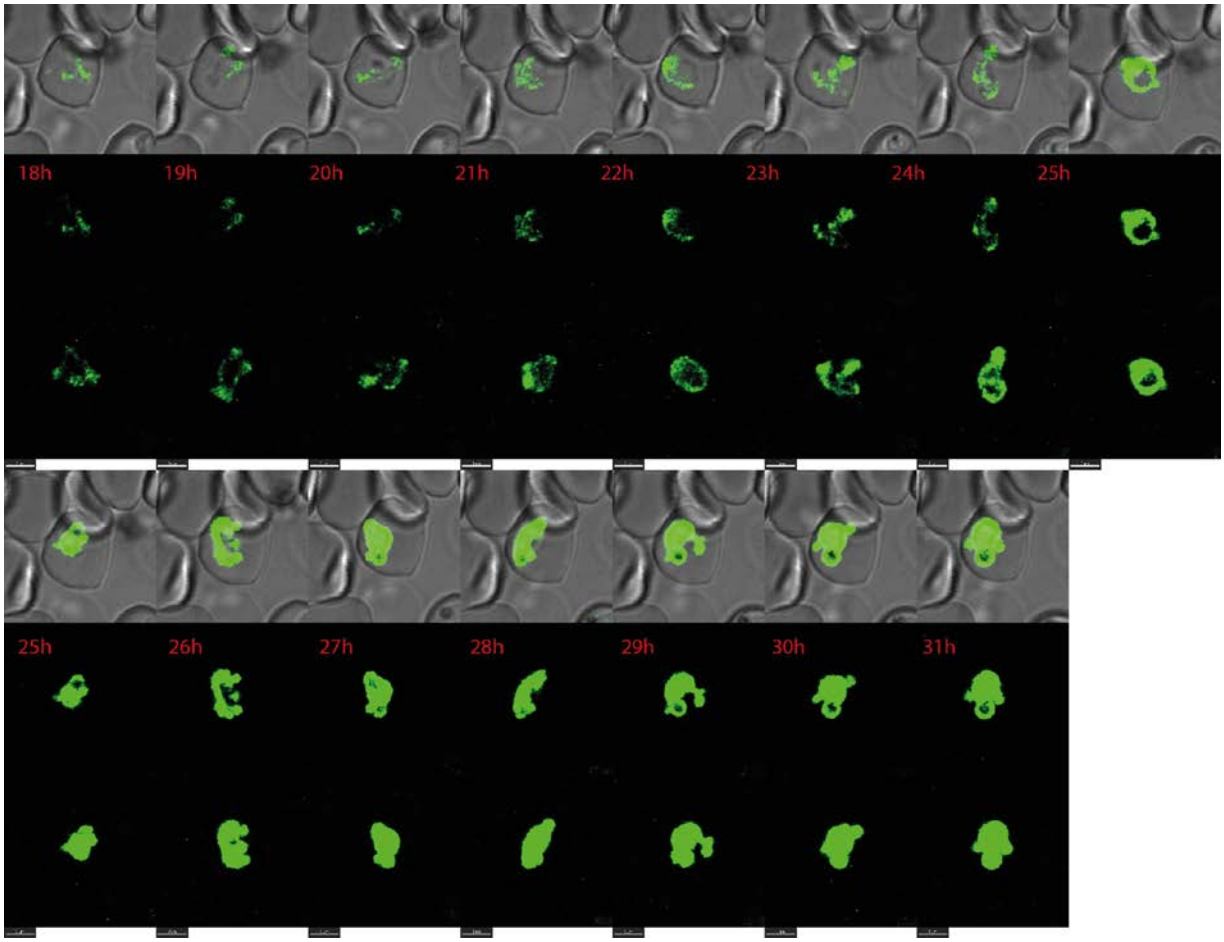

Fig. 3.2.5 Visualization of the PV developmental in Rex2ΔTM-Sp-GFP transgenic parasites. Time lapse microscopy, stacks were taken in 1 hour intervals. Shown are 47 hours of development; red numbers: hours before and post schizonts rupture; upper row: overlay of slices of the DIC and GFP channel; middle row: slices of the GFP channel; Bottom row: 3D reconstructions of image stacks; size bar: 3 µM; n= 8.

Reinvasion of new RBCs is a sign of proper parasite development and was made premise for the parasites being counted in the quantifications of the examined phases of schizont PV biogenesis.

After reinvasion, no Rex2ΔTM-Sp-GFP was observable in the PV of early ring stage parasites, consistent with a lack of expression of transgenes in early rings under the control of the *crt* promoter (Grüring *et al*., 2011). The signal of Rex2ΔTM-Sp-GFP gradually appeared from 6 hours post invasion (hpi) but remained comparably low until the parasite reached the transition to the trophozoite stage after which the intensity increased rapidly (fig. 3.2.5, 25 to 32

hpi). The strong fluorescence signal in these stages precluded a detailed analysis of these stages in this experiment, In order to analyze the PV biogenesis for theses stages, extractions of this data set are shown with decreased fluorescent intensity in fig. 3.2.6.

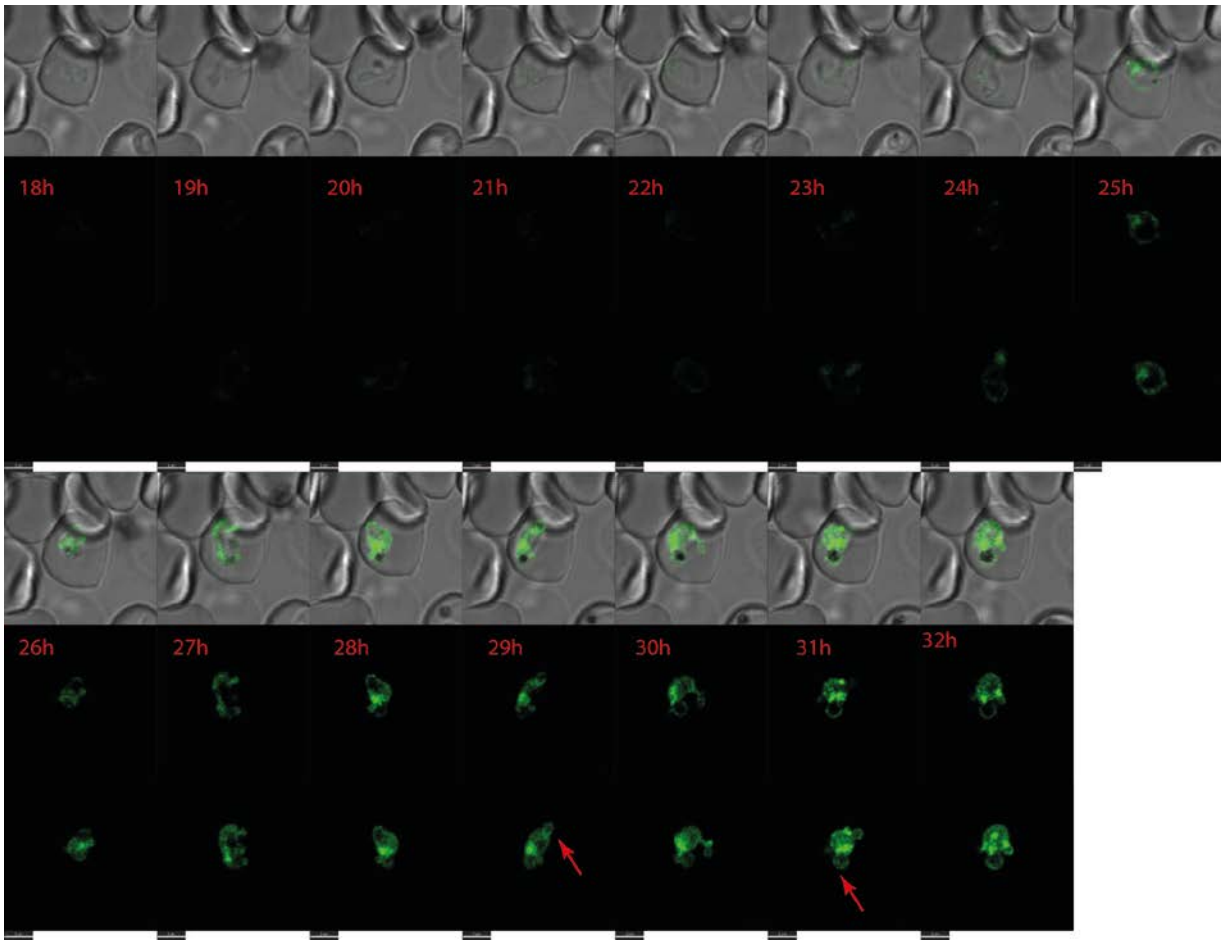

Fig. 3.2.6 Extraction of time-lapse experiments of the PV development in Rex2ΔTM-Sp-GFP parasites, covering ring to trophozoite stages. Extracted time series from time-lapse microscopy experiment (fig. 3.2.5), stacks had been taken in 1 hour intervals. Shown are 15 hours of development, starting at 18 hours post schizont rupture; red numbers: hours post schizonts rupture; upper row: overlay of slices of the DIC and GFP channel; middle row: slices of the GFP channel; Bottom row: 3D reconstructions of GFP image stacks; size bar: 3 µM; red arrows: indication of PV extensions; n= 8.

Decreasing the fluorescence intensity revealed that in young trophozoites, the Rex2ΔTM-Sp-GFP signal in the PV appeared smooth (fig. 3.2.6, 24 to 32h). In addition to the signal around the parasite extensions were observable that did not

match with the DIC indicating the periphery of the parasite cell (fig. 3.2.6, red arrows). There are known extensions of the PV, the TVN (Bahri & Haldar, 1994; Bannister *et al*., 2000) and the cavity (Grüring *et al*., 2011; Kruse, 2014; PhD thesis). Such extensions were frequently observed in this life cycle phase (6 of n=8 young trophozoites analyzed), however, without an additional marker protein whether a given extension contains parasite cytoplasm, these two structures cannot be distinguished. This was therefore further studies using a double transgenic parasite line (see section 3.2.1.2.1). In conclusion these data indicate that prior to the strawberry phase, the Rex2ΔTM-SP-GFP defined PV appears smooth with frequent extensions reaching into the host cell cytoplasm.

3.2.1.2.1 Improved visualization of PV development in double transgenic parasite expressing parasite internal mCherry

In order to track the PV biogenesis and at the same time distinguish between the parasites PV and its cytoplasm, a double fluorescent artificial reporter cell line was established. This cell line expressed two marker proteins: Exp-1Sp-GFP (PV) and the red fluorescent protein mCherry fused to FKBP (parasite cytosol). Both marker proteins are transcribed on the same mRNA molecule under the *crt* genes promoter region, but taking advantage of a viral 2A skip peptide, translation of this mRNA leads to two independent proteins (Fig. 3.2.7, A;. Skip peptides lead to termination of the amino acid chain but not to a stop of the translation process, therefore a second protein is translated from the same mRNA), Hence, Exp-1Sp-GFP^{crt} and FKBP-mCherry were expressed as individual proteins (Fig. 3.2.7, A). The FKBP had no function in this cell line but remained with mCherry due to the original purpose of the parental plasmid this construct was derived of (see Materials and Methods, section 2.7).

Fluorescence imaging confirmed the localization of Exp-1Sp-GFP^{crt} in the PV and the mCherry fusion protein was detectable in the parasites cytoplasm (fig. 3.2.7).

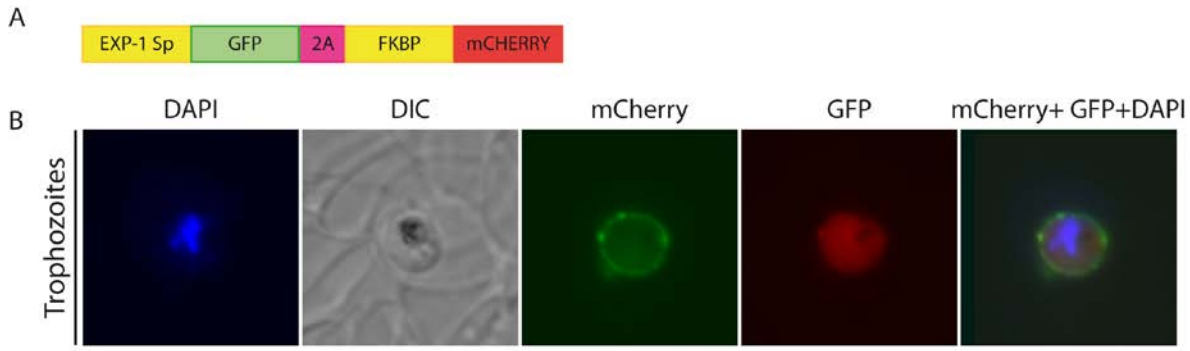

Fig. 3.2.7 Exp1-SP-GFP^{crt} localized at the PV and FKBP-mCherry in the cyctoplasm of trophozoite stage parasites. (A) Schematic depiction of the Exp1-SP-GFP-2A-FKBP-mCherry construct. (B) Live cell fluorescent microscopy images of the Exp1-SP-GFP^{crt} and FKBP-mCherry expressing parasites. DAPI: Nuclear staining; DIC: Differential interference contrast.

In order to examine the PV biogenesis of this double fluorescent artificial reporter cell line time-lapse microscopy experiments were carried out. A representative experiment is shown in fig 3.2.8. This experiment started 19 hours before rupture when the PV had a smooth appearance. Around 13 hours before rupture, the parasites reached the strawberry phase as evident by the characteristic rough appearance of the PV. The start of the strawberry phase around 14 hours before rupture and its duration of 5 hours was comparable to that observed previously with the Rex2ΔTM-Sp-GFP reporter cell line (Fig. 3.2.8, -14 h to -9 h). The strawberry phase was immediately followed by a, 5 hours lasting, gap phase, starting 9 hours before rupture (fig.3.2.8; -9 h to -4h). Thereafter, three hours before rupture, the Exp1-Sp-GFP^{crt} fluorescence was observable around the newly formed merozoites until rupture (fig. 3.2.8, -3 h to 0 h). The reinvaded rings did not show any marker protein expression during the 7 hours imaging post invasion (fig. 3.2.8; 0 to 6h).

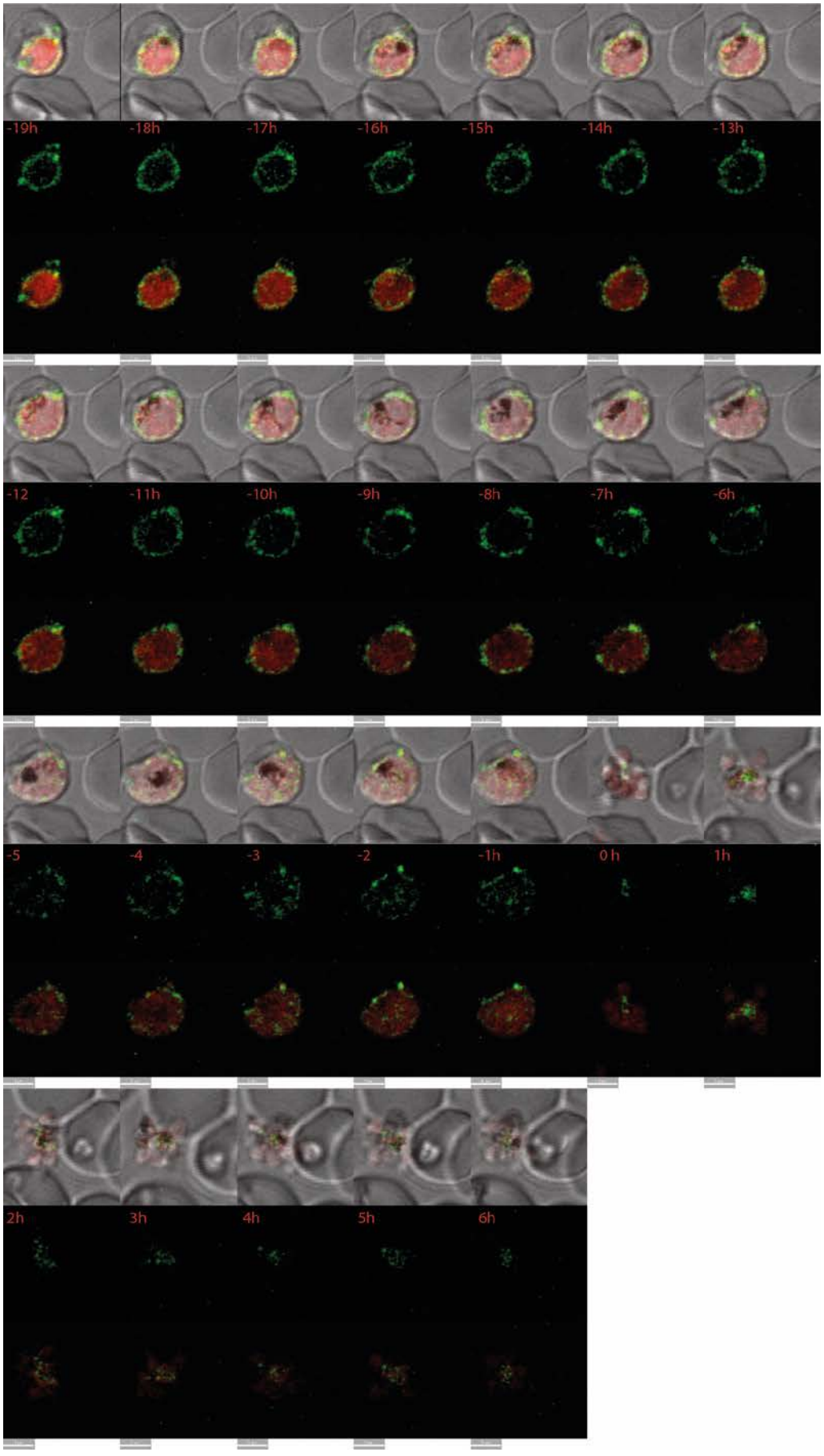
-19h
-18h
-17h
-16h
-15h
-14h
-13h
-12
-11h
-10h
-9h
-8h
-7h
-6h
-5
-4
-3
-2
-1h
0 h
1h
2h
3h
4h
5h
6h

Fig. 3.2.8 Visualization of the PV in relation to the parasites cyctoplasm. Time- lapse microscopy of Exp1-SP-GFP^{crt} and FKBP-mCherry expressing parasites, stacks were taken in 1 hour intervals. Upper row: single slice images of overlaid DIC, mCherry and GFP signals; row below: single sliced GFP signal; bottom row: single slice overlay of mCherry and GFP signals. Hours before and post schizonts rupture/reinvasion (red numbers); size bar: 3 µM; n= 5.

In order to analyze the PV biogenesis and to characterize the extensions of earlier developmental stages, an extract of a time-lapse experiment of the Exp1-SP-GFP-2A-FKBP-mCherry cell line, showing the development from exemplary parasite development from early trophozoite stage to its strawberry phase, is shown in fig. 3.2.9. In the single sliced images the two marker protein signals were better distinguishable than in the 3d reconstructions. The experiment started with a young trophozoite, showing two kind of extensions, one surrounded by the Exp1-SP-GFP^{crt}, containing no cytosolic FKBP-mCherry signal (Fig. 3.2.9; 1h; white arrow) and the second extensions appeared surrounded by the GFP fusion protein and contained the mCherry marker protein (fig. 3.2.9; 1h; red arrow). The parasites cavity is described as parasites extension, consisting of PPM and PVM and filled with host cell cytoplasm (Grüring *et al*,, 2011; Kruse, 2014; unpublished data), appearing in two different phenotypes: the invaginated and the protrusion form (Kruse, 2014; PhD thesis). And the tubovesicoular network (TVN) is known to be originated from the PVM as an rather immobile tubular extension and no parasites cytosol was found in the volume of it (Elmendorf & Haldar, 1994; Lauer *et al*., 1997; Grüring *et al.*,2011). It was previously hypothesized that the protrusion form of the cavity might contain parasites cytosol. Put previous analyses only showed barely detectable amounts of parasites cytosol, depending of on the diameter of the examined cavity (F. Kruse, 2014; PhD thesis). The second type of extension visible at the parasites periphery, lacking matching DIC signals, was not filled with parasites cytosol (fig. 3.2.9; white arrows). Both types of extensions, one filled with the cytosolic expressed mCherry, the other without, are moving at the parasites surface (fig. 3.2.9; 2h to 4h and 5h to 8h); concluding from this the observed extensions could be protrusion cavities. Even though it was not shown before, the extension filled with parasites cytosol might be a protrusion cavity as

well, due to its mobility but the characteristic notch appearance was not consistently observable.

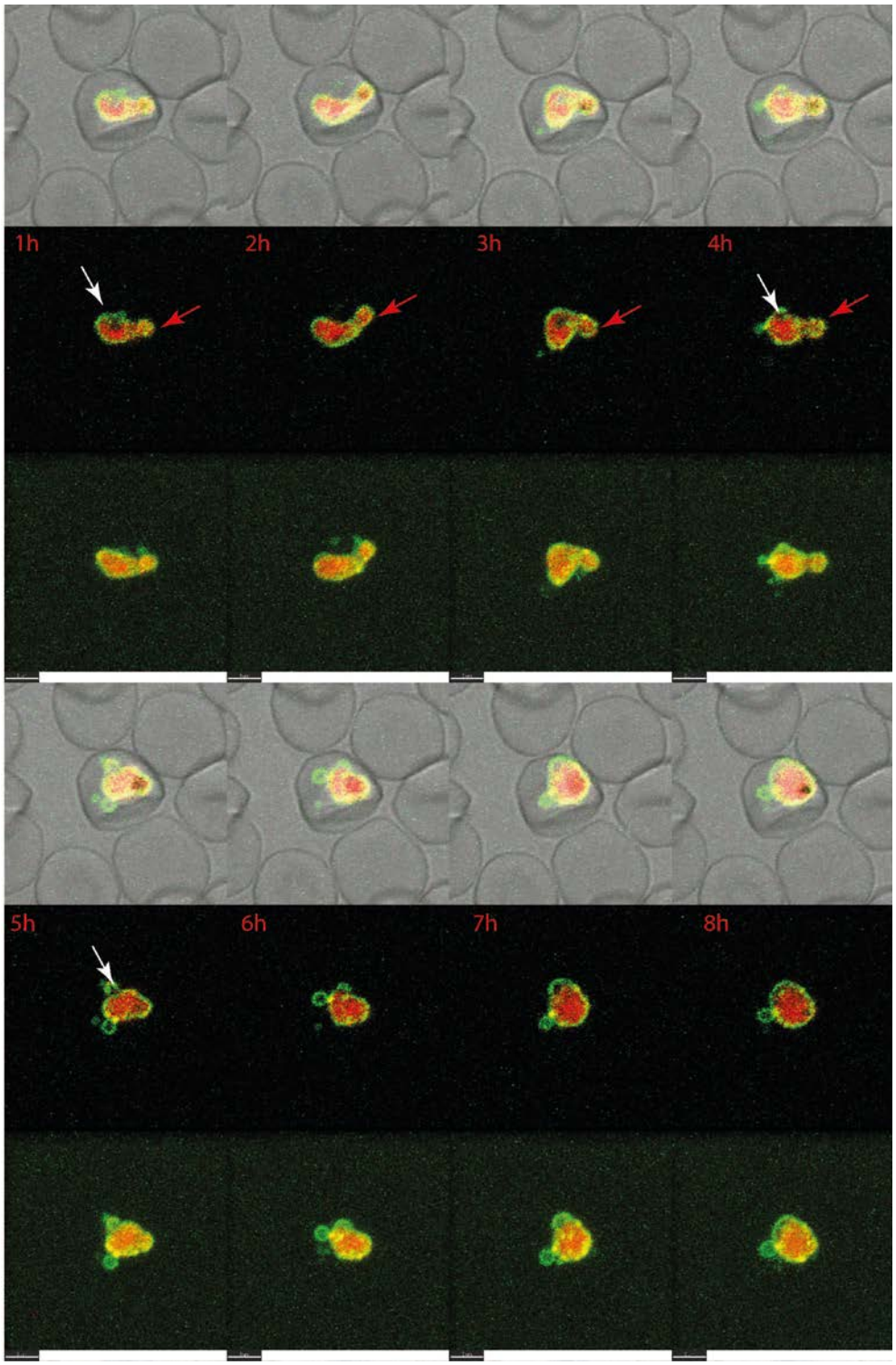

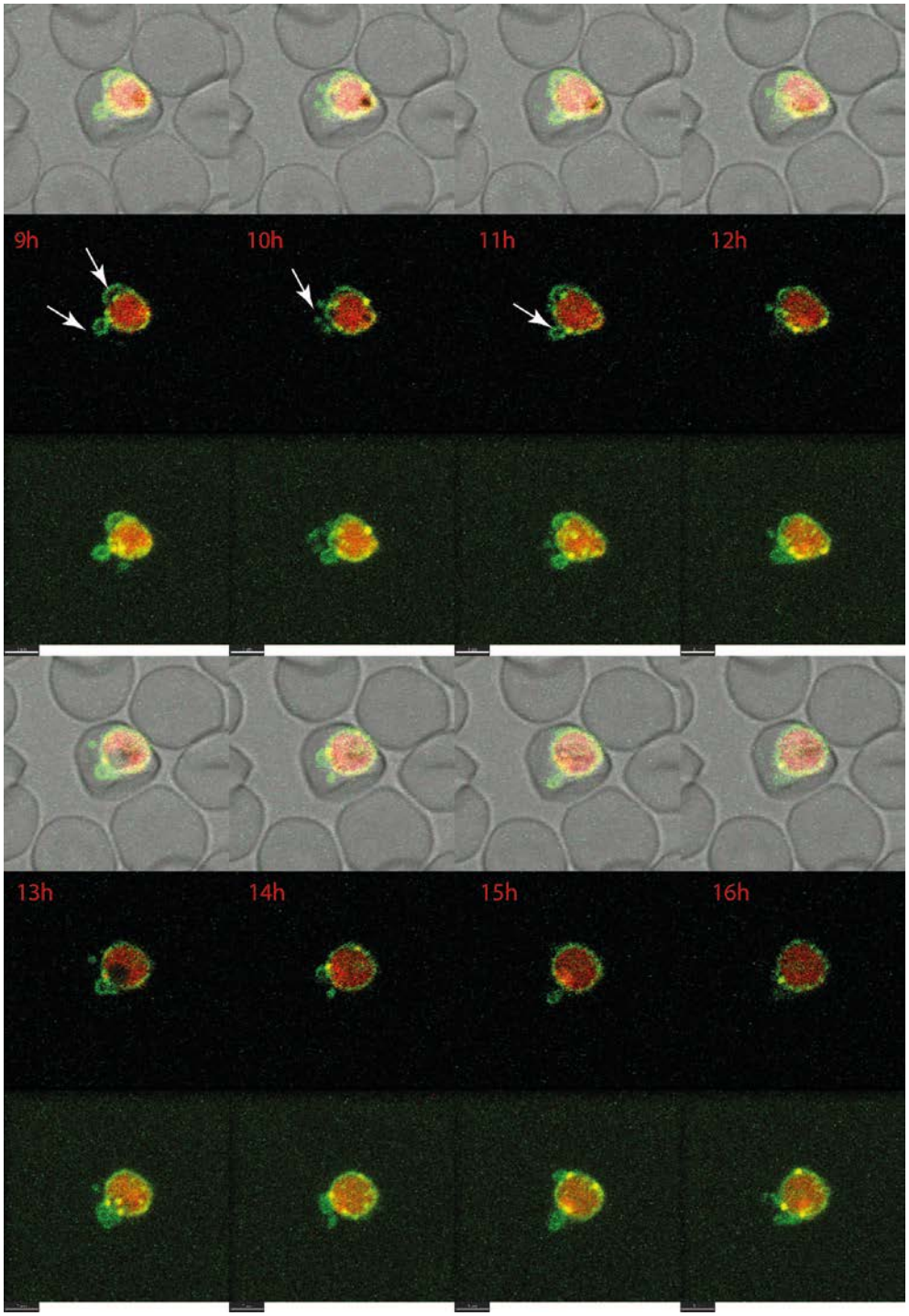

Fig. 3.2.9 Visualization of Exp1-SP-GFP^{crt} and FKBP-mCherry expressing parasites, from trophozoites to strawberry phase. Time- lapse experiment of Exp1-SP-GFP^{crt} and FKBP-mCherry parasites, stacks were taken in 1 hour intervals. Shown 16 hours of development (red numbers); Upper row: single slice images of overlaid DIC, mCherry and GFP signals; row below: single sliced images of GFP and mCherry signals; bottom row: 3d reconstruction of overlaid mCherry and GFP signals. size bar: 3 µM; n=4.

3.2.2 Visualization of the PV with resident marker proteins

The visualization and examination of artificial reporter constructs, by time- lapse microscopy, revealed some remarkable and reproducible phases of the PV, indicating the possibility to divide the asexual cycle into sub-phases. These phases could be used to more easily stage individual parasites and may indicate functional stages during schizogony. In order to further explore this possibility and assess whether the these phases are also evident in proteins naturally occurring in the PV, time- lapse microscopy was carried out with PV resident proteins fused to GFP.

3.2.2.1 PF14_0046-GFP (PF3D7_1404900)

The parasite protein PF14_0046 fused to GFP (PF14_0046-GFP) was shown to localize to the PV in previous studies (Heiber, *et al*., 2013). Expression of this construct was under the control of the *crt* promoter region and therefore expected from early trophozoite to the schizont stage (of blood stage parasites). Live cell imaging with the PF14_0046-GFP expressing parasites showed GFP fluorescence in the periphery of trophozoite stage parasites. In late schizonts, the fluorescence surrounded the newly formed merozoites. In both stages the marker protein co-localized with the membrane marker Bodipy-TR-ceramide (fig. 3.2.10), confirming the published PV localization (Heiber *et al*., 2013). In agreement with the expression profile typically observed with the *crt* promoter, no PF14_0046-GFP was found in ring stage parasites (fig. 3.2.10).

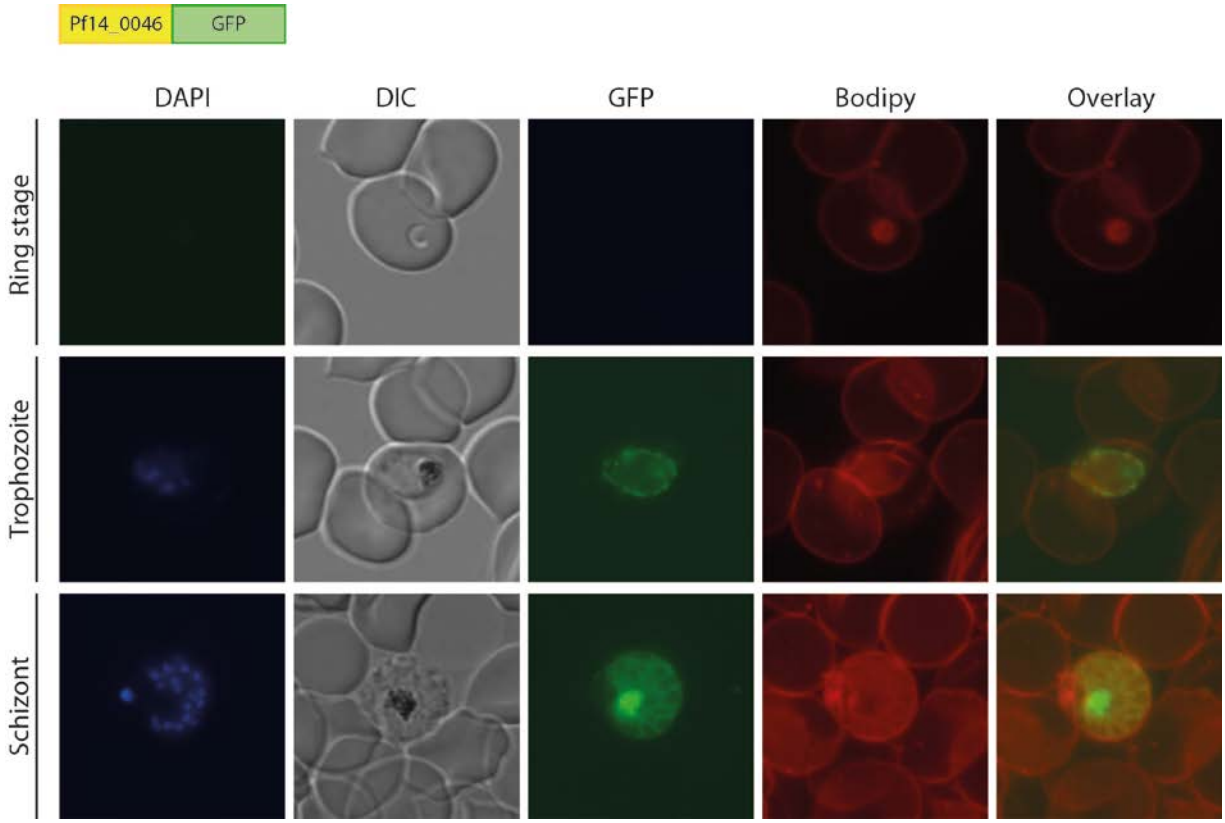

Fig. 3.2.10 PF14_0046-GFP localized to the PV in trophozoite and schizont stage parasites. A schematic depiction of the PF14_0046-GFP construct is shown above the image panels. Images show the PF14_0046-GFP fluorescence in live parasites. DAPI: Nuclear staining; DIC: Differential interference contrast microscopy; Bodipy: membranes stained with Bodipy-TR-C5-ceramide.

The PV biogenesis based on the PF14_0046-GFP signal was analyzed using of time-lapse microscopy. Compared to the intensities of marker proteins of artificial reporters (section 3.2.1), the fluorescence intensity of the PF14_0046-GFP cell line was considerably lower. Nevertheless, 6 experiments with interpretable results were obtained where the quality standard of reinvasion was fulfilled.

A representative experiment is shown in fig. 3.2.11. This experiment started 22 hours before rupture. The fluorescence of PF14_0046-GFP was observable, equally distributed, until 15 hours before rupture (fig. 3.2.11; 22 to 15 hours before rupture). The PV appeared not as smooth as it did with the artificial reporters (compare section 3.2.1), maybe as a consequence of the weaker fluorescence

intensity. And the signal of the marker protein appeared a more dotted distribution pattern, with accumulations in some foci (fig. 3.2.11).
Nevertheless, around 14 hours before rupture, a change was perceptible: the PV showed the characteristic rough appearance of a strawberry phase, which persisted for 6 hours (fig.3.2.11; 14 to 8 hours before rupture). Appearance and onset of the strawberry phase of the PF14_0046-GFP parasites was comparable for all 6 cells (onset 15 to 11 hours before rupture; duration from 5 to 7 hours).

Immediately after the strawberry phase the parasite reached the gap phase, which lasted 5 hours (fig. 3.2.11, -7h to -4h; white arrow head indicating the gap). In the cell in this experiment (fig. 3.2.11), the gap showed only slight movement, while other cells showed gaps with changing positions (fig. 3.2.11) as reported for the artificial reporters. In all 6 interpretable experiments of the PF14_0046-GFP expressing parasites, the gap-phase was reached 7 to 5 hours before rupture and lasted 2 to 4 hours. In the representative experiment shown in fig. 3.2.11, the final phase of PV development occurred three hours before rupture. The marker protein was visible inside the parasite, surrounding the newly formed merozoites, until the schizont ruptured (fig. 3.2.11; -3h to 0h) and reinvasion took place (fig. 3.2.11; 0h).

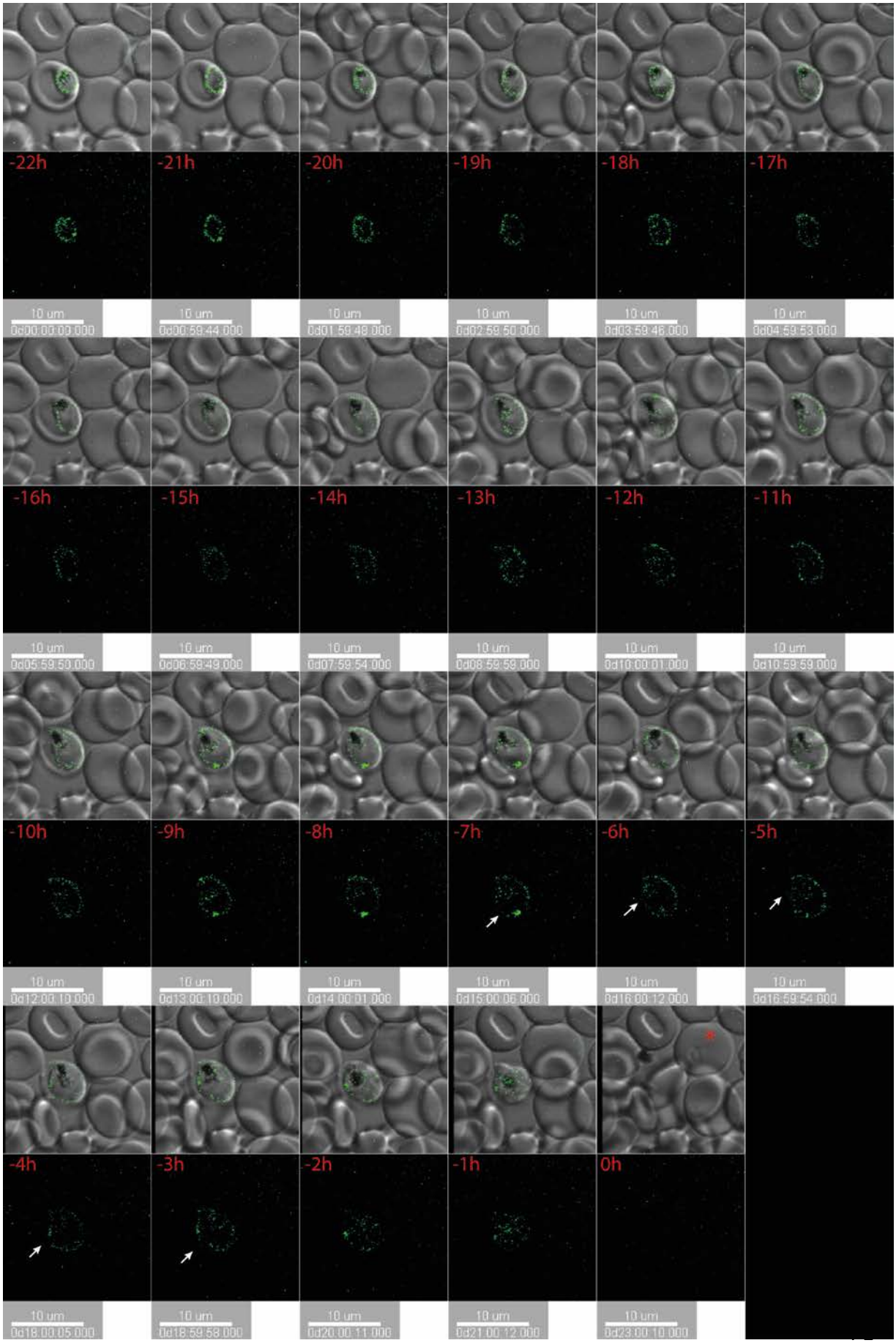
-22h
-21h
-20h
-19h
-18h
-17h
-16h
-15h
-14h
-13h
-12h
-11h
-10h
-9h
-8h
-7h
-6h
-5h
-4h
-3h
-2h
-1h
0h
10 um

Fig. 3.2.11 Visualization of the development of PF14_0046-GFP parasites, from trophozoite stage to reinvasion. Time- lapse microscopy, stacks were taken in 1 hour intervals. Shown are slices of images of the different observed channels. Upper row: overlay DIC, and GFP signals; row below: GFP signal. Red numbers indicate hours before (-) and post (+) schizont rupture/reinvasion; size bar: 10 µM, indicating duration of experiment below the bar; white arrow head: gap; red asterisk: Reinvasion; n= 6

To illustrate more details for the PF14_0046-GFP expressing parasites, another exemplary time-lapse experiment of the corresponding cell line is shown in fig. 3.2.12. This experiment lasted only 12 hours, but showed a slightly brighter fluorescence signal. The experiment already started with a strawberry phase parasite, matching the time point in its life cycle, 11 hours before rupture (fig. 3.2.12; -11h). The strawberry phase persisted for three more hours (fig. 3.2.12; -11h to -9h) before the parasites entered the gap-phase (fig. 3.2.12; -8h; white arrow heads). This parasite showed two to three gaps, two were either merged or one gap vanished within one hour (fig. 3.2.12; -7 to -6h). The third gap showed not major movement (fig.3.2.12; -8h to -4h). This phase lasted 4 hours (3.2.12; -8h to -4h). Thereafter the marker protein was visible inside the parasite, encompassing the newly formed merozoites (3.2.12; -3h to 0h).

In conclusion, the newly found PV phases of later blood stage parasites, which were discovered with the use of artificial reporter cell lines, could also be observed with the residing PV protein reporter PF14_0046-GFP. The newly discovered phases of PV morphology were comparable in time of appearance respective to parasite rupture and total duration.

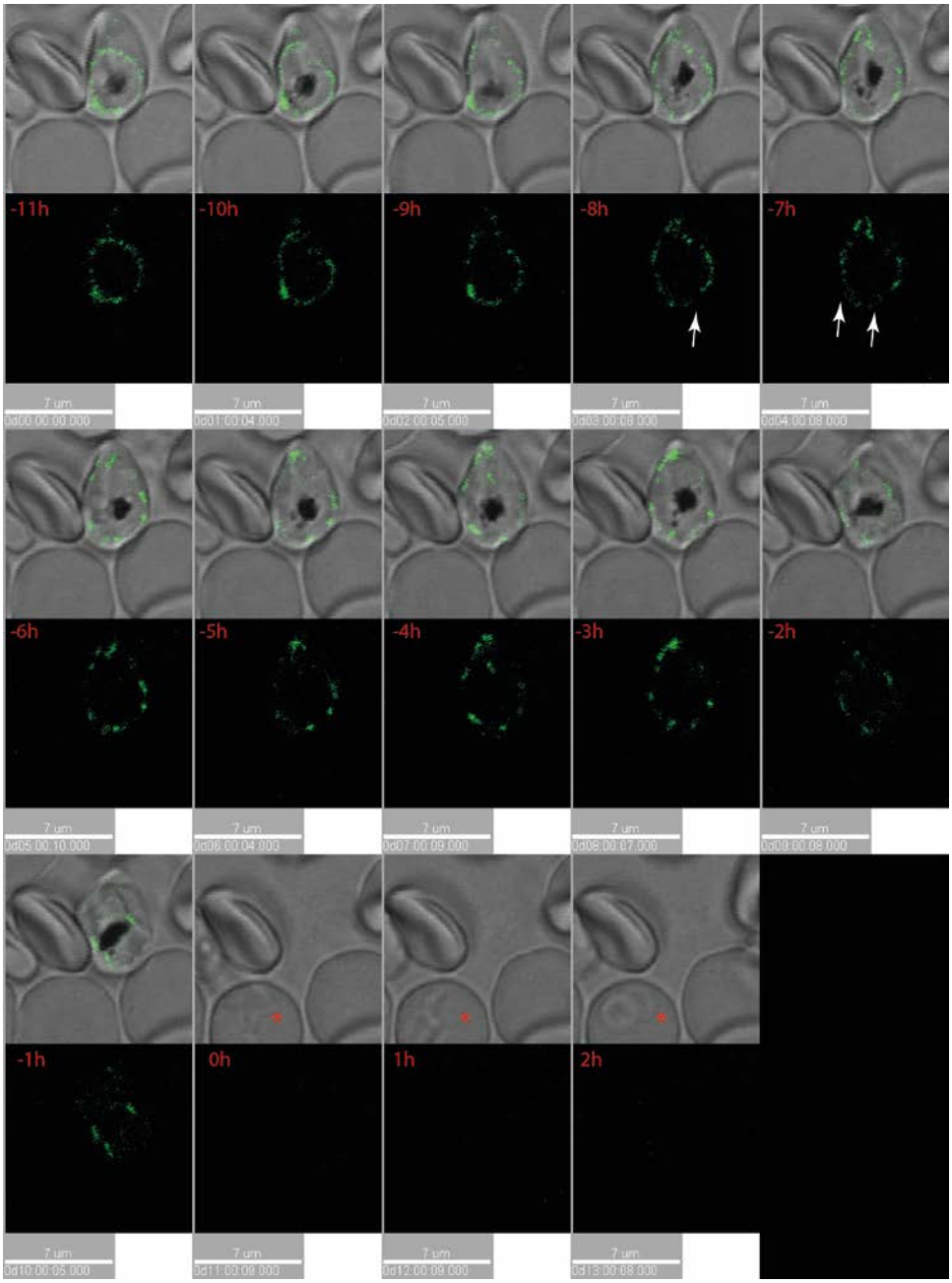

Fig. 3.2.12 Visualization of PF14_0046-GFP expressing parasites, schizont to ring stages. Time- lapse microscopy, images were taken in 1 hour intervals. Single sliced images are shown. Upper row: overlay of DIC, and GFP signals; row below: GFP signal. Hours before and post schizonts rupture/reinvasion (red numbers); size bar: 7 µM; white arrows indication gaps; red asterisk: reinvaded parsites.

3.2.2.2 PF11_0175-GFP (PF3D7_1116800)

The HSP-101 protein (PF11_0175) is a well- characterized protein resident in the PV and on the inner side of the PVM. It is part of the PTEX translocon complex (deKoning-Ward *et al*., 2009; Bullen *et al*., 2012; Beck *et al*., 2014). HSP101 was proposed to be present in distinct sites of the PV (Riglar et al., 2013), and therefore was analyzed as a marker for a potentially protein-specific appearance of PV development. A cell line expressing PF11_0175 fused to GFP (PF11_0175-GFP) was already available from previous work and was shown to localize to the parasites periphery (Heiber *et al*., 2013). In time-lapse experiments marker protein appeared smoothly at the PV in in young and later trophozoite (Fig.3.2.14), and in the later trophozoites the Pf11-0175-GFP was found in foci as well as smooth areas around the parasite (Fig.3.2.13).

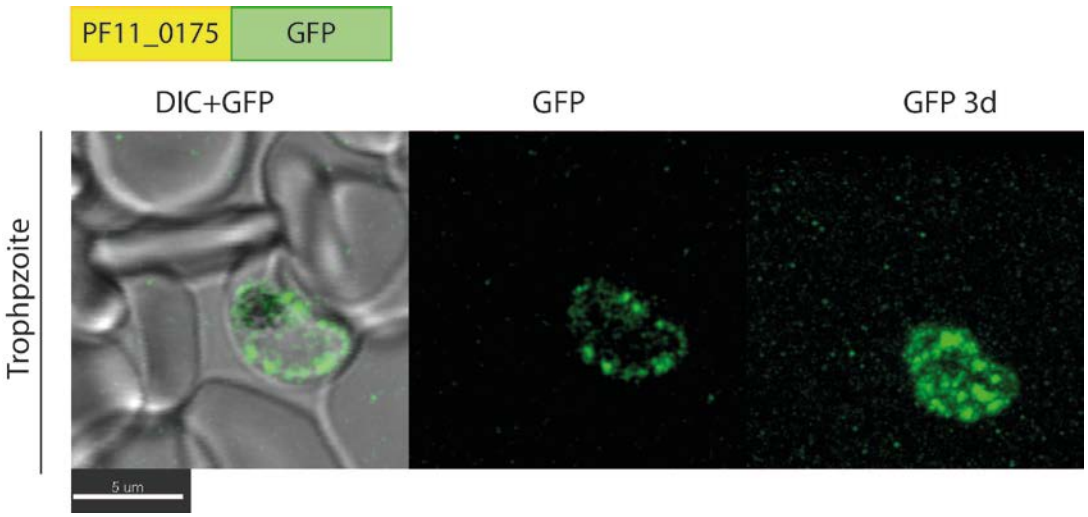

Fig. 3.2.13 Extracts from time-lapse experiments, showing the distribution in the PV of PF11_0175-GFP parasites. Schematic depiction of the PF11_0175 construct is shown above the image panels. The images are extracted time points of time-lapse microscopy experiments of PF11_0175-GFP expressing trophozoite. Single sliced imaged of merged DIC and GFP signals (left side), the single sliced GFP signal (middle) and 3d reconstructed GFP signal from stack of images (right side); size bar: 5µM.

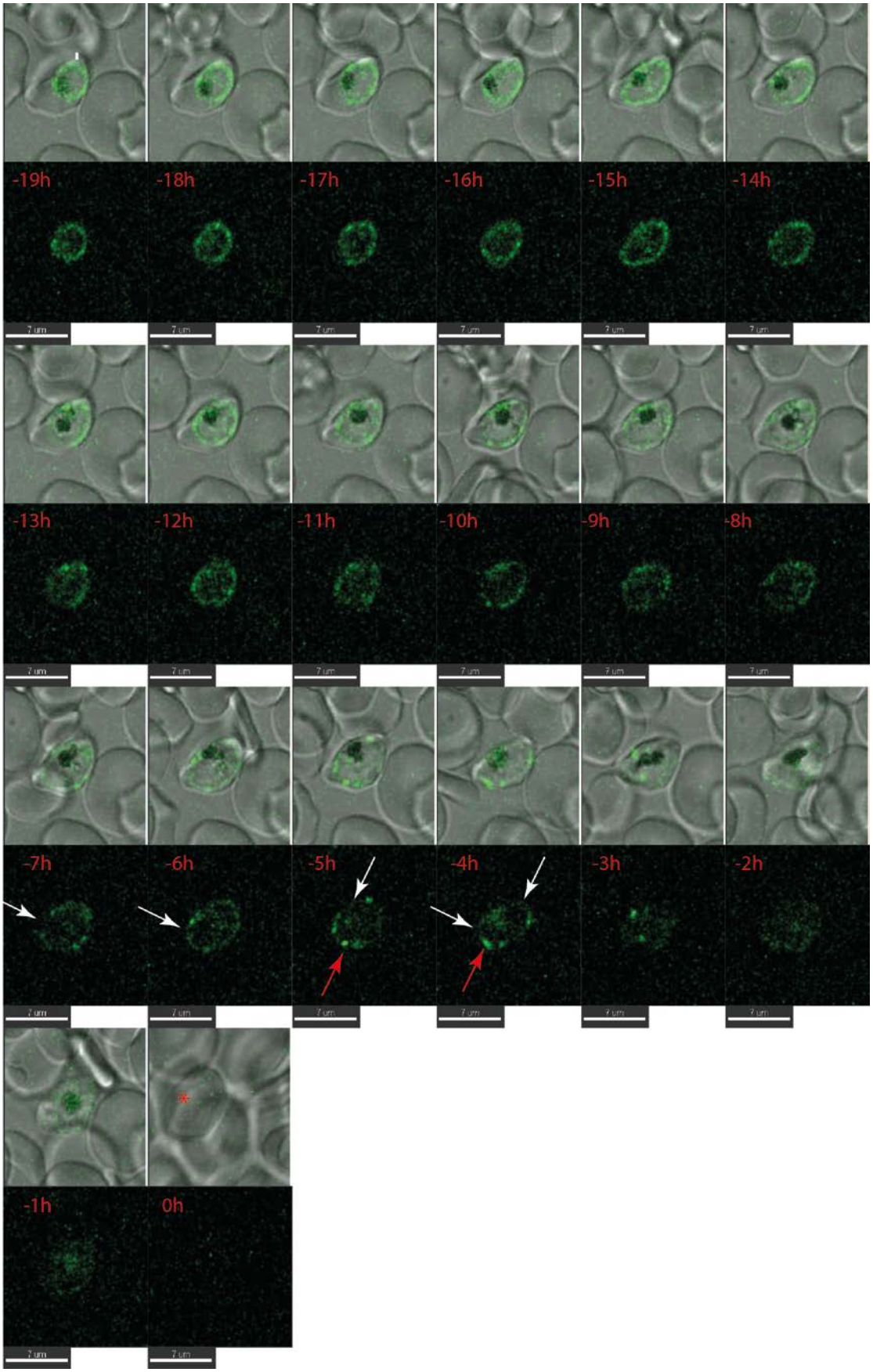
-19h
-18h
-17h
-16h
-15h
-14h
-13h
-12h
-11h
-10h
-9h
-8h
-7h
-6h
-5h
-4h
-3h
-2h
-1h
0h

Fig. 3.2.14 Time-lapse microscopy of PF11_0175-GFP expressing parasites. Images show single slices of a stack acquired in 1 hour intervals. Upper row: overlay of DIC, and GFP signals; row below: GFP signal. Hours before and post schizonts rupture/reinvasion (red numbers); size bar: 7 µM; white arrows indication gaps; red arrows indication marker protein foci; red asterisk: Reinvasion; n=2.

For unknown reasons, parasites expressing PF11_0175-GFP did not survive as well as other cell lines and only few time-lapse experiments met the premise of reinvading RBCs. On a number of occasions experiments also terminated shortly before the expected rupture. The time-lapse experiment shown in 3.2.14 is one of only two experiments meeting this requirement. However, the appearance of the PV biogenesis for the PF11_0175-GFP observed in these experiments was similar in 4 more experiments where no reinvasion could be documented.

The experiment shown in fig 3.2.14 started 19 hours before rupture with a trophozoite stage parasites. Initially PF11_0175-GFP appeared smoothly at the PV. The parasites reached what resembled a strawberry phase 15 hours before rupture and this phase persisted for 8 hours (fig. 3.2.14, -15 to -8h). Thereafter the parasite entered the gap phase seven hours before rupture (fig. 3.2.12, -7h; white arrows) which lasted four hours (fig. 3.2.14, -7h to -4h; white arrows). In contrast to the other reporters, accumulations of Pf11_0175-GFP were visible in addition to the gaps (fig. 3.2.14; -7h to -4h; red arrow). Two foci were still visible, when the PF11_0175-GFP was found inside the parasite surrounding the newly formed merozoites, three hours before rupture (fig. 3.2.14; -3h until 0h). For the second counted experiment, the strawberry phase occurred 16 hours before rupture and continued until the parasite reached the gap phase 7 hours before rupture. Again foci, albeit fainter, were visible during the gap phase until 3 hours before rupture, giving an appearance of a mixed strawberry and gap phase. The final phase of merozoite formation was difficult to observe due to the weakness of the GFP signal.

In conclusion, the newly described phases were also observable with the PF11_0175-GFP in a comparable timing in relation to rupture and with a similar

appearance. However, in addition, PF11_0175-GFP was also present in additional foci at the PV, but the number, intensity and frequency of appearance of these foci did not seem to follow a discernible pattern, potentially because of the limited number of observations made.

All examined and scored parasites for the different time-lapse experiments, using different reporters, are summarized in table 2. Correlating the onset of the strawberry phase with the movement of the FV (table 2).

Table 2: Summary of observed PV biogenesis phases for different cell lines

Cell line	Strawberry Phase (hours before schizonts rupture)	FV movement (yes/no)	Gap phase (hours before rupture)
artificial reporters			
Rex2ΔTM-SP-GFP	**12**	**yes**	**8**
	16	**yes**	**7**
	14	**yes**	**7**
	12	**yes**	**5**
	13	**yes**	**7**
	14	**yes**	**8**
	11	**yes**	**5**
	14	**yes**	**8**
EXP-1-SP*crt* FKBP-mCherry	**13**	**yes**	**9**
	12	**yes**	**7**
	12	**yes**	**8**
	14	**yes**	**9**
	13	**yes**	**7**
resident protein reporter			
PF14_0046-GFP	**11**	**yes**	**5**
	13	**yes**	**8**
	12	**yes**	**4**
	13	**yes**	**4**
	9	**yes**	**5**
	14	**yes**	**7**
PF11_0175-GFP	**15**	**yes**	**7**
	16	**yes**	**7**

3.2.3 Morphology of newly discovered phases during PV biogenesis

In the previous section new phases of PV biogenesis during the parasites asexual life cycle were described, for both, artificial and parasites protein reporters (see section 3.2.1 und 3.2.2). These phases were termed the strawberry and the gap phase and were more closely analyzed 3D reconstructions of exemplary parasites, expressing the REX2ΔTM-SP-GFP, the EXP1-SP-GFP^{crt} and FKBP-mCherry and the parasites resident PF14_0046-GFP. As only a single time point was imaged, a higher quality image was possible as opposed to the time- lapse images.

Membranes of infected RBCs were stained with Bodipy-TR-C5-ceramide to visualize the parasite and host cell compartments (fig. 3.2.15, 16 and 3.2.17).

An exemplary single optical section through a strawberry phase parasite is shown in 3.2.15. The GFP signal appeared in the expected interrupted pattern (3.2.15; A) and in the 3d reconstructions stacked images of the same cell, this marker protein distribution was confirmed (3.2.15; B). The DAPI staining showed the presence of four nuclei, indicating that the parasite already entered the schizont stage (fig. 3.2.15).

In fig. 3.2.16 a single optical section through a late strawberry phase parasite is shown (fig. 3.2.14; A). The overlays of the GFP and the Bodipy membrane staining pointed out, that in the spaces where the marker protein was lacking, the membrane signal appeared smooth and not interrupted (Fig. 3.2.14; A; Overlays). A 3d reconstruction from stacks of images of the same cell confirmed this finding (fig. 3.2.14; B; white arrows). Hence, the pattern of marker proteins cannot be attributed to a morphological change visible with the membrane marker Bodipy-TR-C5-Ceramide

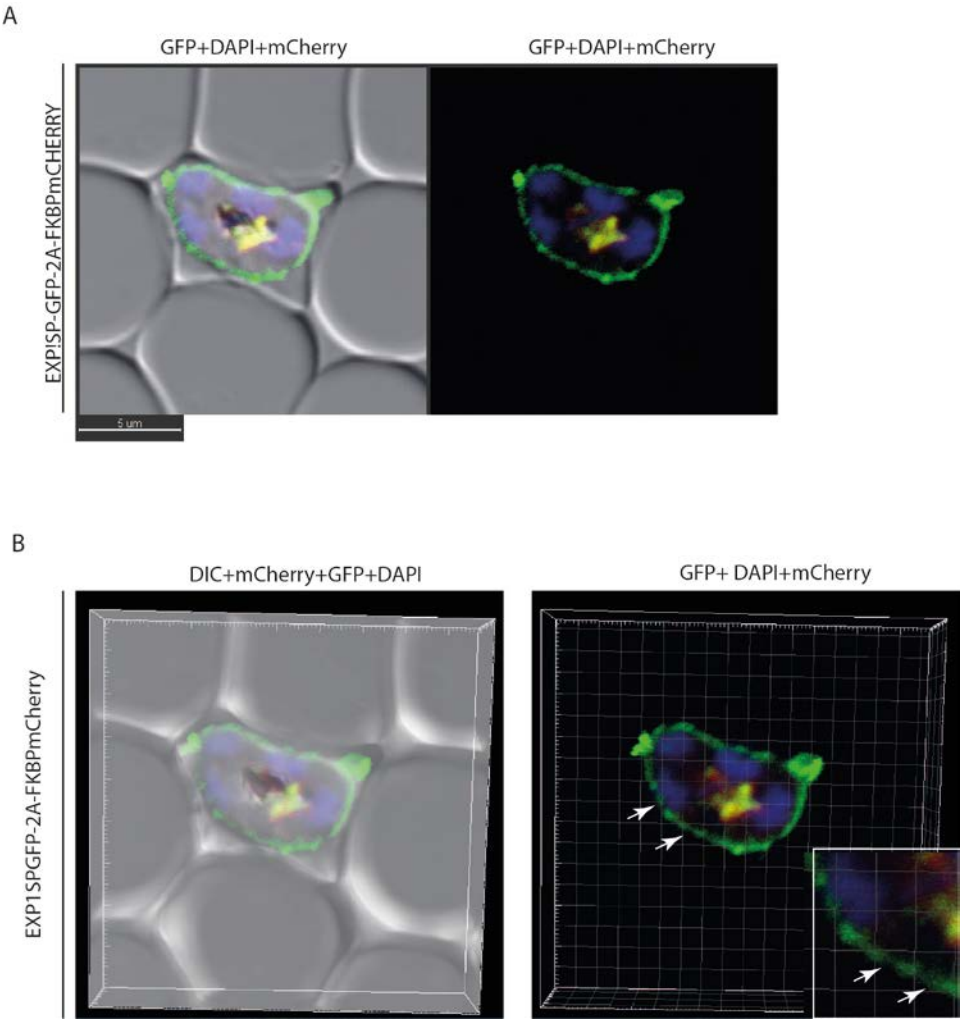

Fig. 3.2.15 Single slice image and 3d reconstructions of a strawberry phase of a EXP1-SP-GFP^{crt} and FKBP-mCherry expressing schizont. Confocal microscopy of EXP1-SP-GFP^{crt} and cytosolic-FKBP-mCherry expressing parasites (A) single slice images; left: overlay of the DIC, DAPI, GFP and mCherry signals; right picture: merge of GFP, DAPI and mCherry signals. (B) From stacked images reconstructed 3d images; left side: overlay of DIC, GFP, DAPI and mCherry; right side: merge of DAPI, GFP and mCherry signal. The cytosolic FKBP-mCherry was barely detectable, it was bleached out immediately under the used microscopy conditions. DAPI: nuclear staining; size bar: 5 µM; white box: zoom of partial PV; white arrows, indicting the spaces between GFP protein signals.

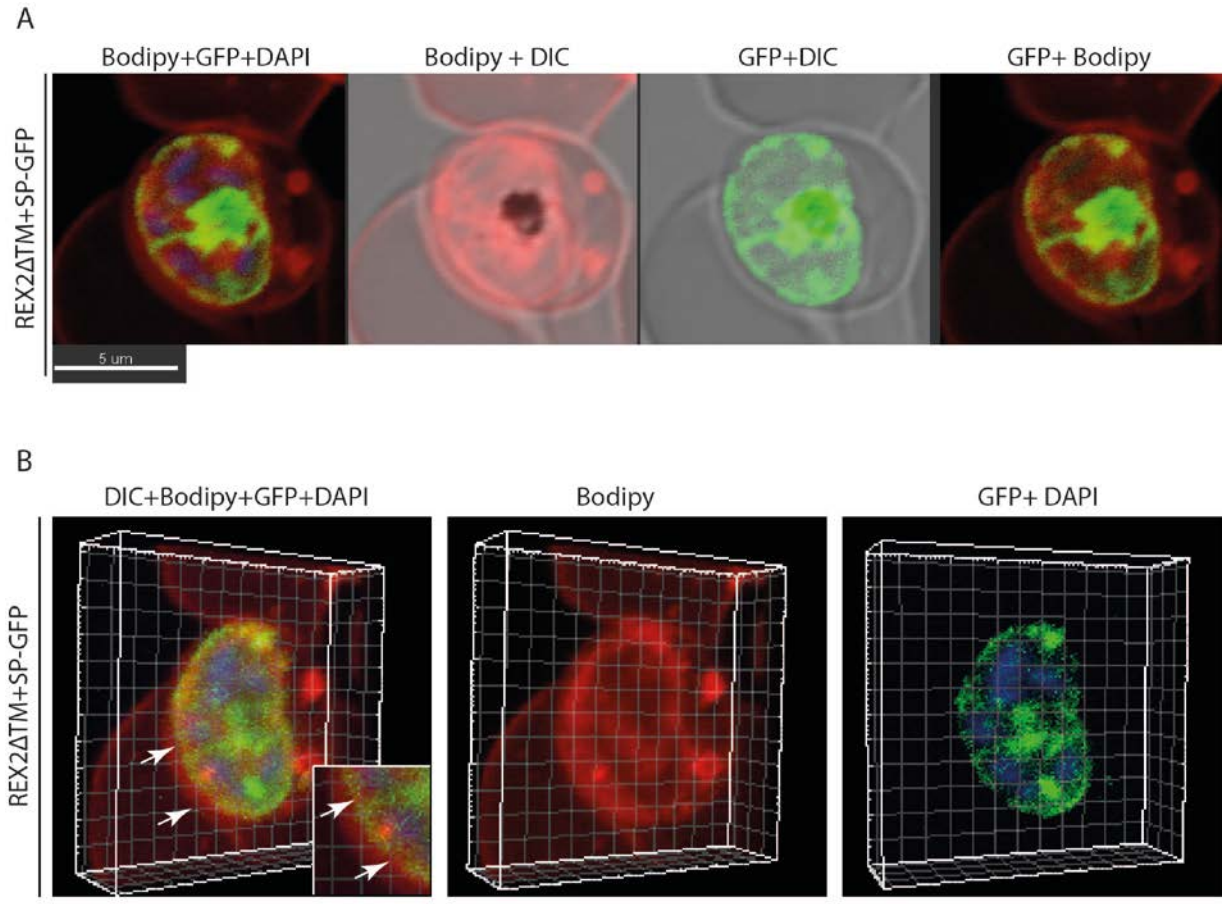

Fig. 3.2.16 Morphology of late strawberry phase of REX2ΔTM-SP-GFP schizont, single slice and 3d reconstruction. REX2ΔTM-SP-GFP expressing parasites, co-stained with a membrane marker. (A) Depicted as single slice images; far left: overlay of DAPI, GFP and Bodipy signals; second: merge of DIC and Bodipy; third: merge of GFP and DIC; right side: merge of GFP and Bodipy. (B) From stacks of images reconstructed 3d images; left side: overlay of GFP, DAPI and Bodipy; white box in the right bottom corner a zoom of partial PV and membrane staining; middle: Bodipy; right side: merge of DAPI and GFP signal. DAPI: nuclear staining; Bodipy: Bodipy-TR-C5-ceramide; size bar: 5 µM.

A representative gap phase parasite is shown in fig. 3.2.17. The 3D reconstruction shows GFP was found around the parasites, showing foci, but with two clearly visible gaps (fig. 3.2.17, white arrows). This parasite is at a very late stage of its development as judged by the number of nuclei and its size, consistent with a gap stage (Fig. 3.2.17, Bodipy + GFP + DAPI and GFP + DAPI).

Co-staining with the Bodipy-TR-C5-Ceramide membrane marker, revealed that the gaps in GFP fluorescence were not reconciled with the membrane marker, suggesting absence of the protein but not of membrane.

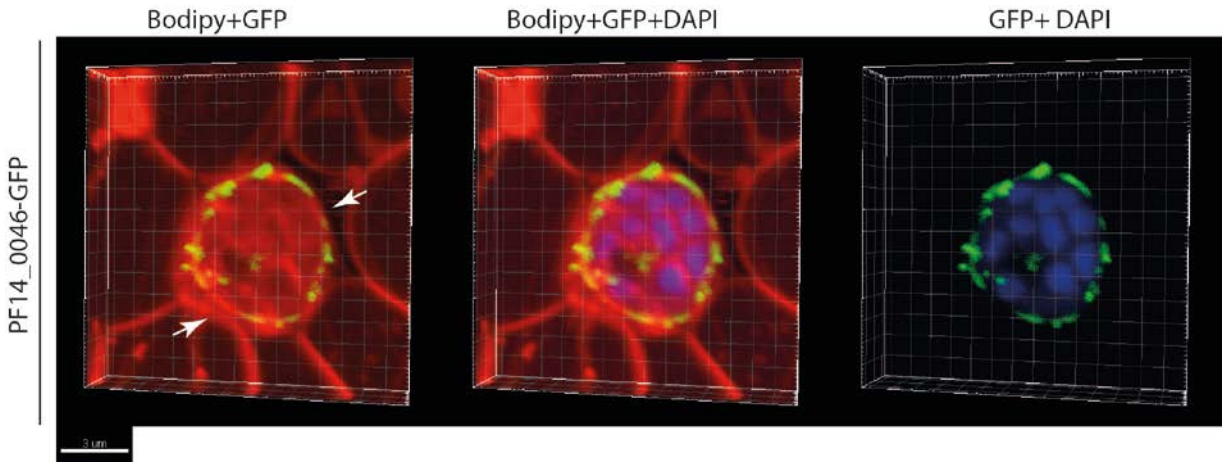

Fig. 3.2.17 3d reconstruction of a PF14_0046-GFP gap-phase parasite. Images show a 3D representation, reconstructed from a z-stack taken throughout the entire infected; white arrows indication the gaps; DAPI: nuclear staining; Bodipy: Bodipy-TR-C5-ceramide; size bar: 3 µM.

Chapter 4: Discussion

The parasitophorous vacuole (PV) is a highly specialized compartment, the *Plasmodium* parasites resides and develops (Liehl *et al.*, 2015). It is surrounded by its membrane (PVM), which is formed during the invasion of a merozoite into its host cell. The material of the PVM is derived of host cell membrane, but already during invasion its protein and lipid content is altered by the parasite (Dluzewski, 1992; Ward, 1993; Lingelbach and Joiner, 1998).

During its early development in the red blood cell, the parasite modifies the host cells surface and its cytoplasm by exporting parasite proteins (Grüring *et al*., 2011). These exported proteins, as well as vital nutrients, have to pass the PV and the two membranes surrounding it. In the last few years more and knowledge was gained on the transport mechanisms mediating these processes. For instance a putative protein translocation complex termed PTEX was found at the inner face of the PVM and was shown to be essential for protein export (Elsworth et a., 2014; Beck *et al*., 2014). For the first time there is also evidence pointing to the origin of the nutrient pore (Gold *et al*). In addition several further proteins of unknown function have been described for the PVM (Spielmann *et al*., 2012). In contrast to this, only a few studies focused on the biogenesis of the PV/PVM compartment (among others Behari and Haldar, 1994; Haldar *et al*., 2001; Haldar *et al*., 2002) most likely due to the limited microscopy abilities to study this compartment in the rather delicate blood stage of the parasites.

Recently, Spielmann and Grüring established 4d microscopy for *P. falciparum* blood stages (Spielmann & Grüring, 2012), which opened the door for structural and morphological studies of the PV and its membrane (PVM). By the use of fluorescent reporters the PV and PVM can be visualized and tracked over time (Grüring *et al*., 2011). In this thesis 4d microscopy was used to examine the biogenesis of the PV/PVM and the putative regulation of one member of its most abundant protein family, the early transcribed membrane proteins (Spielmann and Beck, 2000), was analyzed.

4.1 Putative translational repression of ETRAMP2

Translational repression has been described for some members of the ETRAMP family, e.g. UIS3 and UIS4 in rodent malaria parasites (Müller *et al*., 2005 (b); Silvie *et al*., 2014). Previous studies had also shown discrepancies in the mRNA and protein level of ETRAMP2 in *P. falciparum* blood stage schizonts (Spielmann *et al*., 2003). The ETRAMP2 protein was detectable by western blot analysis only from early ring stage parasites to early trophozoite stages, while the mRNA of *etramp2* could be detected only in late stage schizonts. Because the protein was detectable immediately after the invasion of a new RBC, it was concluded that the *etramp2* gene is transcribed in schizont stages parasites, but that the mRNA is not translated until the beginning of the ring stage and stored somehow before. This kind of translational repression is already known for members of the ETRAMP protein family at the transition of sporozoite stage to the hepatocyctic phase (Silvie *et al.*, 2014), suggesting a crucial role of the protein during invasion or establishing the new developmental stage. It is further a common mechanism in other systems such as in human oocytes (Chapat and Corbo, 2014) and in other *P. falciparum* live cycle stages (Guerriro *et al*, 2014; Cui *et al*, 2015).

In this study the EXP-1-SP-GFP^{etramp2}, an artificial reporter cell line, had been used to examine the putative translational regulation of ETRAMP2, under the control of the *etramp2* 5´UTR, in blood stage schizonts. Time-lapse experiments were conducted with this cell line to observe the ETRAMP- specific onset of translation of the GFP marker protein. These experiments revealed an unexpected appearance of GFP signals in the late schizont, more precisely 90 to 60 minutes before schizont rupture, in all observed cells (n=15), suggesting an onset of the translation of the GFP fusion protein in late schizonts. One possible explanation for this result was, that due to the episomal nature of this artificial EXP-1-SP-GFP^{etramp2} reporter, an abundance of mRNA with *etramp2* 5'UTRs could lead to a leaky repression of translation for example by dilution of regulatory proteins involved in the repression.

To test this hypothesis, immunofluorescence assays (IFAs) with antibodies against the endogenous ETRAMP2, of both, the reporter cell line and the wild type *P. falciparum* 3d7 cell line, were conducted. As expected, ETRAMP2 was detected in late blood stages of the EXP-1-SP-GFP^{etramp2} expressing parasites, but also in the 3d7 wild type parasites (fig. 3.1.4). The intensity of the fluorescent signal was lower in the late schizont stagesthan the intensity of the signal in ring stage parasites (fig. 3.14; B). This suggests that ETRAMP2 is already expressed in the late schizont stage, but at a lower level than in ring stages. The newly formed merozoites might get an initial basic equipment for their invasion process or establishment of an immediately functioning PVM. More ETRAMP protein is then added immediately after invasion and during ring stage development, until the level of drops during transition to the trophozoite stage when other ETRAMPs take over (Spielmann *et al*., 2003). While the lower levels of ETRAMP in Schizonts may indicate less protein in this stage than after invasion, it cannot be excluded that this might be due to the limitations of the technique used, as IFAs are not suitable for a reliable quantification of protein amounts.Several factors influence the strength of the fluorescence signal in IFA, for example the accessibility of the antigen. It is therefore possible that ETRAMP2 is expressed equally in both developmental stages.

The onset of translation, shown in this study, is reminiscent of the recent findings of MacKeller and colleagues during their studies of ETRAMPs of the rodent malaria parasite *P. yoelli* (MacKellar *et al*., 2011). These authors showed that the myc-tagged version of the *P. yoelli* ETRAMP PY03652 was detectable from the early ring stages until the start of schizogony. In the early schizont stage the protein signal vanished and reappeared again in Schizonts when the new daughter merozoites were formed. In those merozoite the PY03652-myc was detectable in foci at the apical end of the merozoites, most likely co-localizing with the secretory organelles, suggesting a crucial role of PY0352 during the invasion and the early blood stage development (MacKellar *et al*., 2011). The localization of an ETRAMP at the secretory organelles was shown the first time by MacKellar *et*

al., but most recently a similar distribution pattern was shown for the newly identified *P. vivax* ETRAMP PvETRAMP11.2 (Cheng *et al*., 2015). The results shown in this thesis may suggest that the onset of *etramp2* mRNA translation is comparable to that of PY03652. Nevertheless, this does not necessarily contradict translational repression at earlier stages of schizont development or that repression is only partial. However, given the fact that this effect then would be much less drastic than initially expected, it is unclear if this is an avenue worth pursuing further. It would require careful quantitative gene and protein expression studies. In addition, it might be interesting to localize ETRAMP2, for example by co-localization with markers of the secretory organelles needed for invasion. Such studies might reveal further parallels to the ETRAMPs to P. yoelii and P. vivax and might ultimately contribute to the elucidation of the function of ETRAMPs that still remains enigmatic.

4.2 Visualization of the PV biogenesis

In order to examine the biogenesis of the parasitophorous vacuole (PV), two generally different types of reporters were used. The first type of reporter was artificial and consisted only of a signal peptide fused to a fluorescent marker protein under the control of different 5´UTRs, to obtain marker protein secretion into the PV at specific times in the developmental cycle of the parasite.

The other type of reporter was used to examine possible protein-specific localizations of PV resident proteins. For this the 5'UTR of PfCRT, which is almost constitutively active (from the middle ring stage until the end of schizogony) (Le Roch *et al*., 2004), was used for expression of the protein of interest fused C-terminally to green fluorescent protein (GFP) (Haase *et al*., 2009; Grüring *et al*., 2011).

4.2.1 Artificial reporter constructs

The EXP-1-SP-GFP^{etramp2} was used to examine the PV from early ring to trophozoite stages. Ring stage parasites have been described as slowly growing

stages. Nevertheless, they are highly mobile, regarding their position in the RBC and frequently change their shape from a circular form to an amebic form and vice versa (Grüring *et al*., 2011). In this study we additionally observed the marker protein distribution in the parasites PV, revealing interesting patterns, especially for the amebic ring stage parasite. 3d reconstructions of stacks taken with a confocal microscope indicated that the marker proteins accumulated at the end of the arm-like extensions, forming a cap-like structure. The reporter was barely detectable elsewhere in the parasite during that stage (fig 3.2.2). A similar type of protein distribution has been described by Riglar and colleagues before but was ascribed a localisation specific for PTEX components and EXP-1 (Riglar *et al*., 2013). They showed that EXP-2 and HSP-101, as core components of PTEX, and EXP-1, used as a PVM marker in this study, are all localized in the same PVM domains and distributed to the end of the amebic extensions to domains from which rhoptry-associated protein 1 (RAPI), a PV marker, was excluded (Riglar *et al*., 2013). They concluded that this particular distribution of the translocon to the end of the amebic extensions is associated with protein export. In the thesis presented here a similar distribution was observed with an artificial reporter, suggesting a general structural distribution of the PV proteins to the end of the amebic extensions. It might therefore be that the PV space is larger at the amoebic extensions, whereas the distance between PPM and PVM is narrower in the regions of the arms closer to the parasite center. Whether this has any functional relevance for this compartment, remains to be determined. It is also puzzling that Rap1 showed a different distribution, indicating that this rhoptry protein inserted into the PV during invasion may show a protein specific loc. It also indicates that the presence of proteins in other areas than the ‘caps’ is possible, somewhat contradicting the PPM-PVM distance hypothesis. This would also mean that there are so far unknown targeting mechanism that direct proteins into subcompartments of the PV. In this respect it is interesting to not that ETRAMPs and EXP1 are found in individual subdomains (Spielmann *et al*., 2003) which might contribute to the spatial organization of the PVM and PV. .

A known structure of the parasite to increase the surface of the PVM and expand it through the host cell cytosol is the tubovesicular network (TVN) (Bahri & Haldar, 1994; Elmendorf & Haldar, 1994). The TVN was shown to be essential for parasite nutrient uptake (Lauer *et al*., 1997). Recently, a structure reminiscent of the TVN of blood stage parasites was identified in the liver stage of the rodent malaria species *P. berghei* (Grützke *et al*., 2014). However, it is still unclear if this structure is highly species-specific and if it fulfills the same function as the TVN of *P. falciparum* blood stages. Data from Matz and colleagues suggest, that it represents a membranous structure that differs strongly from the TVN. They showed that this tubular lumen in *P. berghei* liver stages is a highly specialized compartment that is very dynamic as compared to the TVN of *P. falciparum* blood stages. Furthermore, in contrast to the *P. falciparum* TVN, its formation was not affected by the use of the sphingomyelin synthase inhibitor PPMP and it was not consistently stainable with Bodipy-TR-C5-Ceramide (Lauer *et al*., 1997; Elmendorf & Haldar, 1994; Matz *et al*., 2015). From their findings Matz and colleagues suggested an evolutionary conserved tubular system for protein trafficking (Matz *et al*., 2015).

Riglar *et al*. also suggested that the observed localization of PTEX compounds is specific for a conserved protein trafficking function, although in this case it was not present in large extensions (Riglar *et al*., 2013). The findings of this thesis, showing the same accumulation pattern of the artificial reporter at the end of the amebic ring stage parasites suggest that this localization is not specific for PTEX compounds at this particular developmental stage. It might be a general strategy of the parasite bring the trafficking machinery closer to the host cell but maybe also other PV/PVM proteins, with different functions like nutrient exchange, into the host cell cytosol during this stage of massive host cell modification (Grüring *et al*., 2011) and may also fulfill a function similar to the TVN which is absent in the early ring stage parasites (Tamez *et al*., 2008).

The time-lapse experiments of the artificial reporters, expressed under the control of the *crt* promoter, where used to analyze the subsequent PV biogenesis. In young trophozoite stages of Rex2ΔTM-SP-GFP expressing parasites, the PV

appeared smooth, but extensions were observable that did not match with the parasite border visible in the DIC channel (fig. 3.2.5). Two different kinds of PV extensions are known, the TVN (Langreth *et al*., 1978; Elmendorf and Haldar, 1994) and the recently described cavity (Grüring *et al*., 2011; Kruse, 2014; Kruse and Spielmann, PhD thesis). The TVN is known to originate from the PV and it supposedly is essential for parasites nutrient uptake and blood stage development (Lauer *et al*., 1997). The cavity was identified as a large increase of the parasites PVM and PPM. It appears in two different forms in blood stage parasites: the invaginated and the protrusion form (F. Kruse, 2014; PhD thesis). While the invaginated form was filled with host cell cytosol, the protrusion form of the cavity may contain detectable parasite cytosol, although in rather low amounts. In the DIC channel the cavity, irrespective if a protrusion is present or not, is visible as notch at the parasites surface (Grüring *et al*., 2011; F. Kruse, 2014; PhD thesis).

In our studies we were not able to distinguish clearly between TVN and cavity types of extensions, since we only used reporters for the PV, such as the Rex2ΔTM-SP-GFP cell line. Although the cavity can often be identified in the DIC channel, a clear cavity marker like PfEHD (F. Kruse, 2014; PhD thesis) would have been necessary. In order to investigate whether membranous extensions are filled with host cell cytosol or with parasite cytosol, a double fluorescent cell line was established, expressing EXP-1-SP-GFP^{crt} as a PV marker and FKBP-mCherry as a marker for the parasite cytoplasm. By using a viral skip peptide both proteins were translated from one mRNA. Interestingly some extensions, observable during the young trophozoite stages of these parasites, were filled with parasites cytosol, showing a clear mCherry marker protein signal. The parasites cytosol protrusions were as mobile as the other protrusions observed, and changed their shapes and positions frequently. The cavity was described as highly mobile structure by the 4d imaging studies of Güring and Kruse (Grüring *et al*., 2011; F. Kruse, 2014;PhD thesis). Those parasite protrusions that could be confirmed by their notch appearance in the DIC Channel, were always those without parasites cytosol, this indicates that some of the extensions detected were cavities but the remainder of extensions could not be classified. The presence of

parasite cytosol was so far only inferred from its architecture but never observed (F. Kruse, 2014; PhD thesis) and it could not be confirmed in this study.

With both artificial reporter cell lines, the PV appeared smooth over most of the trophozoite stage. Approximately 11 to 16 hours before schizont rupture, the distribution of the PV reporter changed and it appeared rough, like the surface of a strawberry. This phase was termed ‘strawberry’ phase and occurred concomitantly with the movement of the food vacuole to the center of the parasite, which was described to be characteristic for the transition of trophozoite to schizont stage, occurring 10 to 15 hours before schizonts rupture (Grüring *et al*.,2011). In table 2 the onset of this phase and its correlation with the FV movement are summarized, showing that the strawberry phase appearance always correlated with the movement of the FV to the center of the parasite, suggesting a general, structural change during this developmental stage.
After the strawberry phase one or more gaps appeared at the PV. These gaps appeared approximately 9 to 5 hours before schizont rupture and lasted for 3 to 5 hours. Usually one or two gaps were visible in 3d reconstructions from taken stacked images through the entire cell, which are able to move and possibly fuse.

These two different but distinct phases, the strawberry and the gap phase, occurred in all cells that met the inclusion criteria, suggesting them as general phases of PV development and possibly indicating larger rearrangements of the parasite during this time. The gap phase was immediately followed by the formation of daughter merozoites, schizont rupture and reinvasion of a new RBC, which were previously documented (Grüring *et al*., 2011).

4.2.2 PV resident protein reporter constructs

To analyze potential protein-specific localizations of marker proteins during blood stage development, transgenic cell lines expressing the previously characterized PF14_0046- and the PF11_0175- GFP reporters (Heiber *et al*., 2013) were imaged. For both transgenic parasites cell lines the GFP marker was observable in foci at the PV, more distinct for the PF11_0175-GFP reporter. This distribution of

the marker protein in foci was thought to be due to the protein specific localization. For PF11_0175 (HSP101 - a PTEX component), its localization to the PV facing side of the PVM is known (deKoning-Ward *et al.,* 2009; Bullen *et al*., 2012). For PF14_0046 the localization was not determined in detail, but was assumed to be the PV (Heiber *et al*., 2013).

Nonetheless, the observation of these cell lines expressing PV resident proteins in time-lapse experiments revealed the occurrence of the here newly identified phases of the PV summarized in table 2. The appearance and the timing of onset and duration was comparable. Furthermore, the strawberry phase always correlated with the afore mentioned FV movement to the parasite's center. The strawberry phase continued for 4 to 7 hours and was immediately followed by the gap phase. The gap phase continued for three to four hours and was followed by the distribution of the marker protein around the newly formed merozoites and finally the schizonts ruptured and reinvasion occurred. It hence can be concluded that the newly discovered phases are a general feature of the PV not related to a specific marker.

The general nature of the observed phases indicates sub-phases of the parasite live cycle in red blood cell and raises the question about the underlying processes leading to these morphological phases. According to our observations, at this stage of parasites development, the parasite schizogony is already taking place. This can be concluded from the presence of four DAPI stained nuclei in the early strawberry phase (Fig. 3.2.15). However, this particular sub-stage was observed occurring in a time frame of 16 to 11 hours before rupture, so the number of observable nuclei would most likely differ. Another sub-stage of late schizont development was described as the stage of segmentation of newly formed daughter merozoites, the segmenter stage, from 38 to 48 hours post invasion, representing the last 10 hours of schizont stage development (Sam-Yellowe, 1988; Doerig *et al*., 2000;). This stage is characterized by the formation of daughter merozoites from the central, hemozoin containing, residual body (Sam-Yellowe, 1988; Doerig *et al*., 2000; Bannister et a., 2003).

Co-staining with the Bodipy-TR-C5-Ceramide membrane marker revealed that the interruptions in GFP fluorescence were not reconcilable with the membrane marker, suggesting absence of the protein but not of the membrane. This could occur if the PVM and PPM are situated so closely together, that the marker protein is physically excluded from the gaps. Those kind of morphological changes could lead to distinct pattern of GFP marker protein distribution at the PV and may suggest a structural PV organization pattern or even a more general structure-changing mechanism in the parasites biogenesis.

These newly identified sub-stages of schizont stages suggest specific functions. The strawberry-phase reproducible occurred in the transition stage from trophozoite to schizonts, and therefore during early schizogony, or together with the onset of schizogony. Suggesting the strawberry appearance of the PV might a lead to structural events in order to incorporate the highly needed lipids during this active phase of nuclear division. The PV might expand in order to create space for the following time of branching of the mitochondria and apicoplasts, this massive branching of the organelles was shown to take place at a comparable time during schizont stages for liver stage parasites (Stanway *et al*., 2009). Proteases, known to play a role during blood stage schizonts schizogony, like the *P. falciparum* cyclic GMP (cGMP)-dependent protein kinase (PfPKG) might have a crucial role in destabilizing existing PVM structures (Taylor *et al*., 2010) in order to rearrange for daughter merozoites formation, leading to the distinct pattern of the reporterprotein at the PV.

For the gap-stage parasites the structural rearrangements must be more significant, firstly to the massive amount of membranes compounds needed because if the segmentation of the daughter parasites. And secondly due to the imminent membrane break downs in order to administer the merozoites egress. There are some different kinds of hypothesis of how merozoite egress occurs. The membrane fusion model of Winograd *et al*. (1999); The ‘explosive rupture’ model of Glushakova *et al*. (2005) in which the schizont forms a short-lived ‘flower’ structure; the ‘inside-out’ model (Wickham *et al*., 2003) in which PVM breakdown precedes RBC membrane rupture; The ‘outside-in’ model in which the RBC

membrane is degraded first, allowing release of merozoites surrounded by the PVM, which is eventually degraded in an exo-erythrocytic step (Salmon*et al*.,2001; Soni *et al*., 2005). But naturally-given all this break down hypothesis deal with proteases conclusion, previous work has shown that egress of asexual blood-stage forms in *P. falciparum* is dependent on the activity of least one calcium-dependent kinase, CDPK5 (Dvorin *et al*., 2010). For *P. berghei* blood stages four proteins were shown to act specifically on the rupture of the PVM, the MDV-1/PEG3, PbGEST and Actin II, while the perforin-like proteins protein 2 (PPLP2) has a function restricted to RBC membrane rupture. It remains unclear how all these mechanisms could possible work together but it reveals the complexity of the sub-stage. Further experiments, using inhibitors for the specific proteases could be quite informative.

The different changes in the distribution of soluble PV proteins appeared to be highly orchestrated. Although the descriptive data shown in this work cannot elucidate the mechanisms, the time of their occurrence suggests that they are evident to extensive structural rearrangements during schizogony. These phases of schizont development need to be further analyses in order to confirm them as highly specific sub-stages of the late blood stage development of the parasite, and to understand the structural mechanisms behind this process.

But newly identified sub-stages could be used to stage the blood stage parasites more precisely, until now this was barely achievable. By the use of markers at the PV, the sub-stages can easily be used for time-wise orientation and for staging of the parasites.

LITERATURE

Agrawal, S., Chung, D.W., Ponts, N., van Dooren, G.G., Prudhomme, J., Brooks, C.F., Rodrigues, E.M., Tan, J.C., Ferdig, M.T., Striepen, B.*, et al.* (2013). An apicoplast localized ubiquitylation system is required for the import of nuclear-encoded plastid proteins. PLoS pathogens *9*, e1003426.

Aikawa, M. (1971). Parasitological review. *Plasmodium*: the fine structure of malarial parasites. Experimental parasitology *30*, 284-320.

Ansorge, I., Paprotka, K., Bhakdi, S., and Lingelbach, K. (1997). Permeabilization of the erythrocyte membrane with streptolysin O allows access to the vacuolar membrane of Plasmodium falciparum and a molecular analysis of membrane topology. Molecular and biochemical parasitology *84*, 259-261.

Ariey, F., Witkowski, B., Amaratunga, C., Beghain, J., Langlois, A.C., Khim, N., Kim, S., Duru, V., Bouchier, C., Ma, L.*, et al.* (2014). A molecular marker of artemisinin-resistant Plasmodium falciparum malaria. Nature *505*, 50-55.

Ashley, E.A., Dhorda, M., Fairhurst, R.M., Amaratunga, C., Lim, P., Suon, S., Sreng, S., Anderson, J.M., Mao, S., Sam, B.*, et al.* (2014). Spread of artemisinin resistance in Plasmodium falciparum malaria. The New England journal of medicine *371*, 411-423.
Ashley, E.A., and White, N.J. (2014). The duration of Plasmodium falciparum infections. Malaria journal *13*, 500.

Bannister, L.H., Hopkins, J.M., Dluzewski, A.R., Margos, G., Williams, I.T., Blackman, M.J., Kocken, C.H., Thomas, A.W., and Mitchell, G.H. (2003). Plasmodium falciparum apical membrane antigen 1 (PfAMA-1) is translocated within micronemes along subpellicular microtubules during merozoite development. Journal of cell science *116*, 3825-3834.

Bannister, L.H., Hopkins, J.M., Fowler, R.E., Krishna, S., and Mitchell, G.H. (2000). Ultrastructure of rhoptry development in Plasmodium falciparum erythrocytic schizonts. Parasitology *121 (Pt 3)*, 273-287.

Bannister, L.H., Hopkins, J.M., Fowler, R.E., Krishna, S., and Mitchell, G.H. (2000). A brief illustrated guide to the ultrastructure of Plasmodium falciparum asexual blood stages. Parasitology today *16*, 427-433.

Bano, N., Romano, J.D., Jayabalasingham, B., and Coppens, I. (2007). Cellular interactions of Plasmodium liver stage with its host mammalian cell. International journal for parasitology *37*, 1329-1341.

Baruch, D.I., Gamain, B., Barnwell, J.W., Sullivan, J.S., Stowers, A., Galland, G.G., Miller, L.H., and Collins, W.E. (2002). Immunization of Aotus monkeys with a functional domain of the Plasmodium falciparum variant antigen induces protection against a lethal parasite line. Proceedings of the National Academy of Sciences of the United States of America *99*, 3860-3865.

Baruch, D.I., Pasloske, B.L., Singh, H.B., Bi, X., Ma, X.C., Feldman, M., Taraschi, T.F., and Howard, R.J. (1995). Cloning the *P. falciparum* gene encoding PfEMP1, a malarial variant antigen and adherence receptor on the surface of parasitized human erythrocytes. Cell *82*, 77-87.

Baum, J., Chen, L., Healer, J., Lopaticki, S., Boyle, M., Triglia, T., Ehlgen, F., Ralph, S.A., Beeson, J.G., and Cowman, A.F. (2009). Reticulocyte-binding protein homologue 5 - an essential adhesin involved in invasion of human erythrocytes by Plasmodium falciparum. International journal for parasitology *39*, 371-380.

Baum, J., Maier, A.G., Good, R.T., Simpson, K.M., and Cowman, A.F. (2005). Invasion by *P. falciparum* merozoites suggests a hierarchy of molecular interactions. PLoS pathogens *1*, e37.

Baum, J., Richard, D., Healer, J., Rug, M., Krnajski, Z., Gilberger, T.W., Green, J.L., Holder, A.A., and Cowman, A.F. (2006). A conserved molecular motor drives cell invasion and gliding motility across malaria life cycle stages and other apicomplexan parasites. The Journal of biological chemistry *281*, 5197-5208.

Beck, J.R., Muralidharan, V., Oksman, A., and Goldberg, D.E. (2014). PTEX component HSP101 mediates export of diverse malaria effectors into host erythrocytes. Nature *511*, 592-595.

Besteiro, S., Michelin, A., Poncet, J., Dubremetz, J.F., and Lebrun, M. (2009). Export of a Toxoplasma gondii rhoptry neck protein complex at the host cell membrane to form the moving junction during invasion. PLoS pathogens *5*, e1000309.

Boddey, J.A., Carvalho, T.G., Hodder, A.N., Sargeant, T.J., Sleebs, B.E., Marapana, D., Lopaticki, S., Nebl, T., and Cowman, A.F. (2013). Role of plasmepsin V in export of diverse protein families from the Plasmodium falciparum exportome. Traffic *14*, 532-550.

Bozdech, Z., Llinas, M., Pulliam, B.L., Wong, E.D., Zhu, J., and DeRisi, J.L. (2003). The transcriptome of the intraerythrocytic developmental cycle of Plasmodium falciparum. PLoS biology *1*, E5.

Bozdech, Z., Zhu, J., Joachimiak, M.P., Cohen, F.E., Pulliam, B., and DeRisi, J.L. (2003). Expression profiling of the schizont and trophozoite stages of Plasmodium falciparum with a long-oligonucleotide microarray. Genome biology *4*, R9.

Braks, J.A., Mair, G.R., Franke-Fayard, B., Janse, C.J., and Waters, A.P. (2008). A conserved U-rich RNA region implicated in regulation of translation in Plasmodium female gametocytes. Nucleic acids research *36*, 1176-1186.

Bullen, H.E., Charnaud, S.C., Kalanon, M., Riglar, D.T., Dekiwadia, C., Kangwanrangsan, N., Torii, M., Tsuboi, T., Baum, J., Ralph, S.A.*, et al.* (2012). Biosynthesis, localization, and macromolecular arrangement of the Plasmodium falciparum translocon of exported proteins (PTEX). The Journal of biological chemistry *287*, 7871-7884.

Casares, S., Brumeanu, T.D., and Richie, T.L. (2010). The RTS,S malaria vaccine. Vaccine *28*, 4880-4894.

Cesbron-Delauw, M.F., Gendrin, C., Travier, L., Ruffiot, P., and Mercier, C. (2008). Apicomplexa in mammalian cells: trafficking to the parasitophorous vacuole. Traffic *9*, 657-664.

Chapat, C., Corbo, L. (2014), Novel roles oft he CCR4-NOT complex, WIREs RNA, 5: 883-901

Chen, Q., Heston, J.B., Burkett, Z.D., and White, S.A. (2013). Expression analysis of the speech-related genes FoxP1 and FoxP2 and their relation to singing behavior in two songbird species. The Journal of experimental biology *216*, 3682-3692.

Cheng, Y.J., Lee, C.H., Lin, Y.P., Huang, J.Y., Su, C.C., Chang, W.T., and Yang, B.C. (2008). Caspase-3 enhances lung metastasis and cell migration in a protease-independent mechanism through the ERK pathway. International journal of cancer Journal international du cancer *123*, 1278-1285.

Cogswell, F.B. (1992). The hypnozoite and relapse in primate malaria. Clinical microbiology reviews *5*, 26-35.

Collins, W.E., and Jeffery, G.M. (2007). Plasmodium malariae: parasite and disease. Clinical microbiology reviews *20*, 579-592.

Cooke, B.M., Buckingham, D.W., Glenister, F.K., Fernandez, K.M., Bannister, L.H., Marti, M., Mohandas, N., and Coppel, R.L. (2006). A Maurer's cleft-associated protein is essential for expression of the major malaria virulence antigen on the surface of infected red blood cells. The Journal of cell biology *172*, 899-908.

Cowman, A.F., Baldi, D.L., Healer, J., Mills, K.E., O'Donnell, R.A., Reed, M.B., Triglia, T., Wickham, M.E., and Crabb, B.S. (2000). Functional analysis of proteins involved in *Plasmodium falciparum* merozoite invasion of red blood cells. FEBS letters *476*, 84-88.
Cowman, A.F., and Crabb, B.S. (2006). Invasion of red blood cells by malaria parasites. Cell *124*, 755-766.

Cox-Singh, J., and Culleton, R. (2015). *Plasmodium knowlesi*: from severe zoonosis to animal model. Trends in parasitology *31*, 232-238.

Crabb, B.S., Triglia, T., Waterkeyn, J.G., and Cowman, A.F. (1997). Stable transgene expression in Plasmodium falciparum. Molecular and biochemical parasitology *90*, 131-144.

Crompton, P.D., Kayala, M.A., Traore, B., Kayentao, K., Ongoiba, A., Weiss, G.E., Molina, D.M., Burk, C.R., Waisberg, M., Jasinskas, A.*, et al.* (2010). A prospective analysis of the Ab response to *Plasmodium falciparum* before and after a malaria season by protein microarray. Proceedings of the National Academy of Sciences of the United States of America *107*, 6958-6963.

Cui, L. Linder, S and Miao, J (2015), Translational regulation during stage transitions in malaria parasites. Annals oft he New York Academy of Science, 1342: 1-9.

Cummings, P. (2010). Carryover bias in crossover trials. Archives of pediatrics & adolescent medicine *164*, 703-705.

Daily, J.P., Le Roch, K.G., Sarr, O., Fang, X., Zhou, Y., Ndir, O., Mboup, S., Sultan, A., Winzeler, E.A., and Wirth, D.F. (2004). In vivo transcriptional profiling of *Plasmodium falciparum*. Malaria journal *3*, 30.

Dembele, L., Gego, A., Zeeman, A.M., Franetich, J.F., Silvie, O., Rametti, A., Le Grand, R., Dereuddre-Bosquet, N., Sauerwein, R., van Gemert, G.J.*, et al.* (2011). Towards an in vitro model of *Plasmodium* hypnozoites suitable for drug discovery. PloS one *6*, e18162.

Desai, M., ter Kuile, F.O., Nosten, F., McGready, R., Asamoa, K., Brabin, B., and Newman, R.D. (2007). Epidemiology and burden of malaria in pregnancy. The Lancet Infectious diseases *7*, 93-104.

Dluzewski, A.R., Mitchell, G.H., Fryer, P.R., Griffiths, S., Wilson, R.J., and Gratzer, W.B. (1992). Origins of the parasitophorous vacuole membrane of the malaria parasite, *Plasmodium falciparum*, in human red blood cells. Journal of cell science *102 (Pt 3)*, 527-532.

Dluzewski, A.R., Nash, G.B., Wilson, R.J., Reardon, D.M., and Gratzer, W.B. (1992). Invasion of hereditary ovalocytes by *Plasmodium falciparum* in vitro and its relation to intracellular ATP concentration. Molecular and biochemical parasitology *55*, 1-7.

Doerig, C., Chakrabarti, D., Kappes, B., and Matthews, K. (2000). The cell cycle in protozoan parasites. Progress in cell cycle research *4*, 163-183.

Dondorp, A.M., Nosten, F., Yi, P., Das, D., Phyo, A.P., Tarning, J., Lwin, K.M., Ariey, F., Hanpithakpong, W., Lee, S.J.*, et al.* (2009). Artemisinin resistance in *Plasmodium falciparum* malaria. The New England journal of medicine *361*, 455-467.

Dondorp, A.M., Yeung, S., White, L., Nguon, C., Day, N.P., Socheat, D., and von Seidlein, L. (2010). Artemisinin resistance: current status and scenarios for containment. Nature reviews Microbiology *8*, 272-280.

Drew, D.R., Sanders, P.R., and Crabb, B.S. (2005). *Plasmodium falciparum* merozoite surface protein 8 is a ring-stage membrane protein that localizes to the parasitophorous vacuole of infected erythrocytes. Infection and immunity *73*, 3912-3922.

Eksi, S., and Williamson, K.C. (2011). Protein targeting to the parasitophorous vacuole membrane of *Plasmodium falciparum*. Eukaryotic cell *10*, 744-752.

Elmendorf, H.G., and Haldar, K. (1994). *Plasmodium falciparum* exports the Golgi marker sphingomyelin synthase into a tubovesicular network in the cytoplasm of mature erythrocytes. The Journal of cell biology *124*, 449-462.

Elsworth, B., Matthews, K., Nie, C.Q., Kalanon, M., Charnaud, S.C., Sanders, P.R., Chisholm, S.A., Counihan, N.A., Shaw, P.J., Pino, P.*, et al.* (2014). PTEX is an essential nexus for protein export in malaria parasites. Nature *511*, 587-591.

Formaglio, P., Tavares, J., Menard, R., and Amino, R. (2014). Loss of host cell plasma membrane integrity following cell traversal by *Plasmodium* sporozoites in the skin. Parasitology international *63*, 237-244.

Glushakova, S., Yin, D., Li, T., and Zimmerberg, J. (2005). Membrane transformation during malaria parasite release from human red blood cells. Current biology: CB *15*, 1645-1650.

Goldberg, D.E., and Slater, A.F. (1992). The pathway of hemoglobin degradation in malaria parasites. Parasitology today *8*, 280-283.

Goldberg, D.E., and Slater, A.F. (1992). The pathway of hemoglobin degradation in malaria parasites. Parasitology today *8*, 280-283.

Guerreiro, A; Deligianni, E (2014), Genome-wide RIP-Chip analysis of translational repressor-bound mRNAs in the *Plasmodium* gametocyte. Genome Biology 2014, 15:493

Graewe, S., Rankin, K.E., Lehmann, C., Deschermeier, C., Hecht, L., Froehlke, U., Stanway, R.R., and Heussler, V. (2011). Hostile takeover by *Plasmodium*: reorganization of parasite and host cell membranes during liver stage egress. PLoS pathogens *7*, e1002224.

Graewe, S., Stanway, R.R., Rennenberg, A., and Heussler, V.T. (2012). Chronicle of a death foretold: *Plasmodium* liver stage parasites decide on the fate of the host cell. FEMS microbiology reviews *36*, 111-130.

Gregson, A., and Plowe, C.V. (2005). Mechanisms of resistance of malaria parasites to antifolates. Pharmacological reviews *57*, 117-145.

Gruring, C., Heiber, A., Kruse, F., Flemming, S., Franci, G., Colombo, S.F., Fasana, E., Schoeler, H., Borgese, N., Stunnenberg, H.G.*, et al.* (2012). Uncovering common principles in protein export of malaria parasites. Cell host & microbe *12*, 717-729.

Gruring, C., Heiber, A., Kruse, F., Ungefehr, J., Gilberger, T.W., and Spielmann, T. (2011). Development and host cell modifications of *Plasmodium falciparum* blood stages in four dimensions. Nature communications *2*, 165.

Gruring, C., and Spielmann, T. (2012). Imaging of live malaria blood stage parasites. Methods in enzymology *506*, 81-92.

Grutzke, J., Rindte, K., Goosmann, C., Silvie, O., Rauch, C., Heuer, D., Lehmann, M.J., Mueller, A.K., Brinkmann, V., Matuschewski, K.*, et al.* (2014). The spatiotemporal dynamics and membranous features of the *Plasmodium* liver stage tubovesicular network. Traffic *15*, 362-382.

Gunther, S., McMillan, P.J., Wallace, L.J., and Muller, S. (2005). *Plasmodium falciparum* possesses organelle-specific alpha-keto acid dehydrogenase complexes and lipoylation pathways. Biochemical Society transactions *33*, 977-980.

Haase, S., Herrmann, S., Gruring, C., Heiber, A., Jansen, P.W., Langer, C., Treeck, M., Cabrera, A., Bruns, C., Struck, N.S.*, et al.* (2009). Sequence requirements for the export of the *Plasmodium falciparum* Maurer's clefts protein REX2. Molecular microbiology *71*, 1003-1017.

Haldar, K. (1994). Ducts, channels and transporters in *Plasmodium*-infected erythrocytes. Parasitology today *10*, 393-395.

Haldar, K., Elmendorf, H.G., Das, A., Li, W.L., Ferguson, D.J., and Elford, B.C. (1994). In vitro secretory assays with erythrocyte-free malaria parasites. Methods in cell biology *45*, 221-246.

Hanson, J., Hossain, A., Charunwatthana, P., Hassan, M.U., Davis, T.M., Lam, S.W., Chubb, S.A., Maude, R.J., Yunus, E.B., Haque, G*., et al.* (2009). Hyponatremia in severe malaria: evidence for an appropriate anti-diuretic hormone response to hypovolemia. The American journal of tropical medicine and hygiene *80*, 141-145.

Hanssen, E., Dekiwadia, C., Riglar, D.T., Rug, M., Lemgruber, L., Cowman, A.F., Cyrklaff, M., Kudryashev, M., Frischknecht, F., Baum, J*., et al.* (2013). Electron tomography of *Plasmodium falciparum* merozoites reveals core cellular events that underpin erythrocyte invasion. Cellular microbiology *15*, 1457-1472.

Hehl, A.B., Lekutis, C., Grigg, M.E., Bradley, P.J., Dubremetz, J.F., Ortega-Barria, E., and Boothroyd, J.C. (2000). Toxoplasma gondii homologue of *Plasmodium* apical membrane antigen 1 is involved in invasion of host cells. Infection and immunity *68*, 7078-7086.

Heiber, A., Kruse, F., Pick, C., Gruring, C., Flemming, S., Oberli, A., Schoeler, H., Retzlaff, S., Mesen-Ramirez, P., Hiss, J.A*., et al.* (2013). Identification of new PNEPs indicates a substantial non-PEXEL exportome and underpins common features in *Plasmodium falciparum* protein export. PLoS pathogens *9*, e1003546.

Heussler, V., Sturm, A., and Langsley, G. (2006). Regulation of host cell survival by intracellular *Plasmodium* and *Theileria* parasites. Parasitology *132 Suppl*, S49-60.
Jiang, J.B., Li, G.Q., Guo, X.B., Kong, Y.C., and Arnold, K. (1982). Antimalarial activity of mefloquine and qinghaosu. Lancet *2*, 285-288.

Johnson, D.J., Fidock, D.A., Mungthin, M., Lakshmanan, V., Sidhu, A.B., Bray, P.G., and Ward, S.A. (2004). Evidence for a central role for PfCRT in conferring *Plasmodium falciparum* resistance to diverse antimalarial agents. Molecular cell *15*, 867-877.

Keeley, A., and Soldati, D. (2004). The glideosome: a molecular machine powering motility and host-cell invasion by Apicomplexa. Trends in cell biology *14*, 528-532.

Klemba, M., and Goldberg, D.E. (2005). Characterization of plasmepsin V, a membrane-bound aspartic protease homolog in the endoplasmic reticulum of *Plasmodium falciparum*. Molecular and biochemical parasitology *143*, 183-191.

Kruse, Florian; PhD thesis (2014). Charakterizierung einer Phosphatidyliniositol-4,5-bisphostphat-angereicherten Struktur der Plasmamembran des humanen Malaria Erregers *Plasmodium falciparum* (Welch, 1987)

de Koning-Ward TF1, Gilson PR, Boddey JA, Rug M, Smith BJ, Papenfuss AT, Sanders PR, Lundie RJ, Maier AG, Cowman AF, Crabb BS (2009). A newly discovered protein export machine in malaria parasites. Nature. 2009 Jun 18;459(7249):945-9. doi: 10.1038/nature08104.

Kriek, N., Tilley, L., Horrocks, P., Pinches, R., Elford, B.C., Ferguson, D.J., Lingelbach, K., and Newbold, C.I. (2003). Characterization of the pathway for transport of the cytoadherence-mediating protein, PfEMP1, to the host cell surface in malaria parasite-infected erythrocytes. Molecular microbiology *50*, 1215-1227.

Kyes, S., Christodoulou, Z., Pinches, R., Kriek, N., Horrocks, P., and Newbold, C. (2007). Plasmodium falciparum var gene expression is developmentally controlled at the level of RNA polymerase II-mediated transcription initiation. Molecular microbiology *63*, 1237-1247.

Kyes, S.A., Kraemer, S.M., and Smith, J.D. (2007). Antigenic variation in *Plasmodium falciparum*: gene organization and regulation of the var multigene family. Eukaryotic cell *6*, 1511-1520.

Langreth, S.G., Jensen,J.B., Reese, R.T., and Trager, W. (1978). Fine structure of human malaria in vitro. The Journal of protozoology *25*, 443-452.

Langreth, S.G., Nguyen-Dinh,P., and Trager, W. (1978). *Plasmodium falciparum*: merozoite invasion in vitro in the presence of chloroquine. Experimental parasitology *46*, 235-238.

Lauer, S.A., Rathod, P.K., Ghori, N., and Haldar, K. (1997). A membrane network for nutrient import in red cells infected with the malaria parasite. Science *276*, 1122-1125.

Laufer, M.K. (2009). Monitoring antimalarial drug efficacy: current challenges. Current infectious disease reports *11*, 59-65.

Le Roch, K., Sestier, C., Dorin, D., Waters, N., Kappes, B., Chakrabarti, D., Meijer, L., and Doerig, C. (2000). Activation of a Plasmodium falciparum cdc2-related kinase by heterologous p25 and cyclin H. Functional characterization of a *P. falciparum* cyclin homologue. The Journal of biological chemistry *275*, 8952-8958.

Le Roch, K.G., Johnson, J.R., Florens, L., Zhou, Y., Santrosyan, A., Grainger, M., Yan, S.F., Williamson, K.C., Holder, A.A., Carucci, D.J.*, et al.* (2004). Global analysis of transcript and protein levels across the *Plasmodium falciparum* life cycle. Genome research *14*, 2308-2318.

Ling, I.T., Florens, L., Dluzewski, A.R., Kaneko, O., Grainger, M., Yim Lim, B.Y., Tsuboi, T., Hopkins, J.M., Johnson, J.R., Torii, M.*, et al.* (2004). The *Plasmodium falciparum* clag9 gene encodes a rhoptry protein that is transferred to the host erythrocyte upon invasion. Molecular microbiology *52*, 107-118.

Ling, J., Baird, J.K., Fryauff, D.J., Sismadi, P., Bangs, M.J., Lacy, M., Barcus, M.J., Gramzinski, R., Maguire, J.D., Kumusumangsih, M.*, et al.* (2002). Randomized, placebo-controlled trial of atovaquone/proguanil for the prevention of *Plasmodium falciparum* or Plasmodium vivax malaria among migrants to Papua, Indonesia. Clinical infectious diseases : an official publication of the Infectious Diseases Society of America *35*, 825-833.

Lingelbach, K., and Przyborski, J.M. (2006). The long and winding road: protein trafficking mechanisms in the *Plasmodium falciparum* infected erythrocyte. Molecular and biochemical parasitology *147*, 1-8.

Lisewski, A.M., Quiros, J.P., Ng, C.L., Adikesavan, A.K., Miura, K., Putluri, N., Eastman, R.T., Scanfeld, D., Regenbogen, S.J., Altenhofen, L.*, et al.* (2014). Supergenomic network compression and the discovery of EXP1 as a glutathione transferase inhibited by artesunate. Cell *158*, 916-928.

Mackellar, D.C., O'Neill, M.T., Aly, A.S., Sacci, J.B., Jr., Cowman, A.F., and Kappe, S.H. (2010). *Plasmodium falciparum* PF10_0164 (ETRAMP10.3) is an essential parasitophorous vacuole and exported protein in blood stages. Eukaryotic cell *9*, 784-794.

MacKellar, D.C., Vaughan, A.M., Aly, A.S., DeLeon, S., and Kappe, S.H. (2011). A systematic analysis of the early transcribed membrane protein family throughout the life cycle of *Plasmodium yoelii*. Cellular microbiology *13*, 1755-1767.

Maier, A.G., Rug, M., O'Neill, M.T., Beeson, J.G., Marti, M., Reeder, J., and Cowman, A.F. (2007). Skeleton-binding protein 1 functions at the parasitophorous vacuole membrane to traffic PfEMP1 to the *Plasmodium falciparum*-infected erythrocyte surface. Blood *109*, 1289-1297.

Maier, A.G., Rug, M., O'Neill, M.T., Beeson, J.G., Marti, M., Reeder, J., and Cowman, A.F. (2007). Skeleton-binding protein 1 functions at the parasitophorous vacuole membrane to traffic PfEMP1 to the *Plasmodium falciparum*-infected erythrocyte surface. Blood *109*, 1289-1297.

Maier, A.G., Rug, M., O'Neill, M.T., Brown, M., Chakravorty, S., Szestak, T., Chesson, J., Wu, Y., Hughes, K., Coppel, R.L.*, et al.* (2008). Exported proteins required for virulence and rigidity of *Plasmodium falciparum*-infected human erythrocytes. Cell *134*, 48-61.

Mair, G.R., Braks, J.A., Garver, L.S., Wiegant, J.C., Hall, N., Dirks, R.W., Khan, S.M., Dimopoulos, G., Janse, C.J., and Waters, A.P. (2006). Regulation of sexual development of *Plasmodium* by translational repression. Science *313*, 667-669.

Mair, G.R., Lasonder, E., Garver, L.S., Franke-Fayard, B.M., Carret, C.K., Wiegant, J.C., Dirks, R.W., Dimopoulos, G., Janse, C.J., and Waters, A.P. (2010). Universal features of post-transcriptional gene regulation are critical for *Plasmodium* zygote development. PLoS pathogens *6*, e1000767.

Matthews, K., Kalanon, M., Chisholm, S.A., Sturm, A., Goodman, C.D., Dixon, M.W., Sanders, P.R., Nebl, T., Fraser, F., Haase, S.*, et al.* (2013). The *Plasmodium* translocon of exported proteins (PTEX) component thioredoxin-2 is important for maintaining normal blood-stage growth. Molecular microbiology *89*, 1167-1186.

Matz, J.M., Goosmann, C., Brinkmann, V., Grutzke, J., Ingmundson, A., Matuschewski, K., and Kooij, T.W. (2015). The *Plasmodium berghei* translocon of exported proteins reveals spatiotemporal dynamics of tubular extensions. Scientific reports *5*, 12532.

McMillan, P.J., Stimmler, L.M., Foth, B.J., McFadden, G.I., and Muller, S. (2005). The human malaria parasite *Plasmodium falciparum* possesses two distinct dihydrolipoamide dehydrogenases. Molecular microbiology *55*, 27-38.

Medana, I.M., and Turner, G.D. (2006). Human cerebral malaria and the blood-brain barrier. International journal for parasitology *36*, 555-568.

Medana, I.M., and Turner, G.D. (2006). Human cerebral malaria and the blood-brain barrier. International journal for parasitology *36*, 555-568.

Meis, J.F., Jap, P.H., Verhave, J.P., and Meuwissen, J.H. (1983). Ultrastructural studies of a vesicle system associated with endoplasmic reticulum in exo-erythrocytic forms of *Plasmodium* berghei. The Journal of protozoology *30*, 111-114.

Meis, J.F., Verhave, J.P., Jap, P.H., and Meuwissen, J.H. (1983). An ultrastructural study on the role of Kupffer cells in the process of infection by *Plasmodium berghei* sporozoites in rats. Parasitology *86 (Pt 2)*, 231-242.

Meis, J.F., Verhave, J.P., Jap, P.H., Sinden, R.E., and Meuwissen, J.H. (1983). Ultrastructural observations on the infection of rat liver by *Plasmodium berghei* sporozoites in vivo. The Journal of protozoology *30*, 361-366.

Menard, D., Ariey, F., and Mercereau-Puijalon, O. (2013). [*Plasmodium falciparum* susceptibility to antimalarial drugs: global data issued from the Pasteur Institutes international network]. Medecine sciences : M/S *29*, 647-655.

Miller, S.K., Good, R.T., Drew, D.R., Delorenzi, M., Sanders, P.R., Hodder, A.N., Speed, T.P., Cowman, A.F., de Koning-Ward, T.F., and Crabb, B.S. (2002). A subset of *Plasmodium falciparum* SERA genes are expressed and appear to play an important role in the erythrocytic cycle. The Journal of biological chemistry *277*, 47524-47532.

Mota, M.M., Hafalla, J.C., and Rodriguez, A. (2002). Migration through host cells activates Plasmodium sporozoites for infection. Nature medicine *8*, 1318-1322.

Mota, M.M., and Rodriguez, A. (2002). Invasion of mammalian host cells by *Plasmodium* sporozoites. BioEssays : news and reviews in molecular, cellular and developmental biology *24*, 149-156.

Muller, I.B., Walter, R.D., and Wrenger, C. (2005). Structural metal dependency of the arginase from the human malaria parasite *Plasmodium falciparum*. Biological chemistry *386*, 117-126.

Mundwiler-Pachlatko, E., and Beck, H.P. (2013). Maurer's clefts, the enigma of *Plasmodium falciparum*. Proceedings of the National Academy of Sciences of the United States of America *110*, 19987-19994.

Mundwiler-Pachlatko, E., and Beck, H.P. (2013). Maurer's clefts, the enigma of *Plasmodium falciparum*. Proceedings of the National Academy of Sciences of the United States of America *110*, 19987-19994.

Noedl, H., Wongsrichanalai, C., Miller, R.S., Myint, K.S., Looareesuwan, S., Sukthana, Y., Wongchotigul, V., Kollaritsch, H., Wiedermann, G., and Wernsdorfer, W.H. (2002). *Plasmodium falciparum*: effect of anti-malarial drugs on the production and secretion characteristics of histidine-rich protein II. Experimental parasitology *102*, 157-163.

Nussenzweig, R.S. (1967). Increased nonspecific resstance to malaria produced by administration of killed Corynebacterium parvum. Experimental parasitology *21*, 224-231.

Nussenzweig, R.S., and Nussenzweig, V. (1989). Antisporozoite vaccine for malaria: experimental basis and current status. Reviews of infectious diseases *11 Suppl 3*, S579-585.

Nussenzweig, R.S., Vanderberg, J., Most, H., and Orton, C. (1967). Protective immunity produced by the injection of x-irradiated sporozoites of *Plasmodium berghei*. Nature *216*, 160-162.

Nussenzweig, V., and Nussenzweig, R.S. (1989). Rationale for the development of an engineered sporozoite malaria vaccine. Advances in immunology *45*, 283-334.

Nussenzweig, V., and Nussenzweig, R.S. (1989). Circumsporozoite proteins of malaria parasites. Bulletin et memoires de l'Academie royale de medecine de Belgique *144*, 493-504.

Nyalwidhe, J., and Lingelbach, K. (2006). Proteases and chaperones are the most abundant proteins in the parasitophorous vacuole of *Plasmodium falciparum*-infected erythrocytes. Proteomics *6*, 1563-1573.

O'Donnell, R.A., Saul, A., Cowman, A.F., and Crabb, B.S. (2000). Functional conservation of the malaria vaccine antigen MSP-119across distantly related *Plasmodium* species. Nature medicine *6*, 91-95.

Ogutu, B.R., Apollo, O.J., McKinney, D., Okoth, W., Siangla, J., Dubovsky, F., Tucker, K., Waitumbi, J.N., Diggs, C., Wittes, J.*, et al.* (2009). Blood stage malaria vaccine eliciting high antigen-specific antibody concentrations confers no protection to young children in Western Kenya. PloS one *4*, e4708.

Pinheiro, M.M., Ahmed, M.A., Millar, S.B., Sanderson, T., Otto, T.D., Lu, W.C., Krishna, S., Rayner, J.C., and Cox-Singh, J. (2015). *Plasmodium knowlesi* genome sequences from clinical isolates reveal extensive genomic dimorphism. PloS one *10*, e0121303.

Plowe, C.V. (2005). Antimalarial drug resistance in Africa: strategies for monitoring and deterrence. Current topics in microbiology and immunology *295*, 55-79.

Plowe, C.V., Doumbo, O.K., Djimde, A., Kayentao, K., Diourte, Y., Doumbo, S.N., Coulibaly, D., Thera, M., Wellems, T.E., and Diallo, D.A. (2001). Chloroquine treatment of uncomplicated *Plasmodium falciparum* malaria in Mali: parasitologic resistance versus therapeutic efficacy. The American journal of tropical medicine and hygiene *64*, 242-246.

Price, R.N., von Seidlein, L., Valecha, N., Nosten, F., Baird, J.K., and White, N.J. (2014). Global extent of chloroquine-resistant *Plasmodium vivax*: a systematic review and meta-analysis. The Lancet Infectious diseases *14*, 982-991.

Prudencio, M., Rodrigues, C.D., Ataide, R., and Mota, M.M. (2008). Dissecting in vitro host cell infection by *Plasmodium* sporozoites using flow cytometry. Cellular microbiology *10*, 218-224.

Rankin, K.E., Graewe, S., Heussler, V.T., and Stanway, R.R. (2010). Imaging liver-stage malaria parasites. Cellular microbiology *12*, 569-579.

Riglar, D.T., and Baum, J. (2013). Static and dynamic imaging of erythrocyte invasion and early intra-erythrocytic development in *Plasmodium falciparum*. Methods in molecular biology *923*, 269-280.

Riglar, D.T., Richard, D., Wilson, D.W., Boyle, M.J., Dekiwadia, C., Turnbull, L., Angrisano, F., Marapana, D.S., Rogers, K.L., Whitchurch, C.B.*, et al.* (2011). Super-resolution dissection of coordinated events during malaria parasite invasion of the human erythrocyte. Cell host & microbe *9*, 9-20.

Riglar, D.T., Rogers, K.L., Hanssen, E., Turnbull, L., Bullen, H.E., Charnaud, S.C., Przyborski, J., Gilson, P.R., Whitchurch, C.B., Crabb, B.S.*, et al.* (2013). Spatial association with PTEX complexes defines regions for effector export into *Plasmodium falciparum*-infected erythrocytes. Nature communications *4*, 1415.

Russo, I., Babbitt, S., Muralidharan, V., Butler, T., Oksman, A., and Goldberg, D.E. (2010). Plasmepsin V licenses *Plasmodium* proteins for export into the host erythrocyte. Nature *463*, 632-636.

Sagara, I., Dicko, A., Ellis, R.D., Fay, M.P., Diawara, S.I., Assadou, M.H., Sissoko, M.S., Kone, M., Diallo, A.I., Saye, R.*, et al.* (2009). A randomized controlled phase 2 trial of the blood stage AMA1-C1/Alhydrogel malaria vaccine in children in Mali. Vaccine *27*, 3090-3098.

Sagara, I., Ellis, R.D., Dicko, A., Niambele, M.B., Kamate, B., Guindo, O., Sissoko, M.S., Fay, M.P., Guindo, M.A., Kante, O.*, et al.* (2009). A randomized and controlled Phase 1 study of the safety and immunogenicity of the AMA1-C1/Alhydrogel + CPG 7909 vaccine for *Plasmodium falciparum* malaria in semi-immune Malian adults. Vaccine *27*, 7292-7298.

Sam-Yellowe, T.Y., Florens, L., Johnson, J.R., Wang, T., Drazba, J.A., Le Roch, K.G., Zhou, Y., Batalov, S., Carucci, D.J., Winzeler, E.A.*, et al.* (2004). A *Plasmodium* gene family encoding Maurer's cleft membrane proteins: structural properties and expression profiling. Genome research *14*, 1052-1059.

Sam-Yellowe, T.Y., Shio, H., and Perkins, M.E. (1988). Secretion of *Plasmodium falciparum* rhoptry protein into the plasma membrane of host erythrocytes. The Journal of cell biology *106*, 1507-1513.

Seder RA, Chang LJ, Enama ME, Zephir KL, Sarwar UN, Gordon IJ, Holman LA, James ER, Billingsley PF, Gunasekera A, Richman A, Chakravarty S, Manoj A, Velmurugan S, Li M, Ruben AJ, Li T, Eappen AG, Stafford RE, Plummer SH, Hendel CS, Novik L, Costner PJ, Mendoza FH, Saunders JG, Nason MC, Richardson JH, Murphy J, Davidson SA, Richie TL, Sedegah M, Sutamihardja A, Fahle GA, Lyke KE, Laurens MB, Roederer M, Tewari K, Epstein JE, Sim BK, Ledgerwood JE, Graham BS, Hoffman SL; VRC 312 Study Team. (2013) Protection against malaria by intravenous immunization with a nonreplicating sporozoite vaccine. *Science 20 September 2013: Vol. 341 no. 6152 pp. 1359-136*

Schofield, A.E., Tanner, M.J., Pinder, J.C., Clough, B., Bayley, P.M., Nash, G.B., Dluzewski, A.R., Reardon, D.M., Cox, T.M., Wilson, R.J.*, et al.* (1992). Basis of unique red cell membrane properties in hereditary ovalocytosis. Journal of molecular biology *223*, 949-958.

Shute, P.G. (1946). The maintenance of a strain of *Plasmodium vivax* through man and mosquito over a period of 21 years. Monthly bulletin of the Ministry of Health and the Emergency Public Health Laboratory Service *5*, 110-112.

Sidhu, A.B., Verdier-Pinard, D., and Fidock, D.A. (2002). Chloroquine resistance in *Plasmodium falciparum* malaria parasites conferred by pfcrt mutations. Science *298*, 210-213.

Silvie, O., Briquet, S., Muller, K., Manzoni, G., and Matuschewski, K. (2014). Post-transcriptional silencing of UIS4 in *Plasmodium berghei* sporozoites is important for host switch. Molecular microbiology *91*, 1200-1213.

Simmons, D., Woollett, G., Bergin-Cartwright, M., Kay, D., and Scaife, J. (1987). A malaria protein exported into a new compartment within the host erythrocyte. The EMBO journal *6*, 485-491.

Slater, A.F. (1992). Malaria pigment. Experimental parasitology *74*, 362-365.

Slater, A.F., and Cerami, A. (1992). Inhibition by chloroquine of a novel haem polymerase enzyme activity in malaria trophozoites. Nature *355*, 167-169.

Smith, J.D., Chitnis, C.E., Craig, A.G., Roberts, D.J., Hudson-Taylor, D.E., Peterson, D.S., Pinches, R., Newbold, C.I., and Miller, L.H. (1995). Switches in expression of Plasmodium falciparum var genes correlate with changes in antigenic and cytoadherent phenotypes of infected erythrocytes. Cell *82*, 101-110.

Spielmann, T., and Beck, H.P. (2000). Analysis of stage-specific transcription in Plasmodium falciparum reveals a set of genes exclusively transcribed in ring stage parasites. Molecular and biochemical parasitology *111*, 453-458.

Spielmann, T., Dixon, M.W., Hernandez-Valladares, M., Hannemann, M., Trenholme, K.R., and Gardiner, D.L. (2006). Reliable transfection of *Plasmodium falciparum* using non-commercial plasmid mini preparations. International journal for parasitology *36*, 1245-1248.

Spielmann, T., Fergusen, D.J., and Beck, H.P. (2003). etramps, a new *Plasmodium falciparum* gene family coding for developmentally regulated and highly charged membrane proteins located at the parasite-host cell interface. Molecular biology of the cell *14*, 1529-1544.

Spielmann, T., and Gilberger, T.W. (2010). Protein export in malaria parasites: do multiple export motifs add up to multiple export pathways? Trends in parasitology *26*, 6-10.

Spielmann, T., Hawthorne, P.L., Dixon, M.W., Hannemann, M., Klotz, K., Kemp, D.J., Klonis, N., Tilley, L., Trenholme, K.R., and Gardiner, D.L. (2006). A cluster of ring stage-specific genes linked to a locus implicated in cytoadherence in *Plasmodium falciparum* codes for PEXEL-negative and PEXEL-positive proteins exported into the host cell. Molecular biology of the cell *17*, 3613-3624.

Spielmann, T., Montagna, G.N., Hecht, L., and Matuschewski, K. (2012). Molecular make-up of the *Plasmodium* parasitophorous vacuolar membrane. International journal of medical microbiology : IJMM *302*, 179-186.

Spycher, C., Klonis, N., Spielmann, T., Kump, E., Steiger, S., Tilley, L., and Beck, H.P. (2003). MAHRP-1, a novel *Plasmodium falciparum* histidine-rich protein, binds ferriprotoporphyrin IX and localizes to the Maurer's clefts. The Journal of biological chemistry *278*, 35373-35383.

Spycher, C., Rug, M., Pachlatko, E., Hanssen, E., Ferguson, D., Cowman, A.F., Tilley, L., and Beck, H.P. (2008). The Maurer's cleft protein MAHRP1 is essential for trafficking of PfEMP1 to the surface of *Plasmodium falciparum*-infected erythrocytes. Molecular microbiology *68*, 1300-1314.

Sridaran, S., McClintock, S.K., Syphard, L.M., Herman, K.M., Barnwell, J.W., and Udhayakumar, V. (2010). Anti-folate drug resistance in Africa: meta-analysis of reported dihydrofolate reductase (dhfr) and dihydropteroate synthase (dhps) mutant genotype frequencies in African *Plasmodium falciparum* parasite populations. Malaria journal *9*, 247.

Stanway, R.R., Mueller, N., Zobiak, B., Graewe, S., Froehlke, U., Zessin, P.J., Aepfelbacher, M., and Heussler, V.T. (2011). Organelle segregation into *Plasmodium* liver stage merozoites. Cellular microbiology *13*, 1768-1782.

Striepen, B. (2013). Parasitic infections: Time to tackle cryptosporidiosis. Nature *503*, 189-191.

Talisuna, A.O., Nalunkuma-Kazibwe, A., Langi, P., Mutabingwa, T.K., Watkins, W.W., Van Marck, E., Egwang, T.G., and D'Alessandro, U. (2004). Two mutations in dihydrofolate reductase combined with one in the dihydropteroate synthase gene predict sulphadoxine-pyrimethamine parasitological failure in Ugandan children with uncomplicated falciparum malaria. Infection, genetics and evolution : journal of molecular epidemiology and evolutionary genetics in infectious diseases *4*, 321-327.

Tamez, P.A., Bhattacharjee, S., van Ooij, C., Hiller, N.L., Llinas, M., Balu, B., Adams, J.H., and Haldar, K. (2008). An erythrocyte vesicle protein exported by the malaria parasite promotes tubovesicular lipid import from the host cell surface. PLoS pathogens *4*, e1000118.

Taylor, H.M., McRobert, L., Grainger, M., Sicard, A., Dluzewski, A.R., Hopp, C.S., Holder, A.A., and Baker, D.A. (2010). The malaria parasite cyclic GMP-dependent protein kinase plays a central role in blood-stage schizogony. Eukaryotic cell *9*, 37-45.

Trager, W., Rudzinska, M.A., and Bradbury, P.C. (1966). The fine structure of *Plasmodium falciparum* and its host erythrocytes in natural malarial infections in man. Bulletin of the World Health Organization *35*, 883-885.

Triglia, T., Healer, J., Caruana, S.R., Hodder, A.N., Anders, R.F., Crabb, B.S., and Cowman, A.F. (2000). Apical membrane antigen 1 plays a central role in erythrocyte invasion by *Plasmodium* species. Molecular microbiology *38*, 706-718.

Turner, A.E. (2006). The efficacy of Adeli suit treatment in children with cerebral palsy.

Developmental medicine and child neurology *48*, 324.

Tyler, J.S., and Boothroyd, J.C. (2011). The C-terminus of Toxoplasma RON2 provides the crucial link between AMA1 and the host-associated invasion complex. PLoS pathogens *7*, e1001282.

Tyler, J.S., Treeck, M., and Boothroyd, J.C. (2011). Focus on the ringleader: the role of AMA1 in apicomplexan invasion and replication. Trends in parasitology *27*, 410-420.

van de Sand, C., Horstmann, S., Schmidt, A., Sturm, A., Bolte, S., Krueger, A., Lutgehetmann, M., Pollok, J.M., Libert, C., and Heussler, V.T. (2005). The liver stage of *Plasmodium berghei* inhibits host cell apoptosis. Molecular microbiology *58*, 731-742.

van Dooren, G.G., and Striepen, B. (2013). The algal past and parasite present of the apicoplast. Annual review of microbiology *67*, 271-289.

Waller, K.L., Cooke, B.M., Nunomura, W., Mohandas, N., and Coppel, R.L. (1999). Mapping the binding domains involved in the interaction between the *Plasmodium falciparum* knob-associated histidine-rich protein (KAHRP) and the cytoadherence ligand *P. falciparum* erythrocyte membrane protein 1 (PfEMP1). The Journal of biological chemistry *274*, 23808-23813.

Wellems, T.E., and Plowe, C.V. (2001). Chloroquine-resistant malaria. The Journal of infectious diseases *184*, 770-776.

White, M.T., Bejon, P., Olotu, A., Griffin, J.T., Riley, E.M., Kester, K.E., Ockenhouse, C.F., and Ghani, A.C. (2013). The relationship between RTS,S vaccine-induced antibodies, CD4(+) T cell responses and protection against *Plasmodium falciparum* infection. PloS one *8*, e61395.

White, M.T., Griffin, J.T., Akpogheneta, O., Conway, D.J., Koram, K.A., Riley, E.M., and Ghani, A.C. (2014). Dynamics of the antibody response to *Plasmodium falciparum* infection in African children. The Journal of infectious diseases *210*, 1115-1122.

White, M.T., Karl, S., Battle, K.E., Hay, S.I., Mueller, I., and Ghani, A.C. (2014). Modelling the contribution of the hypnozoite reservoir to *Plasmodium vivax* transmission. eLife *3*.

Wickham, M.E., Rug, M., Ralph, S.A., Klonis, N., McFadden, G.I., Tilley, L., and Cowman, A.F. (2001). Trafficking and assembly of the cytoadherence complex in *Plasmodium falciparum*-infected human erythrocytes. The EMBO journal *20*, 5636-5649.

WHO, World Malaria Report; 2014

Winograd, E., Clavijo, C.A., Bustamante, L.Y., and Jaramillo, M. (1999). Release of merozoites from *Plasmodium falciparum*-infected erythrocytes could be mediated by a non-explosive event. Parasitology research *85*, 621-624.

Yang, Y., Li, Z., Yang, L., Jackson, M., Turner, A., and Ye, J. (2006). Effect of pH management on brain perfusion during retrograde cerebral perfusion. Asian cardiovascular & thoracic annals *14*, 495-500.

APPENDIX

A

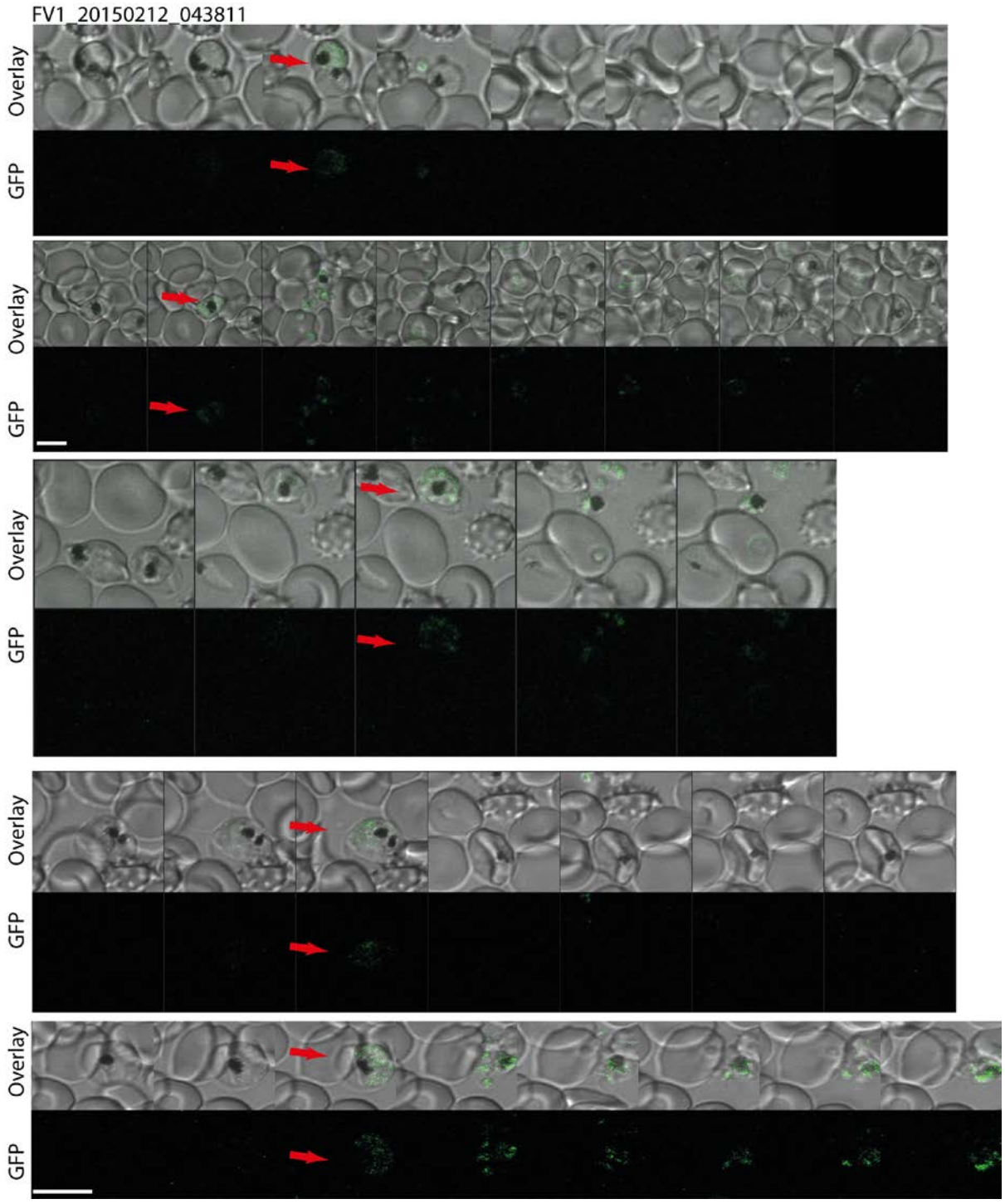
FV1_20150212_043811
Overlay
GFP
Overlay
GFP
Overlay
GFP
Overlay
GFP
Overlay
GFP

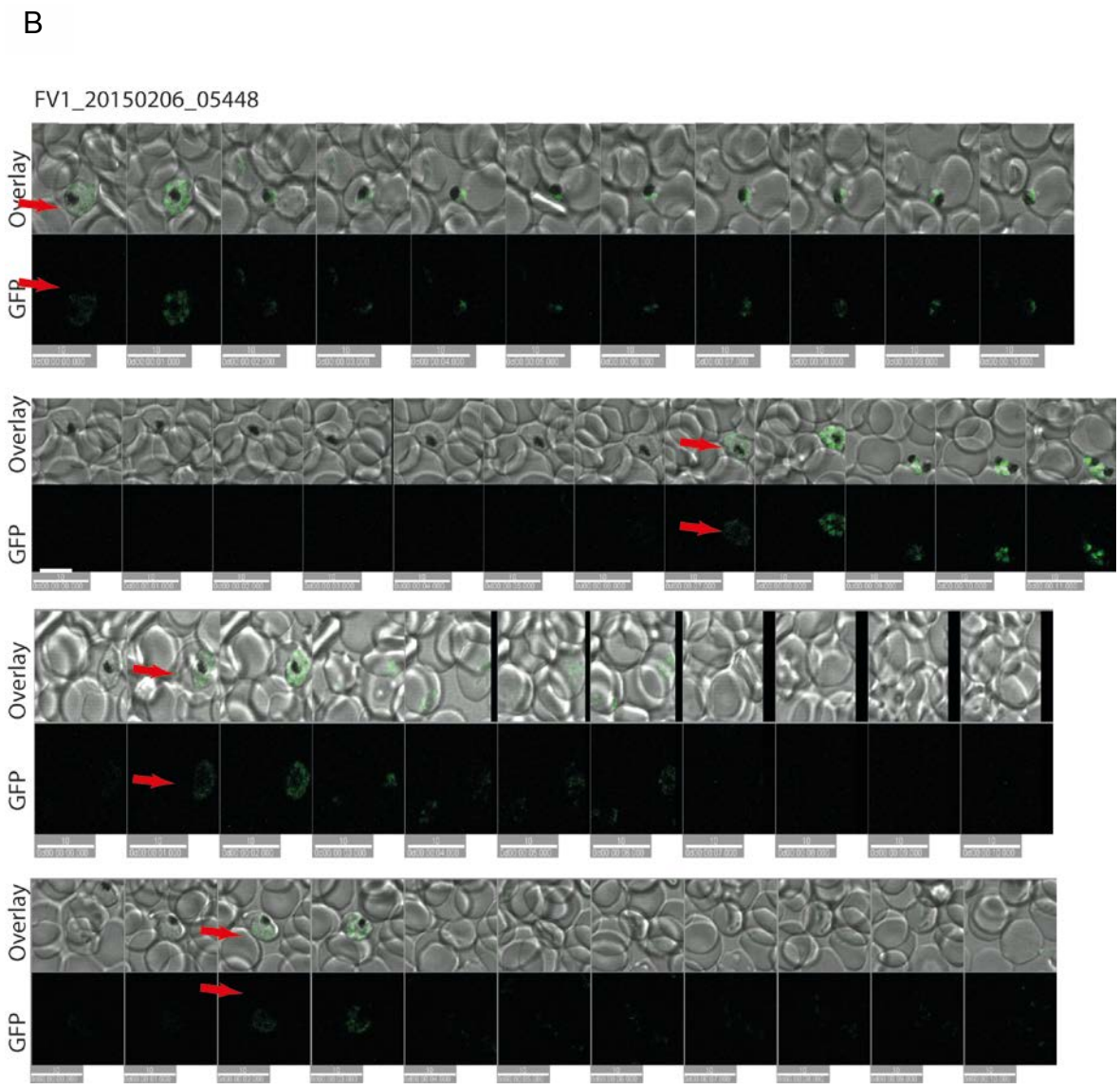

Fig.A1 Time-lapse microscopy experiments of SP-EXP-1-GFP^{etramp2} schizont stages. Four time-lapse experiments focused on schizonts were analyzed, short sequences of single sliced images of exemplary cells of the regarding experiments are shown; stacks were taken in 30 minute intervals; overlay: merged DIC and GFP signals (upper row); GFP signal (bottom row); GFP marker protein expression shortly before schizonts rupture is indicated by red arrows; size bar: 10µM. Fluoview identification numbers are given to characterize the experimental data; A: FV1_2015_0212_043811; B: FV1_20150206_05448.

Danksagung

Ich möchte mich zunächst bei Dr. Tobias Spielmann bedanken, für die Bereitstellung meines Promotionsthemas und die Möglichkeit meine Arbeit bei ihm anzufertigen. Vielen Dank, Tobi, für alles!

Des Weiteren möchte ich mich bei Dr. Markus Heß und Dr. Ulrich Spengler und altona Diagnostics GmbH bedanken, für dieses Projekt der geteilten Doktorarbeit finanziell möglich gemacht.

Ich bedanke mich von Herzen bei allen ehemaligen und jetzigen Mitglieder der AG Spielberger ;) für einfach alles, das schöne Arbeitsklima, die Gespräche, die Menschen, ihr werdet mir fehlen.

Ich danke dir, Dr. Sven Flemming, für all deine Hilfe. Ich kann dir nicht genug danken!

Ich danke meinen Freunden, die mir so verständnisvoll zu Seite standen, mich stets wieder aufgebaut und motiviert haben und immer ein offenes Ohr hatten. Ihr seid die Besten!

Ich danke meiner Familie, auch dem nicht verwandten Teil, für die große Unterstützung und die Hilfsangebote und die aufbauenden Worte!

Ich danke meinen Schwestern, dafür dass ich sie habe, ohne euch wäre ich nichts! Und dir, Anna, danke ich für die praktische Hilfe und für die ständigen Ermunterungen.

Ein ganz besonderer Dank gilt meinen Eltern, die mir immer alles ermöglicht haben und mich stets mit Rat und Tat unterstützen.

Eidesstattliche Versicherung

Hiermit erkläre ich an Eides statt, dass ich die vorliegende Dissertationsschrift selbst verfasst und keine anderen als die angegebenen Quellen und Hilfsmittel benutzt habe.